ENDOTHELIAL JUNCTIONS IN THE PERIODONTAL LIGAMENT MICROVASCULATURE OF YOUNG AND AGED MICE

A reseach report submitted in partial fulfilment
of the requirements for the
Degree of Master of Dental Surgery

by

John Cameron, B.D.Sc. (Qld.), F.R.A.C.D.S.

Department of Dentistry
The University of Adelaide
South Australia

July, 1995

This research report is dedicated to my beloved wife,
Dr Tracey Anne Winning

TABLE OF CONTENTS i

LIST OF FIGURES

LIST OF TABLES

SIGNED STATEMENT

This thesis contains no material which has been accepted for the award of any other degree or diploma in any university and that, to the best of the candidate's knowledge and belief, the thesis contains no material previously published or written by another person, except where due reference is made in the text of the thesis. The author consents to the thesis being made available for photocopying and loan if applicable, if accepted for the award of the degree.

John Cameron
31 July, 1995.

ACKNOWLEDGMENTS

I am grateful to my supervisors, Professor M.R. Sims, Discipline of Orthodontics, Faculty of Dentistry, University of Sydney and Dr. W.J. Sampson, Orthodontics Unit, Faculty of Dentistry, The University of Adelaide, for providing the facilities for this work to be carried out, for advice during experimentation and for their comments during the preparation of this manuscript. I also would like to acknowledge other members of the Department of Dentistry, The University of Adelaide, in particular, Mrs. M Leppard and Ms. V. Hargraves, for their helpful assistance.

I am grateful for assistance and advice that I received from outside the Faculty of Dentistry, in particular, Mr. P. Leppard, and the staff at the Electron Microscope Centre, Flinders Medical Centre, for the use of equipment and advice. Dr. H. Rosser and Dr. K. Crocker, from the Centre for Electron Microscopy and Microstructure analysis, The University of Adelaide, for the use of equipment and helpful assistance; and Dr. R. Correll, Biometrics Unit, CSIRO, for his statistical advice and analyses.

I am grateful to the Faculty of Dentistry for providing support through the Oliver Rutherford Turner Scholarship, for the second year of my candidature.

I would like to acknowledge the support of the Australian Society of Orthodontics Foundation for Research and Education for funding the project.

Finally, I would like to thank my family and friends both from within and outside the university, in particular my wife, Dr. Tracey Winning, for her love, support and assistance in the achievement of my goal.

SUMMARY

Populations in industrialised countries are living longer. One aspect of the proposed theories of the human ageing process relates to alterations in the microvasculature. Vascular permeability, which is directly proportional to changes in the ultrastructural dimensions of endothelial junctional complexes (Bundgaard, 1988), decreases with ageing (Hruza, 1977). An increased number of endothelial junction tight regions correlates with a reduction in permeability of microvessels (Rippe and Haraldsson, 1994). Therefore, any changes in the number and distribution of tight junctions in the microvascular bed endothelium may indicate alterations in vascular permeability with ageing and an effect on orthodontic tooth movement. Any such data from animals would be of value for initial extrapolation to humans.

The general aim of the present study was to investigate the effects of ageing on the morphology of periodontal ligament (PDL) endothelial junctions. The null hypothesis to be tested was that no changes occur in proportions of 'tight' and 'close' regions, and the dimensions of endothelial junctions in the microvascular bed of aged mouse PDL.

Tissue specimens used in the present study were from Freezer's (1984) and Sims' (1987) studies and consisted of molar PDL from four young (35 days) and four aged (365 days) ALCA-strain mice. Anaesthetised mice were perfused with 5.6% glutaraldehyde and 0.9% osmium tetroxide W/V solution in cacodylate buffer. The right and left mandibular first molars and their bony sockets were dissected en block. The tissue blocks were demineralised at 4°C with 0.1M EDTA in 2.5% glutaraldehyde and embedded in resin. The mesiobuccal portion of the PDL was sectioned parallel to the occlusal plane from the alveolar crest to the tooth apex. Sections were collected at 160 µm intervals resulting in 7 to 9 levels per root. Sections were stained and processed for transmission electron microscopy (TEM).

The results of a pilot study showed that within the available PDL samples there were only sufficient numbers of postcapillary-sized venules (PCV) for analysis. Therefore, five PCV with one complete endothelial junction were selected from each level. These junctions were assessed and photographed using a TEM goniometer to allow identification of the junction type, i.e., tight or close junctions. Measurements of widths and lengths along the junctions

were completed on standardised micrographs magnified x150K, using a Manual Optical Picture Analyser (MOP-3) and digital callipers. The junction type and junction dimensions were analysed with a chi-square analysis and a multiple regression technique, respectively, using Genstat^{TM} 5, Release 3 (AFRC Institute of Arable Crops Research, Clarendon Press, Oxford, UK). A value of $p < 0.05$ was taken as significant.

Analysis of the measurement error, using a paired t-test or Wilcoxon signed rank test, indicated there was no significant difference between the measurement at different time intervals. The coefficient of variation for the measurements ranged from 1.8% to 4.8%. The kappa coefficient was used to test the precision in classification of tight and close regions between first and second observations. This calculation yielded a measure of 1.00, indicating that no significant differences were found between the first and second classifications.

The types of junction found were: (1) junctions with tight regions, (2) junctions with close regions, (3) junctions with tight and close regions, and (4) junctions with no tight or close regions. No open or gap junctions were found. A chi-square analysis showed that the junction types changed significantly with age ($p < 0.001$). The percentage of tight regions was 14.1% ± 3.5% higher in the old mice. The percentages of close regions for young and old mice were 88.8% and 74.7%, and for tight regions 11.2% and 25.3%, respectively. The aged mice had an increased proportion of tight /close regions and greater numbers of tight regions at every PDL level ($p < 0.01$). With respect to PDL level (coronal to apical) effects, significantly ($p < 0.05$) higher numbers of tight regions were found at the alveolar crest by comparison with the apex for each age group. The majority of tight junctions (86.1% in young and 90.0% in old mice) were located at the luminal third of the PCV endothelial wall ($p < 0.05$). Close regions also were more common at the luminal third (66.7% in young mice and 65.5% in old mice).

There was no effect of age on endothelial junction length, thickness, or size. For both groups, the junction length at level 160 μm was higher than other PDL levels, but overall this effect was not significant. There was, however, a significant ($p < 0.05$) effect of PDL level for young and old mice, on the thickness of the PCV wall at the location of the endothelial junction. An increased wall thickness occurred from slightly above average at the alveolar

crest, rising to a maximum at 160 μm and then steadily declining towards the apex.

Junction width changed with age. The junction width a third of the distance along the intercellular cleft from the luminal side of the PCV, at the apex of the PDL, was (1) 3.6 nm ± 0.88 nm wider ($p < 0.05$) in old mice, and (2) increased significantly ($p < 0.05$) for young and old mice, from the 960 μm PDL level to the apex. The junction width at the luminal entrance increased significantly ($p < 0.05$) at the apex by comparison with the alveolar crest in each age group. Age had no effect on the location of the junction region between luminal and abluminal limits of the PCV endothelial wall. Junction size did not change with PDL level (coronal to apical). Tight regions were 2.8 ± 2.4 nm shorter than close regions, but this difference was not statistically significant.

There was no effect of age on either pericytic or apericytic PCV or PCV diameter. A smaller (by 2.5 μm) PCV diameter was found in the old mice compared with the young mice, however, this difference was not significant. In young and old mice, the major proportion of randomly assessed PCV were apericytic. The number of pericytic PCV in each age group increased significantly ($p < 0.05$), relative to the total number of PCV, at the alveolar crest by comparison with the apex.

Significantly more ($p < 0.05$) PCV were found for each group in the PDL circumferential bone third, with fewer in the middle third, and a minimum number in the tooth third. In aged mice, there was a significant increase ($p < 0.01$) in the number of PCV located in the tooth third of the PDL, most of which were apericytic PCV ($p < 0.001$). In the PDL middle circumferential third halfway down the young mice PDL, the number of PCV decreased significantly ($p < 0.001$).

In the present study, the null hypothesis was rejected. The demonstration of significant changes in the proportion of tight and close regions found may lead to decreased permeability of the aged PDL microvasculature. Endothelial junction morphology and structural alterations of PCV in the PDL of mice may represent functional modification of PDL microvasculature during ageing. Ionic tracer studies can assess permeability in aged PDL to confirm this hypothesis. Assessment of the clinical significance of these changes is required.

CHAPTER 1 INTRODUCTION

In all industrialised countries at present, there is a trend towards an ageing population which has profound economic, political, and social significance (Sheiham, 1990). Current theories of the ageing process can be classified according to physiological alterations based on "wear and tear" or genome based theories (Harman, 1981; Cotran *et al.*, 1989; Dice, 1993). Aspects of the former group of theories include cross-linking of extracellular proteins and the accumulation of intracellular waste products. These cellular ageing effects acting alone may be responsible for functional changes. Other variables such as differences in patterns of disease and alterations in lifestyle also may be contributory to age related/dependent changes in function (Weisfeldt *et al.*, 1988).

Clearly, disease is of major significance in the ageing population. As highlighted by Goldman (1970), changes in the other parts of the cardiovascular system, which are unrelated to coronary atherosclerosis, and which are proposed to be more widespread, can have a variable effect on cardiovascular disease. It was concluded that greater attention to the normal mechanisms of ageing in the rest of the cardiovascular system unencumbered with disease is warranted.

Maintenance of optimal cellular function is dependent on the circulation which is crucial for the provision of nutrients and removal of waste (Clough, 1991). Alterations in structural or functional aspects of the peripheral vasculature have been implicated in decreased functional capacity of tissues with ageing, for example, active skeletal muscle (Cook *et al.*, 1992) . The accumulation of intracellular waste products and crosslinking of extracellular proteins that occur with age may be attributable to changes in capillary permeability. It is noteworthy that capillary permeability to macromolecules, micromolecules and transvascular fluid movement has been shown to decrease with age (Duran-Reynals, 1946; Wangensteen *et al.*, 1977; Matalon and Wangensteen, 1977; Hruza, 1977).

Capillary and postcapillary venule permeability correlates with intercellular cleft dimensions and tight junction organisation, such that alterations in permeability are in direct proportion to variations in their dimensions (Bundgaard, 1988). The dimensions of these structures can be estimated

using stereological conventions which involve calculation of three dimensional properties of objects from the study of tissues in two dimensions (Gundersen *et al.*, 1988). Other quantitative morphometric aspects of endothelial junction exchange pathways, that is, measurements of junction dimensions, remain to be further explained (Bundgaard, 1988).

The clinical significance of age related alteration in permeability of endothelial junctions in the periodontal ligament (PDL) microvasculature is relevant to the function of the PDL during mastication, tooth eruption, orthodontic tooth movement, and periodontal health and disease. Fluid collection in the apical interstitium (Magnusson, 1968, cited in Burn-Mudoch, 1990; Magnusson, 1973), has been proposed to be involved in production of an eruptive force (Burn-Mudoch, 1988; Moxham, 1988). Altered PDL microvessel permeability with resultant decreased fluid collection may modify the eruptive force involved in continued tooth eruption to maintain occlusal contact. Decreased permeability of aged PDL may be involved in an age associated reduced rate of orthodontic tooth movement (Bridges *et al.*, 1988; Takano-Yamamoto *et al.*, 1992). Age related differences in the rate of orthodontic tooth movement may be related to an alteration in bone turnover through reduced supply of nutrient and, for example, 1,25-dihydroxycholecalciferol (Takano-Yamamoto *et al.*, 1992), and/or removal of waste products (Stutzmann and Petrovic, 1989). It is suggested that an age related decrease in permeability, and the accompaning decrease in waste product removal, may affect the maintenance of periodontal support (Haugen, 1992), and the reported changes in the host response to the causative factors of periodontal disease (Holm-Pedersen *et al.*, 1975; van der Velden, 1984).

Studies of ageing mice PDL have demonstrated alterations in the structure of the microvasculature bed (Sims *et al.*, 1992a; 1992b; 1993). Redistribution of blood vessels across and down the length of the mouse PDL was demonstrated with a reduction in diffusion distances. As noted previously, with increasing age, alterations in microvascular permeability can occur (Hruza, 1977). While these studies (Sims *et al.*, 1992a; 1992b; 1993), examined blood vessel number and size, these parameters may not be directly related to permeability. Investigation of the structure of the endothelium of aged individuals (Gabbiani and Majno, 1977) by assessment of ultrastructural dimensions of endothelial junctional complexes should provide further insight into structural features of the vasculature that are important in determining vascular permeability.

For the present study, the null hypotheses to be tested are that no alterations in dimensions of endothelial junctions occur with increasing age, for example, (1) number of tight and close regions, (2) widths of junctional 'clefts', (3) lengths of junctions from lumen to ablumen, (4) size of tight and close regions, and (5) the relationship between the junction length and the thickness of the endothelial cell wall. The specific aim of the current investigation was to assess these differences in endothelial junction morphology in the PDL microvascular bed of rodent molars under the influence of ageing. A morphometric analysis of PDL junction distribution and relative dimensions in young adult (35 day old) and aged mice (365 day old) was completed using transmission electron microscopy.

CHAPTER 2 AIMS OF THE INVESTIGATION

As vascular permeability is directly proportional to alterations in endothelial junction morphology (Bundgaard, 1988), and decreases with age (Hzura, 1977), the purpose of this study was to evaluate the morphometric data of endothelial junctions in the molar periodontal ligament microvasculature of young and aged mice.

Accordingly, the specific aims of the investigation were:

1) To conduct a TEM examination of young and aged mouse molar PDL vasculature and derive morphometric data of the endothelial junctions investigated.

2) To derive statistical correlations of the junctional dimensions in young adult (35 days) and aged mice (365 days).

3) To test the null hypotheses that, with increasing age, no changes occur in endothelial junction morphology, namely:
    1. proportion of tight and close regions,
    2. width of the intercellular distance between opposing plasma membranes,
    3. length of the diffusion pathway,
    4. size of tight and close regions, and
    5. ratio of the length of the diffusion pathway to the thickness of the endothelial cell wall at the location of the endothelial junction.

CHAPTER 3 LITERATURE REVIEW

3.1 Ageing Theories and the Cardiovascular System

A specific definition of ageing is difficult to provide. Generally it is accepted that 'ageing constitutes a decreasing ability to survive' (Cotran *et al.*, 1989) and is characterised by a universal, progressive, decremental, intrinsic and irreversible biological process (Strehler, 1962, cited in Goldman, 1970; Haugen, 1992).

Physiological changes proposed to explain the ageing process in tissues are based on 'wear and tear'. This group of theories includes tissue damage due to free radicals, cross-linking of extracellular proteins, the accumulation of intracellular waste products and random errors in protein synthesis (Harman, 1981; Cotran *at al.*, 1989; Dice, 1993). Cellular and macromolecular damage results from a variety of environmental insults accompanied with deficient repair mechanisms causing the passive accumulation of errors in cellular constituents, for example, DNA, RNA, lipid and protein (Dice, 1993). The genome-based theories discuss age changes in relation to genes that are programmed for ageing, limited doubling potential of cells or mutations that ultimately result in the death of the cell (Dice, 1993).

Diseases prevalent in aged populations, interactions between the varying influence of ageing alone, and changes due to disease patterns and life styles may hinder elucidation of the aging process (Lakatta, 1993). In Western society, for example, coronary atherosclerosis is present in up to 60% of elderly people. Clearly this disease is of major significance in the ageing population. However, as highlighted by Goldman (1970), changes with age in other parts of the cardiovascular system, for example, in extracellular fluid and blood volume, are suggested to be more universal, and can impact variably on coronary atherosclerosis. It was concluded by Goldman (1970), that investigation of the mechanisms of ageing and not disease related effects, in the rest of the cardiovascular system, is warranted.

The importance of this area of study is supported by Cook *et al.* (1992), who proposed that the decreased functional capacity of active skeletal muscle with ageing may be related to altered structural or functional aspects of the

peripheral vasculature. The microvasculature of the cardiovascular system is crucial for the provision of nutrients and removal of waste to maintain optimal cellular function (Clough, 1991). Age related changes associated with extracellular protein crosslinking and intracellular waste product accumulation may be attributable to changes in the capillary permeability. It has also been demonstrated that a decrease in capillary permeability occurs for macromolecules, micromolecules and transvascular fluid movement with age (Duran-Reynals, 1946; Wangensteen *et al.*, 1977; Matalon and Wangensteen, 1977; Hruza, 1977).

3.2 Microvasculature

"Microvessel" and "microvasculature" define a single blood vessel and a network of microscopic vessels, respectively (Baez, 1977). These components form the smallest units of the cardiovascular system. Circulation helps to maintain homeostasis, that is, conservation of the internal milieu, through the exchange of gases and solutes between blood and the interstitial fluid (Tortora and Grabowski, 1993). Cells are supplied with the necessary nutrients and metabolic waste products are removed (Bundgaard, 1988). This exchange occurs across microvessel walls which play a role in many physiological functions, namely, permeability, uptake, transport, synthesis, and metabolism (Simionescu and Simionescu, 1984). The components of the microvasculature are arterioles, precapillary sphincter areas, arteriovenous anastomoses, arterial and venous capillaries, postcapillary venules, and muscular venules (Baez, 1977).

The capillary wall, the smallest exchange vessel with a luminal diameter of five to 10 μm, consists of a monolayer of simple squamous cells forming an endothelial tube (Simionescu and Simionescu, 1984). Endothelial cell surface coats, complexed with one another via endothelial junctions, are surrounded by secreted basement membrane with or without surrounding perivascular cells on the abluminal side of the blood vessel (Clough, 1991). The ultrastructural morphology of the microvasculature varies between locations according to the functional activity and nature of the surrounding tissue.

Macromolecules are relatively impermeable across microvessel walls, which are necessary to maintain fluid balance between the vascular and interstitial

fluid compartments according to the Starling hypothesis (Vander *et al.*, 1970). However, some macromolecules, for example, antibodies, opsonins, and cytokines permeate to the extravascular compartment and return to the blood plasma via the lymphatic system (Rippe and Haraldsson, 1994). Structural aspects of capillary and postcapillary venule endothelium when compared to other simple epithelia may be associated with relatively high microvascular permeability to water, lipophilic, and small molecular weight hydrophilic molecules of the blood plasma (Palade *et al.*, 1979).

3.2.1 Classification of Microvasculature

In order to study microvascular changes in tissues, classification of blood vessels is necessary. The more commonly used terminology for classification of microvasculature will be reviewed, although it is noted that differences in terms used for classification have been recognised (Baez, 1977; Wiedeman, 1984). Variables used to classify microvessels include lumen diameter, the number of cell layers, endothelial cell wall thickness and morphology, and the perivascular cell type (Bennett *et al.*, 1959; Majno, 1965; Rhodin, 1967, 1968; Baez, 1977; Simionescu and Simionescu, 1984).

Bennett *et al.* (1959) proposed simple classifications of capillaries following study of a range of vertebrate animals (electric eel, mouse, rat, electric catfish). This classification correlates variations in structure with physiological differences in capillary function. Majno (1965) employed the 'degree of completeness of the endothelial layer' to distinguish three types of capillaries: continuous capillaries, fenestrated capillaries, and discontinuous capillaries (sinusoids) with intercellular gaps. The fenestrated capillaries are generally similar in structure to continuous capillaries, but have thinner endothelial cells (20 nm to 40 nm) and are perforated by fenestrae (intracellular openings). These fenestrae are 10 nm or less in diameter, and may be bridged by a thin diaphragm.

Rhodin (1967, 1968) classified the microvascular bed of the fascia of rabbit medial thigh muscle into segments according to vessel diameter and ultrastructural features (Table 3.1). Identification of arterial vessels was based on the number of smooth muscle layers, endothelial and medial relationships and innervation (Rhodin, 1967). Criteria used to identify venous vessels (Rhodin, 1968) were based on the perivascular elements and the vessel relationship to the local vasculature.

Table 3.1: Classification of blood vessels in the microcirculation. (Adapted from Rhodin, 1967, 1968).

Blood vessel type	Lumen calibre	Wall thickness	Endothelial cell morphology	Peri-endothelial cells	Other
Arteriole	100-50 μm	Greater than 6 μm	Cell 0.15 to 2μm in width, few pinocytotic vesicles, upstream cell usually overlaps downstream cell.	2-3 layers of smooth muscle cells, some eosinophils, mast cells and macrophages.	Well developed elastica interna, non-myelinated nerves extending to smooth muscle layer.
Terminal arterioles	Less than 50 μm	Less than 6 μm	Generally as above but with many filaments parallel to the long axis of the blood vessel and with more pinocytotic vesicles.	One layer of smooth muscle cells.	Little elastica interna, nerves closer to vessel wall with more frequent contacts with the smooth muscle layer, some myoendothelial junctions.
Pre capillary	7-15 μm	Less than 5 μm	Cell protrudes towards vessel lumen, nucleus shorter, thicker and more lobulated than above, some cytoplasmic filaments, many pinocytotic vesicles.	One layer of smooth muscle cells.	An increased number of unmyelinated-nerves associated with a decrease in lumen diameter, frequent neuromuscular and myoendothelial junctions.
Venous capillary	4-7 μm	0.5 μm	Some rough endoplasmic reticulum, free ribosomes, mitochondria, vesicles, granules and filaments.	Occasional veil cells and pericytes. Some macrophages, leukocytes, lymphocytes and plasma cells	Endothelium may be fenestrated.
Post-capillary venule	8-30 μm	1.5 μm	Cell rarely less than 0.2 μm thick and generally larger than that of venous capillary. Slight overlapping of adjoining cells.	More pericytes and veil cells than above. Some primitive smooth muscle cells around larger vessels.	Endothelium generally lacks fenestrae. Leukocytes may adhere to endothelial wall.
Collecting venule	30-50 μm	1.7μm	As above	Continuous layer of pericytes and veil cells around vessel. More primitive smooth muscle than above. Smooth muscle cells around larger vessels.	Single layer of veil cells and some collagenous fibrils surround blood vessels.
Muscular venule	50-100 μm	2.0 μm	As above	1-2 layers of smooth muscle cells.	Veil cells form a complete layer around vessel wall. Myoendothelial junctions present.
Small collecting vein	100-300 μm	2-3 μm	As above but with specific endothelial granules.	2 or more layers of smooth muscle cells.	Unmyelinated nerves situated 5-10 μm from muscular layer.

The inner diameter of venous capillaries has been reported to range from 4 to 7 μm (Rhodin, 1968), 5 to 10 μm (Simionescu and Simionescu, 1984), and 8 to 10 μm (Baez, 1977). Capillary wall thickness is normally thin (Baez, 1977), with a luminal diameter to wall thickness ratio of 20:1 (Rhodin, 1968). Continuous capillaries are devoid of fenestrations with wide variation in the number of plasmalemmal vesicles, transendothelial channels and junctional tightness in different vascular beds (Simionescu and Simionescu, 1984). Characteristics of the PDL microvasculature vary from other vascular beds, at different PDL locations, and between species (section 3.3).

Postcapillary venules are reported to have a diameter from 8 to 30 μm (Rhodin, 1968) or from 10 to 50 μm (Simionescu and Simionescu, 1984). They are continuous with two to four venous capillaries (Baez, 1977). The presence of pericytes between the surrounding basal lamina distinguishes pericytic and apericytic types. The endothelium is generally continuous but fenestration can occur (Simionescu and Simionescu, 1984). Vessel wall thickness is relatively thin, ranging from 0.2 to 0.3 μm (Simionescu and Simionescu, 1984), with a luminal diameter to wall thickness ratio of 10:1 (Rhodin, 1968). The relationship between postcapillary venule endothelial wall thickness and permeability is discussed in section 3.5. As the vessel diameter increase to 30 - 50 μm (Rhodin, 1968) a complete layer of pericytes and occasional smooth muscle cells are found. The definition of collecting venules is based on the finding of smooth muscle cells in the vessel wall (Baez, 1977).

3.2.1.1 Perivascular Cells

Periendothelial cells that characterise venous capillaries and postcapillary venules are pericytes and veil cells (Rhodin, 1968). Shepro and Morel (1993) describe pericytes as morphologically, biochemically, and physiologically heterogenous. Luminal diameter and the number of pericytes and veil cells distinguish a venous capillary (< 8 μm diameter) and a postcapillary venule (8 to 30 μm diameter), the latter having a gradual increase in the number of pericytes. The pericyte varies from 150 to 200 μm long and 10 to 25 μm wide (Simionescu and Simionescu, 1984). Pericytes and endothelial cells are closely associated with an intercellular distance of 20 nm (Sims, 1986). In the pericyte cytoplasm, plasmalemmal vesicles which are continuous with each other and the cell surface (Frøkjær-Jensen, 1984), were observed in association with endothelial cells (Sims, 1986). Sims (1986) suggested an interrelated, coordinated function of endothelial cell junctions and pericytes.

Simionescu and Simionescu (1984) describe the perivascular cells as an 'integrated cell system' between different segments of the microvasculature. A gradual transition of periendothelial cell with intermediate features occurs from the smooth muscle cells of the arteriole, the pericytic cells of capillaries and venules, and the smooth muscle cells of the muscular venules. Pericytes are reported to be sparse along capillaries, becoming numerous and 'spidery' on postcapillary venules (Sims, 1986).

Ultrastructural similarities are noted between pericytes and fibroblasts (Rhodin, 1968), but there are some differences, namely that pericytes:

1) are surrounded by the vascular basement membrane present on the abluminal side of the blood vessel and infrequently present on the endothelial side,
2) are most often found associated with venous capillaries, postcapillary venules and collecting venules,
3) have highly branched thin cytoplasmic processes which can make contact with, but do not fuse with the endothelium,
4) have less granular endoplasmic reticulum,
5) have a limited number of pinocytotic vesicles located near or connected with the plasma membrane,
6) display small densities along the cytoplasmic side of the plasma membrane similar in appearance to half-desmosomes.

In a review of pericyte function, Simionescu and Simionescu (1984) summarised their ascribed roles as (1) mechanical support for endothelial cells, (2) contraction regulating regional blood flow, (3) potential phagocytic activity, and (4) a source of undifferentiated mesenchymal cells in repair and inflammation. Pericytes may have other roles in wound healing; and coordination of endothelial cell mitogenesis and function (Sims, 1986); synthesis and secretion of structural components of the basement membrane and extracellular matrix; and synthesis and secretion of vasoactive autoregulating agents (Shepro and Morel, 1993). Of particular relevance to the current study is the relationship between the 'degree of tightness of the interendothelial junctions' resulting in a microvascular barrier and the endothelial area associated with pericytes as well as the ratio of pericytes to endothelial cells (Shepro and Morel, 1993).

Contractile proteins have been identified in pericytes. These include filament bundles of actin, myosin and tropomyosin located near the nucleus and in the

periphery of pericytes (Sims, 1986). Using autoradiography, Chakravarthy *et al.* (1992) showed that bovine retinal microvascular pericytes have receptors for the potent vasoactive peptide endothelin (ET1) which caused contraction of pericytes, at low concentrations (0.1 nM). At greater concentrations (10 nM) ET1 caused muscle-specific actins to aggregate and realign into bundles parallel to the cell's long axis. Chakravarthy *et al.* (1992) suggested that endothelial cell-pericyte interactions may play a role in control of endothelial cell proliferation and microvascular blood flow.

3.3 Periodontal Ligament Vasculature

The PDL is traditionally considered to be a dense, fibrous connective tissue which attaches tooth to alveolar bone. It has an important role in several functions, including: (1) supportive and protective roles during mastication, tooth eruption, and the application of orthodontic forces by providing a cushioning effect for the teeth to absorb forces; and (2) homeostatic, formative, resorptive, sensory and nutritive functions provided by cell populations, connective tissue fibres, blood vessels, and nerves. The PDL is highly vascular by comparison with other connective tissues (Berkovitz, 1990a). The rich vascular supply of the PDL provides the physiologic exchange of nutrients and waste products, and may reflect the high metabolic activity of rapid turnover of both cellular and extracellular elements (Embery, 1990). Large variations in vascular volume exist in different regions of the PDL (Sims, 1983; Freezer and Sims, 1987) and between different animals. This variation highlights the need for adequate sample sizes in investigations of PDL vascular volume (Sims, 1983).

The PDL vasculature of humans and various animals has been reviewed by Edwall (1982). Table 3.2 presents a summary of findings from studies demonstrating the extent of PDL vascularity. The primary vessels supplying the PDL are derived from the inferior and superior alveolar arteries for the mandible and maxilla, respectively, reaching the PDL from three sources, namely: (1) gingival vessels; (2) horizontal transalveolar vessels from the intraseptal vessels communicating with the PDL via perforations in the cribriform plate; (3) apical vessels which course coronally after branching with vessels entering the pulp via the apical foramen.

Table 3.2 Summary of studies on the total vascular bed volume as a percentage of the total PDL volume for various sites in different species.

Vascular vol. (SE)	PDL Site	Method	Study
Mouse			
7.7% (0.6%); 7.3%(0.8%)	Md first molar (mesial)	LM	Gould *et al.* (1977); McCulloch & Melcher (1983)
17%	Md first & second molars	LM	Sims (1980)
7.5% (1%); 8.5% (1.4%)	Md first molar (mesial)	TEM	Freezer (1984); Sims *et al.* (1992a)
10.9%	Md first molar	LM	Sims (1987)
Rat			
22.1% (5.6%)	Md first molar	TEM	Moxham *et al.* (1985)
20.0% to 23.0%	Mx first molar apex	TEM	Lew *et al.* (1989); Clark (1986)
10.2% to 24.6%	Mx first molar	TEM	Sims (unpublished data)
Monkey			
0.5% to 1%	Md incisors	LM	Wills *et al.* (1976)
8.3% (0.4%)	Md second molar	LM	Douvartzidis (1984)
2.6% to 19.7%; 10.8%	Mx incisor apex	TEM	Crowe (1988); Weir (1990)
11.26% (2.72%)	Mx incisor (mesial)	TEM	Parlange & Sims (1993)
Human			
1.63% to 3.5%	Anterior & premolar teeth	LM	Götze (1976, 1980)*
11%	Md premolars	LM	Sims (1980)
8.97% to 9.52%	Md premolars (distal)	TEM	Foong (1994)

PDL: periodontal ligament Mx: maxilla Md: mandible * cited in Parlange & Sims, 1993
LM: light microscope TEM: transmission electron microscope
SE: standard error

The gingival blood vessels are supplied by the greater palatine artery to the palatal gingiva and from the superior labial branches of the facial and infraorbital arteries in the maxilla, and from the sublingual branch of the lingual artery, and branches of the buccal, inferior labial, masseteric and mental arteries in the mandible. Entering the PDL via the crestal region, gingival vessels anastomose with vessels of the cervical region. The vessels of the PDL are thin walled and tend to run parallel to the long axis of the root. A system of capillaries which demonstrate fenestrae is found nearer the bone surface than the tooth (Luke, 1992). Central capillaries are generally devoid of fenestrae (Corpron *et al.*, 1976).

3.3.1 Periodontal Ligament Microvasculature

The PDL microvascular bed includes all vessels located between the alveolar bone and tooth root, and from the alveolar crest to the apex. Based on the classification of ultrastructural features of arterial and venous blood vessels by Rhodin (1967; 1968), the following vessels have been identified in the PDL: terminal arterioles; precapillary sphincters; arterovenous anastomoses; continuous venous capillaries (pericytic or apericytic); fenestrated arterial and venous capillaries and postcapillary venules; postcapillary venules (pericytic or apericytic); collecting venules (pericytic or apericytic); muscular venules and small collecting veins (Corpron *et al.*, 1976; Freezer, 1984; Wong and Sims, 1987). Species specific characteristics of the PDL microvasculature vary for different locations for mice (Corpron *et al.*, 1976; Sims, 1983), rats (Moxham *et al.*, 1985), primates (Lee *et al.*, 1991) and humans (Gilchrist, 1978). Only details of mouse PDL microvasculature will be presented as the present study involves investigation of this animal species.

Periodontal vascular walls contain numerous fenestrations in mice (Corpron *et al.*, 1976) and it is generally believed that they facilitate vascular permeability (Moxham *et al.*, 1985). Casley-Smith (1983) proposed that arterial fenestrae facilitate the passage of fluid and macromolecules into the interstitial tissues, whereas the venous fenestrae facilitate the collection of fluid and macromolecules.

Wong and Sims (1987), using a scanning electron microscopy (SEM) corrosion cast technique, found different patterns of anastomoses between axially oriented postcapillary-sized venules (PCV) and gingival inner (venous) vessels in the occlusal, middle and apical thirds of the mouse PDL. There was a preponderance of PCV as assessed morphometrically which was reflected in the lack of a paired arterial and venous system (Wong and Sims, 1987). Sims (1983) demonstrated that the mouse PDL microvascular bed was mainly venous.

The mouse PDL microvascular bed has an extensive venous pool incorporating approximately 11% of the tissue volume (Sims, 1987). Characteristically, PCV, which are mainly apericytic and may contain fenestrae, comprise 88% of the mouse PDL vascular volume (Freezer and Sims, 1987), thus forming the major component of the mouse PDL microvascular bed. Parlange and Sims (1993) found that PCV comprise 47.2% of the normal marmoset PDL vascular volume. However, the PCV

may be the most sensitive microvessel to experimental extrusive force, but any changes in the PCV are transitory.

According to Sims (1983), mouse microvasculature bed did not conform to Rhodin's (1968) morphological classification. Reported differences in PCV included: (1) an increased ratio of luminal diameter to wall thickness in the cervical and apical regions near 30:1 and 60:1, respectively, compared with Rhodin's ratio of 10:1 for rabbit subdermal postcapillary venules; (2) a paucity of pericytes; (3) the presence of fenestrae; (4) the observation of nerve endings and unmyelinated nerves adjacent to the endothelium. These differences were related to the supportive role the PDL plays during mastication. This role of the vasculature may be extended to include tooth eruption and tooth support as well as supply of nutrients and removal of wastes (Berkovitz, 1990b).

3.3.2 Periodontal Ligament Microvasculature Ultrastructure

The microvasculature has been classified according to ultrastructural features (Bennett *et al.*, 1959; Rhodin, 1967; 1968; 1984a; Simionescu and Simionescu, 1984). Using TEM, Freezer (1984) identified pericytic and apericytic capillaries and PCV in mouse PDL (Table 3.3).

Table 3.3 Ultrastructural features of mouse molar microvasculature*.

Vessel	Internal Diameter	Pericytic Investment	Cell Number[a]	Microvilli[b]
Capillary	4-7 μm	Partial or complete	up to 6 cells	Present
Capillary	4-7 μm	Absent	up to 6 cells	Present
PCV	8-30 μm	Few or absent	up to 9 cells	Present
PCV	8-30 μm	Complete	up to 9 cells	Present

* - Freezer, 1984

a - number of cells in the vessel wall

b - luminal microvilli present at endothelial junctions

PCV - postcapillary-sized venule

Corpron *et al.* (1976) observed cytoplasmic organelles and capillary endothelium ultrastructure using electron microscopy. The structures reported included numerous microvesicles, scattered ribosomes, and small mitochondria, finger-like cytoplasmic projections into the vessel lumen, occasional tight junctions, and endothelial cells surrounded by a basement membrane, but incompletely invested by pericytes. Quantitative data on

these organelles remains to be elucidated. No fenestrae were found in the middle third of the PDL. However, fenestrated capillaries (fenestrations 30 to 50 nm in diameter) were observed in the bone third. Small peripheral arterioles were found in the bone and tooth thirds.

3.4 Endothelial Junctions-Ultrastructure

3.4.1 Cardiovascular System Endothelial Junctions

The general appearance of different junctions has been described by Rhodin (1984b) as shown in Figure 3.1. Evidence that intercellular junctions or 'clefts' are an exchange pathway came from ionic tracer studies using mouse heart or diaphragm (Clough, 1991). Ionic tracers of various sizes are illustrated in Figure 3.1. The ultrastructural characteristics of endothelial junctions differ for each microvascular segment representing the functional activity of the surrounding tissue that the microvessels supply (Simionescu and Simionescu, 1991).

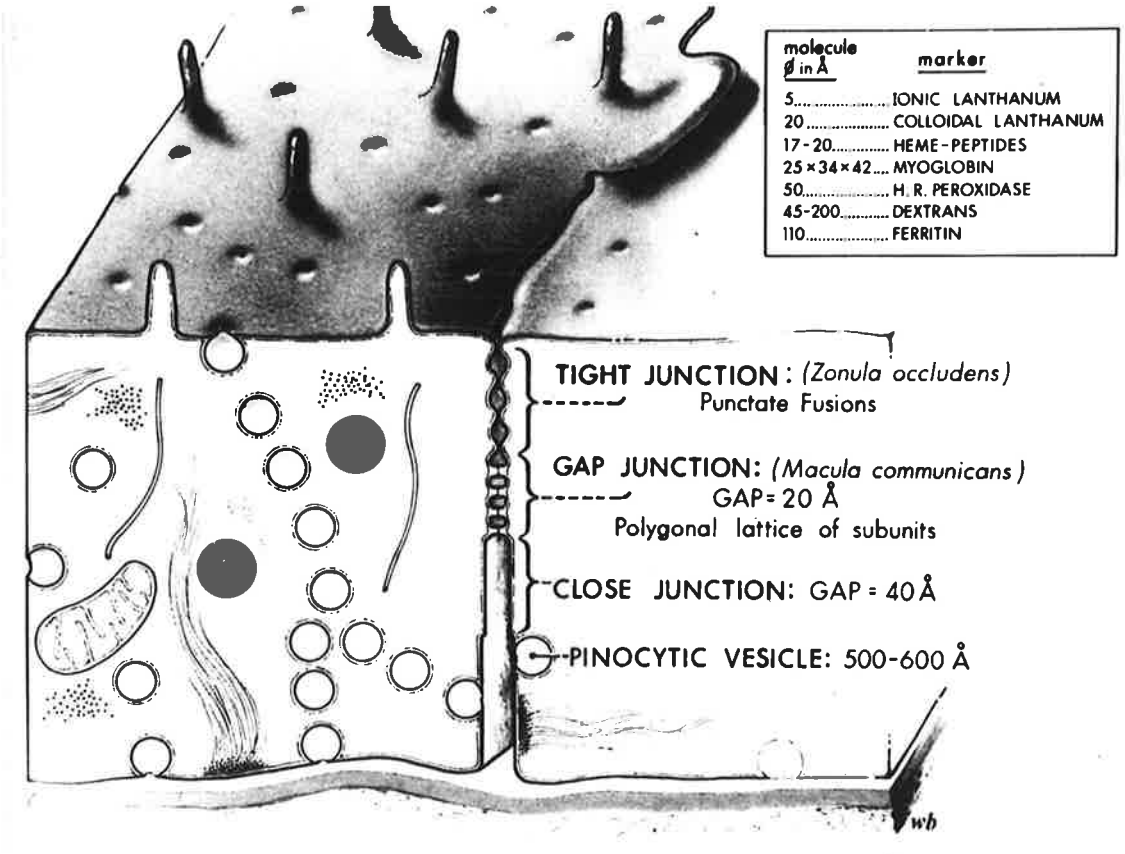

Figure 3.1 General ultrastructural appearance of different endothelial cell junctions. Markers commonly used for testing transendothelial transport in electron microscopy are listed in the box with their molecular diameter (Rhodin, 1984b).

Farquhar and Palade (1963) identified three structural elements of epithelial junctional complexes: (1) a discontinuous zonula adherens; (2) a macula adherens or desmosome at the most distal aspect; (3) a tight junction forming the most apical component. Intercellular junctions that attach endothelial cells to each other consist of two basic forms: occluding (tight) junctions and communicating (gap) junctions (Simionescu and Simionescu, 1984). Using tannic acid perfusion of previously fixed capillaries of mouse diaphragm, Wagner (1988) demonstrated functionally 'tight' regions within the intercellular cleft where the tracer failed to penetrate the clefts, suggesting 'tight' regions are closed routes across the capillary wall.

One of the techniques used to investigate tight junction morphology involves viewing freeze fractured junctions under SEM. Findings from freeze fracture studies demonstrate that tight junctions form an erratic pattern of contact lines between adjacent cells, interrupted by discrete discontinuities in the lines which form a meandering intercellular or extramembranous pathway between the cells (Schneeberger and Karnovsky, 1976). The freeze-fracture technique, however, has limitations, such that junctional tightness cannot be predicted and the fracture plane is through the cellular membranes of the adjacent cells rather than along 'intercellular clefts' (Bundgaard, 1988).
In thin sections, tight junctions or zonula occludens fuse adjacent endothelial cell membranes at punctate appositions which obliterate the intercellular space (Farquhar and Palade, 1963).

Ultrathin (~ 140Å) serial sectioned rat cardiac muscle endothelium demonstrated that these intramembranous strands form a labyrinth of continuous lines of contact between adjacent cells which are circumvented by intercellular clefts following a tortuous pathway from luminal to abluminal aspects (Bundgaard, 1984). Bundgaard (1984) also noted that there were discrete discontinuities or 'pores' (4 nm wide) between the lines of contact of tight junctions (Figure 3.2). It was suggested that water and small hydrophilic molecules diffused through these small 'pores', whereas macromolecules permeate through the intercellular clefts.

Other studies used a tilting stage goniometer to describe tight junction morphology (Ward *et al.*, 1988; Adomson and Michel, 1993). A goniometer enables tilting of a specimen around a single axis (section 4.2.6), which allows examination of areas of apparent fusion between the external laminae of plasma membranes of apposed endothelial cells. Gaps of 5 nm and

2.3 nm between the outer membranes separating tight junctions, have been reported in rat cardiac capillaries (Ward *et al.*, 1988), and in frog mesenteric capillaries (Adomson and Michel, 1993), respectively.

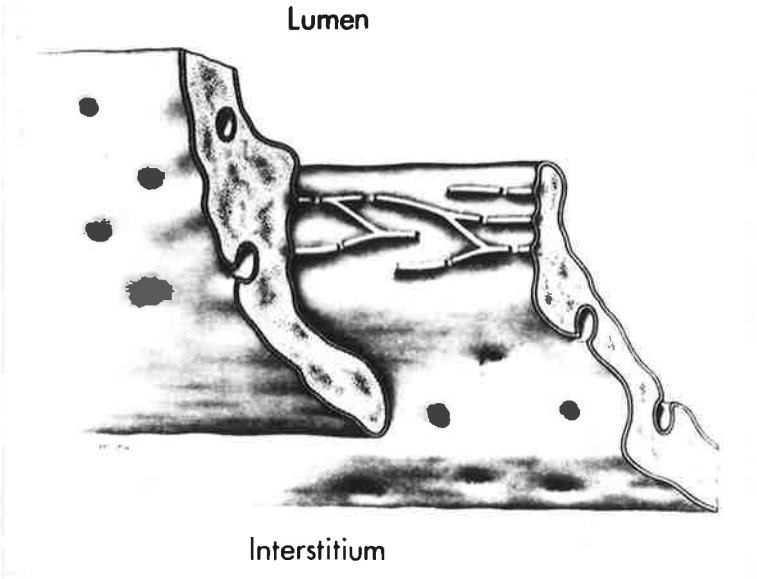

Figure 3.2 Ultrastructural representation of a segment of a capillary wall with the junctional region exposed. An irregular network of lines of contact represent tight junctions circumvented by discontinuities which may allow the passage of hydrophilic solutes (Bundgaard, 1984).

It has been demonstrated that tight junctions found in capillary endothelium form irregular contact lines and grooves between adjacent cells, while those in postcapillary venules (pericytic venules) are loose with discrete discontinuities in the lines (Simionescu *et al.*, 1974; 1975). Simionescu *et al.* (1975) reported an absence of gap junctions in these microvessels which was corroborated by Chintakanon (1990) in the PDL. The number of tight junctions is thought to represent the relative tightness of the junction (Casley-Smith, 1983).

The functions of tight junctions are considered to be as follows:
(1) selective permeability barriers; (2) cell communication via intercellular exchange of ions and small metabolites; and (3) electronic coupling between cells (Simionescu and Simionescu, 1984). Sheridan (1980) has shown interendothelial transfer of dye (Lucifer yellow) can occur via cell-to-cell channels through tight junctions of capillaries and pericytic venules.

In a review of tight junctions, Schneeberger and Lynch (1984) suggested that their resistance can be altered by different physiological requirements or pathological conditions. They concluded modification of tight junctions may have a role in regulating vascular permeability, suggesting possible roles for intracellular second messengers, namely Ca^{++} and cyclic adenosine monophosphate (cAMP), and cytoskeletal elements in the regulatory process. Contractility of the endothelial cytoskeleton (microfilaments, microtubules, and intermediate filaments) functions in endothelial integrity and repair (Gottlieb, 1991). The cytoskeleton may regulate tight junction function, structure and formation via modulation of the movement of protein (Schneeberger and Lynch, 1984).

The close junctions (width ≈ 6 nm) referred to by Casley-Smith (1983), may correspond to the small pores (40 to 50 Å) described by Pappenheimer (1953). These junctions are believed to circumvent tight junction contact lines via discrete discontinuities in the lines of fusion, forming a meandering pathway for the exchange of water, ions and small hydrophilic solutes between plasma and interstitial fluid compartments (Bundgaard, 1988). Casley-Smith (1983) described junctions greater than 30 nm as 'open' junctions which may be seen in injured blood vessels, mostly in the postcapillary venules. Infrequently, open junctions are also found in normal continuous capillaries.

3.4.2 Periodontal Ligament Endothelial Junctions

Studies on endothelial junctions for various other microvascular beds have been extensively reviewed by Simionescu and Simionescu (1984), for example, rat omentum and mesentery, rat diaphragm, rat choroid plexus, lung and brain. The following section will cover PDL endothelial junctions only. In a TEM study of the microvascular bed of the rat PDL based on systematically selected thin sections of tissue, three types of junction were found (Chintakanon, 1990); close junctions (80%), tight junctions (16%) and open junctions (4%). Gap junctions were not seen. Incident to an extrusive load, close junction widths increased in the same animals. Chintakanon (1990) suggested that close junctions are one of the main exchange pathways in the PDL microvasculature, since they comprise the majority of junctions in the vascular bed. It was concluded that the vascular endothelial junctions of the PDL are 'leaky', indicating high permeability (Chintakanon and Sims, 1994).

A number of studies using ionic tracers as markers have shown evidence for endothelial junctions acting as an exchange pathway (Karnovsky, 1967; Cooper *et al.*, 1990; Tang and Sims, 1992; Tang *et al.*, 1993). Using TEM, Cooper *et al.* (1990) demonstrated a 50% increase in the mean number of apical tissue channels/μm^2 (MNTC/μm^2) at 0.2 μm from the rat PDL vascular endothelium following application of an extrusive force. It was suggested that arterial capillaries, venous capillaries and postcapillary venules are important in fluid exchange because following extrusive loads an increase in the tissue channel density was found near these vessels. Tang and Sims (1992) similarly reported a significant increase from 0.10 ± 0.01 to $0.28 \pm 0.01/\mu m^2$ in the mean number of rat PDL tissue channels adjacent to blood vessels following the application of a tensile force. The mean number of tissue channels decreased from the cervical to the apical regions of the PDL. The decrease in the mean number of tissue channels was associated with arterial capillaries, venous capillaries and PCV.

Using TEM analysis, a significant (42%) increase in the mean number of junctions/μm of endothelial perimeter for all vessel types in the full width of rat PDL under tension was demonstrated by Tang *et al.* (1993). Three factors were reported to explain the increase in junctions during a 30-min tension load, namely: (1) the proportion of vessel types change in the tensioned PDL as an inflammatory response (venous and arterial capillary numbers increased with applied tension), and these vessels were associated with more junctions explaining the increase in mean number of junctions/μm; (2) as the luminal diameter of vessels decreased (because of possible stretching and recoil in the endothelial cells) the junction number may not have increased, however, if expressed as a ratio of the vessel perimeter, then the mean number of junctions/μm changes; (3) the results may be influenced by previously closed vessels opening up to give a maximum functional vascular bed. The reported change in the proportion of vessels types within the PDL during a 30-min extrusive load (Tang *et al.*, 1993) may be due to altered vessel geometry placing the vessels into a different catagory.

A significantly positive relationship was reported by Tang *et al.* (1993) when the number of junctions/μm and the MNTC/μm^2 were correlated. Junction types (tight, close, open junctions) were not classified by Tang *et al.* (1993), but were considered as a unit because a goniometer was not available to tilt the specimens. The mean number of junctions/μm for venous capillaries in the middle third and PCV in the tooth-third of the control PDL was $0.017 \pm$

0.04/μm and 0.21 ± 0.04/μm respectively. With extrusion, there was a significant increase in the mean number of junctions/μm for venous capillaries in the middle third to 0.25 ± 0.04/μm and for PCV in the tooth-third to 0.42 ± 0.05/μm.

3.5 The Role of Endothelial Junctions in Capillary and Postcapillary Permeability

Blood plasma and interstitial fluid form the extracellular component of the body's fluid compartment. As blood passes through the microvasculature, oxygen, nutrients, wastes and other metabolic products exchange between plasma and interstitial fluid. The endothelial cell wall is impermeable enough to prohibit loss of some cells and proteins of the blood, but permeable enough for nutrient exchange to occur. Except for protein, solute concentrations between plasma and interstitial fluid are essentially homogenous because of these exchanges. Permeability, or exchange pathways across endothelium, is a physiological phenomenon that occurs via physical and chemical changes in the cells involved. Many pathways have been described (Figure 3.3) for passage of different nutrients and metabolic wastes which may vary between different locations and conditions (Majno, 1965; Renkin, 1977; Casley-Smith, 1983; Simionescu and Simionescu, 1984). Simionescu and Simionescu, (1984) distinguish two hydrophilic (fluid-filled) pathways - transmembranous and extramembranous pathways:

1) Directly across the cell (transmembranous): Water, gases, ions and small hydrophilic molecules are freely and passively exchanged by convection and diffusion via both transmembranous and extramembranous routes. The lipid bilayer of the endothelial cell plasmalemma may permit rapid exchange of lipophilic molecules.

2) Extramembranous pathways defined include:
   - transcellular (vesicles, channels, fenestrae, and diaphragms)
   - intercellular (endothelial junctions) which are well organised and dynamic structures.

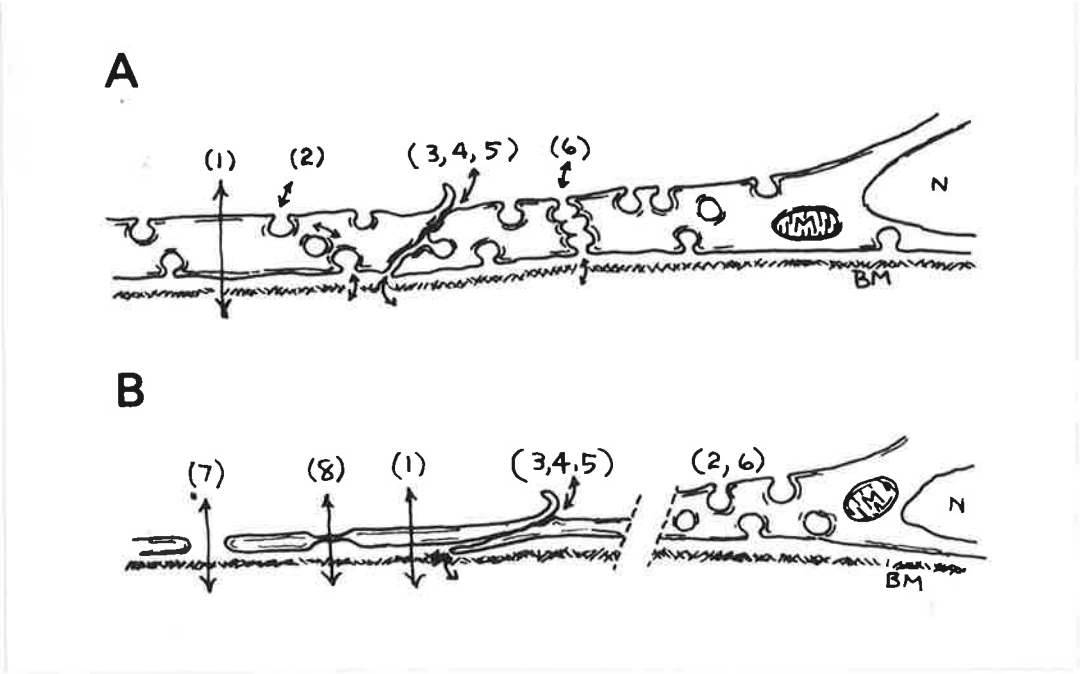

Figure 3.3 Representation of capillary endothelium transport pathways (Renkin, 1977). A, continuous capillaries; B, fenestrated capillaries; (1) direct cellular, (2) vesicular, (3) lateral diffusion, (4) narrow 'small pore' junctions, (5) wide 'leaking' junctions, (6) transitory open channels, (7) open fenestrae, (8) closed fenestrae.

Ultrastructural and physiological studies support an extramembranous route for small solute exchange via clefts, fenestrae and open cell junctions in inflammation (Bundgaard, 1984; Crone and Levitt, 1984; Michel, 1988; Clough, 1991). However, the permeation of macromolecules (diameter greater than 5 nm) are limited by this route (Clough, 1991). It has been suggested that the endothelial cell coat, believed to consist of glycoproteins secreted and regulated by endothelial cells, may restrict macromolecular movement (Michel, 1988; Weinbaum *et al.*, 1992). Bundgaard (1988) defined the exchange of hydrophilic solutes via junctional dimensions (Figure 3.4). These relationships are supported by Clough and Michel (1988), who demonstrated an inverse relation between the length of the intercellular clefts from the luminal to the abluminal side and the permeability of individual frog mesenteric capillaries.

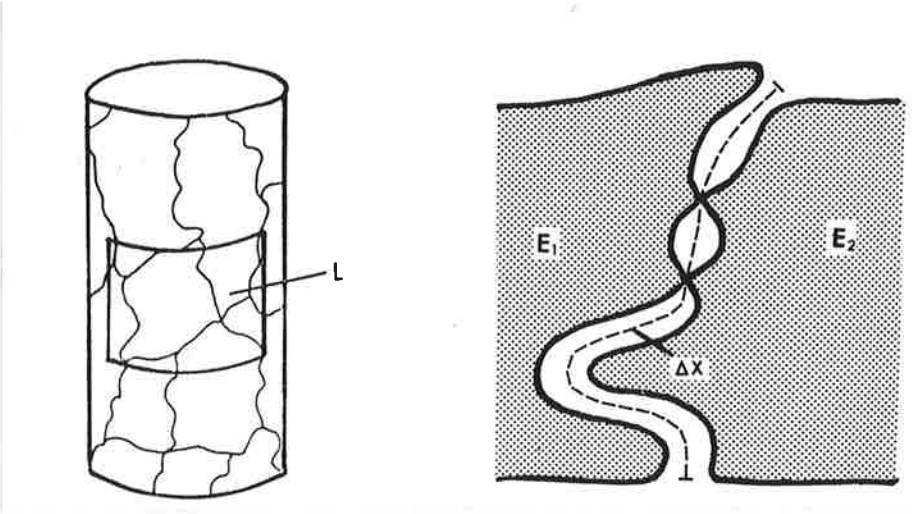

Figure 3.4: Representation of the dimensions of interendothelial junctions of the capillary wall which define the exchange of small hydrophilic solutes by the equation: $P = D \times (L \times W/\Delta X)$. P, permeability; D, diffusion coefficient of the solute; L, average length of the clefts per unit area capillary wall; W, average effective width of the clefts; ΔX, length of the diffusion pathway measured from the luminal to the abluminal side (Bundgaard, 1988).

Capillary and postcapillary venule intercellular clefts are characterised by tight junctions and close junctions (up to 6 nm wide). However, variable proportions of these junctional zones exist dependent on the location of the microvessel within the vascular tree (Simionescu and Simionescu, 1984).

The permeability of the basement membrane surrounding microvessels may be an important factor in transport rates through the less restrictive endothelial pathways, for example, open fenestrae (Renkin, 1977). A fine layer of fibrillar material forms the basement membrane which functions to (1) support endothelial cells, (2) anchor blood vessels to surrounding tissue, and (3) filter the passage of water and small solutes, but retards larger molecules, for example, large tracers carbon ≈ 250 to 300 Å and ferritin ≈ 100 Å (Majno, 1965; Casley-Smith, 1983).

The functional significance of the basement membrane is reflected in its structure. The lack of basal lamina around lymphatic capillaries is considered

to be important for the movement of interstitial macromolecules into lymph vessels (O'Morchoe and O'Morchoe, 1987). Where basal lamina are prominent, e.g., renal glomerular capillaries, they are known to prevent extravasation of plasma proteins.

Quantitative measurements of vascular permeability show variation in permeability between microvessels in the same vascular bed and from vascular bed to vascular bed (Michel, 1988). Clough (1991) argues that differences in the capacity of exchange pathways of different vascular beds accounts for variations in water and small hydrophilic solute permeability but these pathways retard macromolecules similarly. An increase or a decrease in permeability, therefore, may occur via respective changes in the area of the porous segments of the vessel wall, that is, by changes in the number of junctions per unit area of wall (Clough, 1991).

3.5.1 Theoretical Models of Capillary Permeability

Theoretical models have been developed to explain capillary permeability based on experimental studies. Previously accepted models of transendothelial pathways for the passage of solutes are based on cylindrical pore theory or the fibre-matrix theory (Michel, 1988; Clough 1991; Skalak, 1988). A new three dimensional junction-pore-matrix model has been proposed which overcomes the deficiencies of the two previous models (Weinbaum *et al.*, 1992). A brief discussion of these models will follow.

3.5.1.1 Cylindrical Pore Theory

The cylindrical pore model describes a system of two pore sizes within the junctional cleft that are 17 to 22 nm wide. They consist of one or more small pores (5 to 6 nm) and a few sporadic larger pores (10 nm) occurring after cell death and during cell replacement (Weinbaum *et al.*, 1985).

This model (Figure 3.5) has also been called the constricted channel model (Weinbaum *et al.*, 1992) and as previously noted (section 3.4.1), termed a close junction by Casley-Smith (1983), as shown in Figure 3.6, and a small pore by Pappenheimer (1953). Bennett *et al.* (1959) questioned the validity of the applicability of the capillary pore model (Pappenheimer, 1953) to capillaries in general, based on finding different population densities of 'pores' of type A-1 capillaries in muscle and connective tissue in eels.

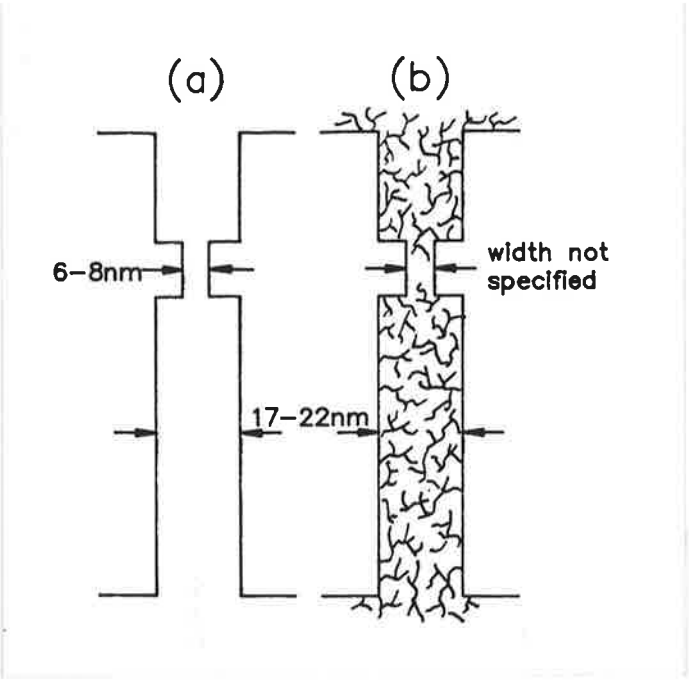

Figure 3.5 Two-dimensional representations of capillary intercellular pathway, (a) constricted channel model, and (b) fiber matrix model (Weinbaum *et al.*, 1992).

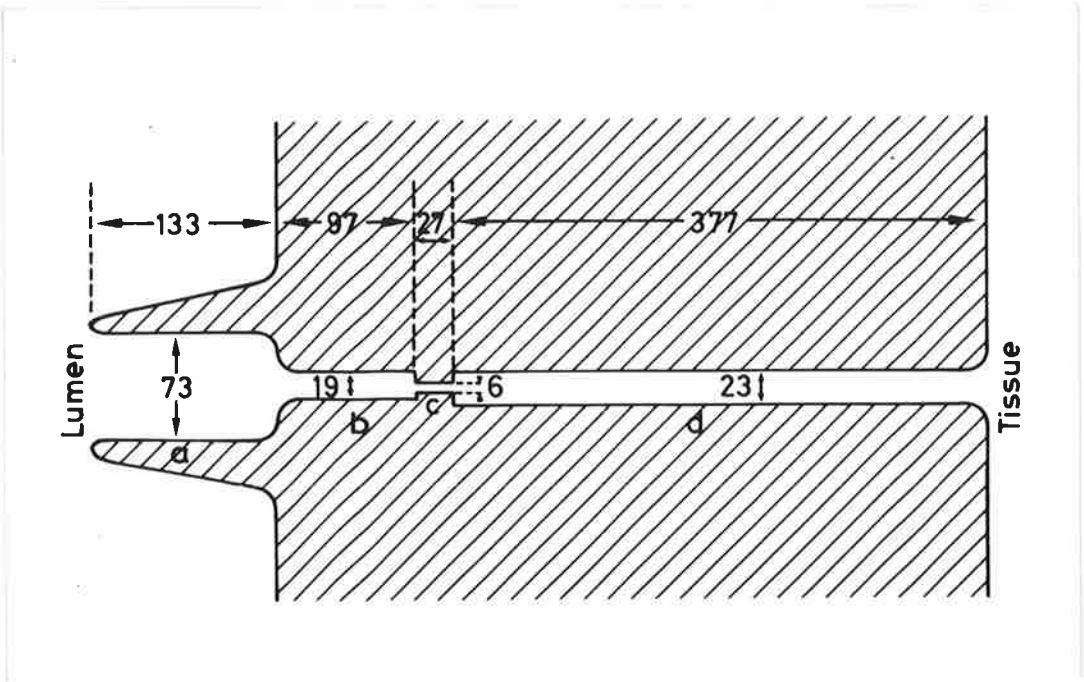

Figure 3.6 Two-dimensional representation of a capillary close junction; dimensions in nm (cited in Casley-Smith, 1983).

Electron microscope tracer studies have shown the small pores to be permeable to horseradish peroxidase, 50 Å in diameter (Karnovsky, 1967), and microperoxidase, 20 Å in diameter (Wissig, 1979).

The cylindrical pore model proposes that the small pores or discontinuities are related to the exchange of small solutes and the larger pores are associated with the permeation of macromolecules (section 3.4.1). Experimental data on filtration measured macroscopically supports the cylindrical pore theory (Michel, 1988). However, the data has not been predictive for coefficients of permeability values similar to those measured *in vivo* (Clough, 1991).

It has been demonstrated that the majority of endothelial cell vesicles previously believed to transport macromolecules via pinocytosis are attached to cell walls (Bundgaard and Frøkjær-Jensen, 1982). The concept of vesicular transport, therefore, has become less important. Filtration through the endothelial cell junctions appeared to be the more likely location of the molecular sieve (Skalak, 1988; Michel, 1988).

3.5.1.2 Fibre-Matrix Theory

The fibre matrix model proposes that the endothelial cell coat, consisting of glycoproteins with an approximate 0.6 nm radius, functions as a molecular sieve which restricts macromolecular movement. Small solute permeability is regulated by small pores or discontinuities in the junctional strand (Clough, 1991; Weinbaum *et al.*, 1992). Tsay *et al.* (1989) described a model which proposed that the small pores form short discrete holes in the junctional strands the size of individual missing proteins. Adamson (1990) recently presented experimental evidence to support this concept, whereby removal of the endothelial cell coat in frog mesenteric capillaries with enzymes resulted in decreased hydraulic resistance by approximately 50%.

3.5.1.3 Three-Dimensional Junction-Pore-Matrix Model

More recently, a more comprehensive three-dimensional model for capillary permeability has been proposed (Weinbaum *et al.*, 1992). This model incorporates aspects of these two previous models with a three-dimensional concept resulting in a junction-pore-matrix model (Figure 3.7). This model attempts to predict hydraulic conductivity and diffusive permeability of capillary endothelium. Clefts with a fibre matrix form its wider parts.

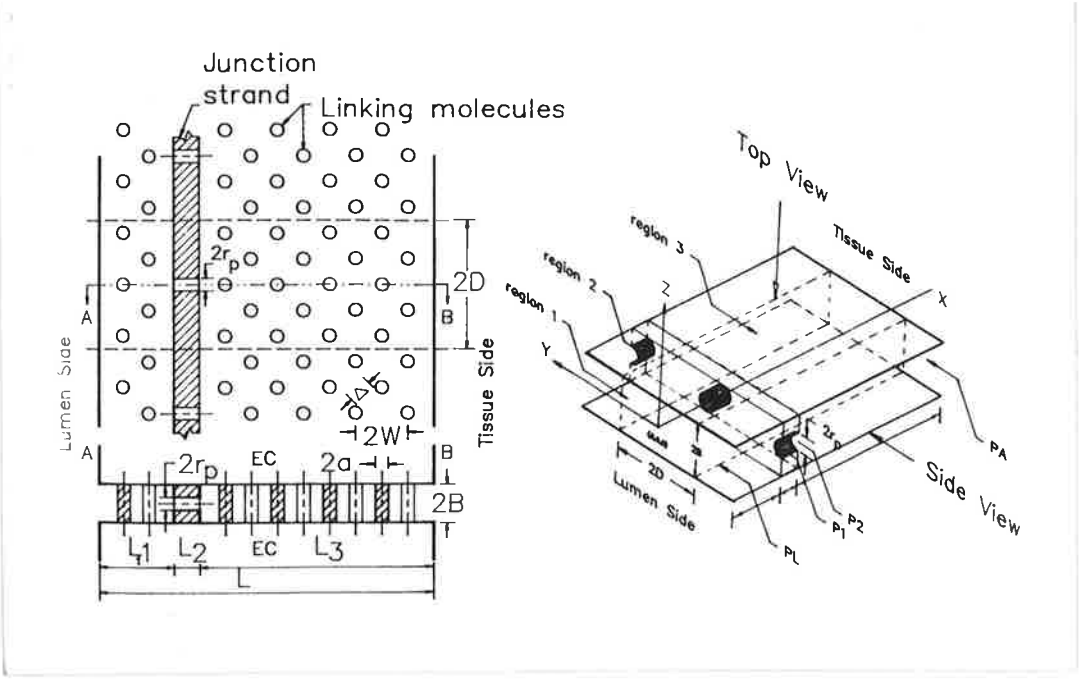

Figure 3.7 Representation of the three-dimensional junction-pore-matrix model of the intercellular cleft (Weinbaum *et al.*, 1992).

As previously noted (section 3.4.1), tight junctions are organised into irregular networks of contact lines between adjacent cells with discrete discontinuities or 'pores' in the lines (Bundgaard, 1988). Phillips *et al.* (1994) proposed a mathematical model, for steady flow through the short discontinuities between tight junction regions. This model predicts that adjacent tight junction regions can either overlap, or are aligned, or are out of alignment with each other.

3.5.2 Endothelial Junction Structure-Function Correlations

Endothelial cells and cell-to-cell junctions are dynamic structures important for regulating vascular permeability, leukocyte extravasation and vascular remodeling (Lampugnani *et al.*, 1993). Recent studies have identified transmembrane adhesive molecules linked to a network of intracellular cytoskeletal proteins (Table 3.4) which form interendothelial junctions (Rubin, 1992; Anderson *et al.*, 1993; Lampugnani *et al.*, 1993). Lampugnani *et al.* (1993) described three different types of endothelial adhesive molecules that are not found in other epithelia: integrins, cadherins and immunoglobulins, for example, platelet endothelial adhesion molecule 1 (PECAM-1). Possible functions for endothelial cell adhesion molecules include: intercellular junction formation and protein-protein interactions involved in signal transduction cascades regulating paracellular permeability.

Table 3.4 Components of interendothelial junctions (Anderson *et al.*, 1993; Lampugnani *et al.*, 1993)

Type of junction	Transmembrane protein	Cytoskeletal protein
Gap junctions	Connexins	Undefined
Close (Adherence) junctions	Cadherins	Catenins, vinculin plakogloblin, a-actinin, zyxin, actin
Tight junctions	Undefined	ZO-1, ZO-2, cingulin

Balda and Anderson (1993) demonstrated two different peripheral membrane proteins ZO-1α^- and ZO-1α^+, defining two classes of tight junction. The distribution of ZO-1 isoforms was demonstrated by RNase protection analysis, immunolocalisation and immunoblotting in normal rat tissues exhibiting cell type specific expression. The authors demonstrated that endothelial junctions, which express the smaller isoform (ZO-1α^-), are more plastic, that is, capable of opening and closing and moving on the plasma membrane. Anderson *et al.* (1993) suggest that cingulin and ZO-2 may be more specific tight junction markers than ZO-1.

Junction number and type differs at different sites of the vascular tree. Tight (occluding) junctions and interjacent gap (communicating) junctions are found in the endothelium of large arteries and arterioles (Simionescu and Simionescu, 1984). Tight junctions impart a low degree of permeability to the endothelium by sealing off the intercellular spaces, whereas gap junctions maintain direct cell-to-cell communication. Postcapillary venules have a loosely arranged junctional system according greater permeability with no gap junctions (Simionescu and Simionescu, 1991). In fenestrated capillaries, a correlation between fenestrae number per unit area of endothelium and permeability has been demonstrated (Levick and Smaje, 1987). Fenestrae have been reported to parallel intercellular clefts as exchange pathways (Clough, 1991).

Tight junctions are complex structures which do not maintain a static configuration. They are able to disorganise and reorganise rapidly to allow exchange of plasma proteins and cells (Anderson *et al.*, 1993). The regulatory mechanisms that open and close endothelial junctions remain undefined. Inflammatory mediators, for example, histamine, increase

permeability resulting in tissue oedema due to a transient formation of endothelial gaps (Wu and Baldwin, 1992). This process may be regulated by mediators binding to specific endothelial membrane receptors generating intracellular signals via second messengers causing cytoskeleton contraction, reorganisation of transmembrane proteins and interendothelial gap opening (Lampugnani *et al.*, 1993). A similar process may occur during leukocyte extravasation, where leukocyte binding to endothelial receptors may stimulate junction opening.

As previously noted (section 3.5), endothelial cell wall permeability correlates with the structure of intercellular cleft dimensions and tight junction organisation, such that alterations in permeability are in direct proportion to variations in their dimensions (Bundgaard, 1988). It was noted that the parameters related to permeability include the length of the cleft per unit area, the width of the cleft, and the depth of the cleft defined as the luminal to abluminal length along the convoluted cleft. This latter dimension is referred to as the diffusion pathway. Investigation of these junction dimensions is necessary (Bundgaard, 1988), to further characterise the relationship between these dimensions and associated changes in permeability.

3.6 Clinical Aspects and the PDL Microvasculature

3.6.1 The Role of the Periodontal Ligament Microvasculature in Function

The PDL is not a static tissue. It has the capacity to remodel, which is a prerequisite for physiologic tooth migration and orthodontic tooth movement. The PDL properties of tensile strength, hydrodynamic damping, viscoelasticity (Picton and Wills, 1978), and remodeling (Schroeder, 1991), are related to the function of the PDL which are as follows (section 3.3): tooth support, proprioception, nutrition, homeostasis, and regeneration. The PDL vasculature plays a role in the mechanism of tooth support for these various PDL functions (Berkovitz, 1990a). The role of the PDL vasculature will be discussed in relation to the following areas: orthodontic tooth movement, tooth eruption and periodontal disease.

3.6.1.1 Microvasculature and Orthodontic Tooth Movement

Orthodontic tooth movement is a result of cellular response to applied mechanical stress to teeth. The PDL vasculature is an essential element in the biology of tooth movement and is the source of nutrients for cells. A light

microscopy and TEM investigation of vascular permeability under load using the hamster cheek pouch as a model demonstrated that with light forces, vascular permeability was increased throughout application and following removal of the load (Iida *et al.*, 1992). This result contrasted with the findings following application of a heavy load, where there was no increase in vascular permeability during application of the force, but following removal of the load, there was marked increase in permeability which was succeeded by stasis. This study provides experimental evidence that vascular permeability is an important factor in the microvascular response to the application of light and heavy loads (Iida *et al.*, 1992).

It is a theorem that orthodontic treatment time in general takes longer in adults than a similar treatment in children. Norton (1988) suggested that vascularity and blood flow decreases with increasing age which may explain the reduced number of progenitor cells in the aging patient. Other studies have shown a reduction of the PDL and alveolar bone cell populations in association with decreased vascularity (Reitan, 1954; Grant and Bernick, 1972). Reduction in numbers of progenitor cells may contribute to the reported delayed healing in aged tissues. However, the reported decreased vascularity in aged PDL may not be applicable to mouse PDL (section 3.6.2; Sims, 1992b).

Bridges *et al.* (1988) demonstrated a greater amount and rate of tooth movement for young (21 to 28 days old) rats compared with adult (90 to 100 days old) rats in response to a 60 gm tipping force. The difference was related to a reduction (except for the late tooth movement phase) in tissue mineral density in the young rats reflecting alveolar bone that was more easily remodeled. Takano-Yamamoto *et al.* (1992) investigated the rate of tooth movement in combination with mechanical force (20 gm) and the local use of 1,25-dihydroxycholecalciferol ($1,25(OH)_2D_3$; a bone resorbing agent) in young (49 days old) and mature (196 days old) rats. It was demonstrated that for the control young and mature rats, the total tooth movement after 20 days was 1.2 mm and 0.5 mm, respectively. Following injection of $1,25(OH)_2D_3$, the rate of tooth movement increased in the old rats to a level approximately equal to the rate in the young rats which was also increased.

Alveolar bone fragments from 120 male patients between 7 and 25 years of age were collected during extraction of mandibular first premolars as part of orthodontic treatment (Stutzmann and Petrovic, 1989). In this study, the

subjects were divided into four groups according to age: 7 to 8, 11 to 13, 16 to 17, and 20 to 25 years of age. Bone fragments were placed in organ culture for 72 hours. Bone metabolism was assessed from alkaline phenylphosphatase activity, uptake of ^{45}Ca and ß-glucuronidase, and acid phenylphosphatase activities (Stutzmann and Petrovic, 1989). These authors demonstrated that an increase in alveolar bone turnover rate occurred after three weeks of orthodontic treatment in young adult males by comparison with only 10 days for the group of growing boys. The results of this study indicated that the clinical effectiveness of fixed orthodontic treatment correlated with an increase in alveolar bone turnover rate.

Consideration of the findings from the previous studies demonstrating alterations in bone turnover in young and older groups suggests that a reduction in permeability of aged PDL may result in altered bone turnover as a result of reduced supply of nutrients and/or impaired removal of waste products (Stutzmann and Petrovic, 1989) and factors related to bone metabolism, for example, $1,25(OH)_2D_3$ (Takano-Yamamoto *et al.,* 1992). However, there are many other control factors for bone modeling and remodeling (Roberts, 1994), for example, mechanical loading, other bone metabolic hormones (parathyroid hormone and calcitonin), growth hormones (for example, epidermal growth factor), local factors or cytokines released during inflammation (for example, prostanoids, interlukin-1), and sex steroids (testosterone and estrogen).

3.6.1.2 Microvasculature and Tooth Eruption

The PDL vasculature has been implicated in generating an eruptive force through intra-vessel blood pressure or by periodontal tissue (hydrostatic) pressure being transmitted through the interstitial fluid (Burn-Murdoch, 1988; Moxham, 1988). An increased endothelial permeability to plasma proteins during molar tooth eruption has been reported (Magnusson, 1968; cited in Burn-Murdoch, 1990). Radiolabelled ^{131}I-fibrinogen has been shown to localise extravascularly in periapical regions of erupting rat incisor teeth (Magnusson, 1973). Magnusson (1973) postulated that a change in vascular permeability caused the observed effusions from blood vessels in the PDL of the erupting rat incisor. Changes in the permeability of the microvasculature of the PDL with resultant uptake of fluid into interstitial tissues may alter the eruptive force involved in continued eruption to maintain occlusal contact. Magnusson's (1973) findings were based on a continuously erupting incisor model, however, and may not be applicable to molar eruption associated with

wear. Burn-Murdoch (1990) concluded that although raised interstitial pressure producing tooth eruption can be demonstrated, it is difficult to determine if changes in capillary permeability are the primary cause of tooth eruption or are secondary to it.

3.6.1.3 Microvasculature and Periodontal Health and Disease

The reported age changes in the periodontium microvasculature (section 3.6) and the reported alterations in permeability of microvasculature of other tissues (section 3.1) may contribute to slower wound healing of the periodontium than has been found to occur with age (van der Velden, 1984; Haugen, 1992). The incidence of periodontal disease and loss of periodontal support increases with age (Grant and Bernick, 1970; van der Velden, 1984; Haugen, 1992). It is suggested that decreased permeability that occurs with ageing, with concomitant reduced removal of waste products, may impact on the host response to the causative factors responsible for periodontal disease and in the maintenance of periodontal support. However, it has been reported that poor oral hygiene was the major predictor of periodontitis and the effect of age on disease progression was considered to be negligible with good oral hygiene (Holm-Pedersen *et al.*, 1975; Abdellatif and Burt, 1987). Other studies support the view that for the majority of the population, severe periodontitis is not a natural consequence of ageing (Loe *et al.*, 1986; Burt, 1994).

3.6.2 Ageing and the Periodontal Microvasculature

Bernick (1962) found that the blood supply to the molar teeth of rats changed in the vascular distribution with age and this alteration, outlined below, was correlated with changes in the rate of apposition of dentine, acellular cementum, and cellular cementum. Vessels supplying the PDL in the young rats (one month old) coursed gingivally parallel to the alveolar bone with no vessels observed on the cemental side. In the older animals (18 months old), there was an association between cellular cementum formation in the apical third of the root and the presence of capillary terminals in or adjacent to the layer of cellular cementum. It was noted that interseptal vessels and their perforating branches progressively decreased. Vascular branches arising from the main periodontal vascular trunk were observed entering areas where cemental resorption was repaired with a "bone like material". These changes were thought to help to maintain functional occlusion with ageing (Bernick, 1962).

Sims *et al.* (1992a) found no arteriosclerotic changes with ageing in the microvascular bed of mouse molar PDL. This study supported the conclusions of an earlier histological study by Severson *et al.* (1978) of eighty periodontal ligaments from twenty four human cadavers ranging in age from 20 to 90 years. It was found that vascularised spaces appeared larger in the older specimens, and these spaces encroached upon areas formerly occupied by periodontal fibres and bone. These studies did not confirm previous findings of arteriosclerotic changes in periodontal vessels of ageing humans (Bernick, 1967; Grant and Bernick, 1970), notably vessel wall thickening and a reduction in the lumen diameter. The changes reported by Severson *et al.* (1978) may have been associated with a larger number of blood vessels within the PDL.

Ageing changes in mouse blood vessel luminal volumes were stereologically assessed by Sims *et al.* (1992a; 1992b; 1993) using TEM. Blood vessel distribution was described as (1) a percentage of the PDL volume, (2) a percentage of the microvascular bed (MVB), and (3) a percentage of tooth, middle and bone circumferential thirds of the PDL. Mean wall thickness of the grouped vessels in young and old mice was 2.78 μm and 1.69 μm respectively. The sample size, however, was small and animal variability was high, but was statistically significant. No significant change occurred in the luminal volume of arterial capillaries between young and old mice (Sims *et al.*, 1992b). Luminal volume of collecting venules (CV) and grouped arteriovenous anastomoses and terminal arterioles (AVA, TA), as a per cent of MVB volume, increased from 31% in young mice to 52% in old mice. The increased AVA and TA luminal volumes shunt blood flow to the increased CV volume, bypassing the capillary bed. These findings suggest that the aged mouse PDL microvascular bed remodels mainly in the AVA, TA and CV segments. The PDL area for the total number of capillaries decreased by 31.5 % (from 2117 μm^2 to 1451 μm^2), and the average thickness of the PDL sheet served by a capillary decreased by 47.6% (from 52.5 μm to 27.5 μm) for young and old animals, respectively. It was suggested that these changes demonstrated in aged mice represent reduced diffusion distances which may balance any decrease in vascular efficiency associated with more blood shunting from AVA, TA to CV in aged mice.

Sims *et al.* (1992a) reported significant regional shifts in microvascular bed architecture, notably a total vascular volume increase of ≈ 1.15 fold, that is,

from 8.5% (SE 1.37%) to 9.8% (SE 1.1%). This study questions the view that blood supply reduces with ageing (Bradley, 1972).

These changes in aged PDL are related to the maintenance of homeostasis, with adequate supply of nutrients and removal of waste products. Alteration of endothelial junction dimensions and the number of tight regions in capillaries and PCV with concomitant changes in permeability may be associated with the previous findings of decreased diffusion distances (Sims *et al.*, 1993). Investigation of the morphology of endothelial junctions of the aged PDL is needed to provide a more complete picture of the various factors involved in the determination of diffusion pathways and vascular efficiency.

CHAPTER 4 MATERIALS AND METHODS

4.1 Laboratory Procedure, Tissue and Section Preparation

The tissue samples, processing and preparation for TEM used in the present investigation were those prepared by Freezer, (1984) and Sims *et al.* (1992a; 1992b). In summary, eight male ALCA-strain mice were housed in constant temperature, humidity and lighting until they reached the required ages of 35-day-old and 365-day-old. Four mice in each group was the final number after losses due to cannibalism, anaesthesia death, incorrect angle of cut through the molars, and lack of matching pairs. During this time, the mice were fed and watered *ad libitum*, with M and V mouse cubes (Charlicks Trading Co., Port Adelaide, SA) and distilled water.

Anaesthesia was produced with intraperitoneal injection of Urethane (30%) in normal saline, at a dose of 30 mg/10 g body weight, using a 1.0 ml disposable hyperdemic syringe with a 26.5 gauge needle. When a response was not obtained by squeezing the foot pad, anaesthesia was deemed surgically adequate. Prior to perfusion of the mice, heparinised saline was injected with a microlitre syringe into the ventral tail vein at a dose of 2 IU/10 g body weight.

Primary fixation was achieved by pulsatile intracardiac perfusion for a minimum of five minutes with 5.6% glutaraldehyde and 0.9% osmium tetroxide in 0.06M cacodylate buffer (pH 7.4). Following perfusion and decapitation, the mandibles were dissected out and sectioned in the midline into right and left halves. The mandibles were kept moist in 0.06M cacodylate buffer and then placed into labelled histokinette baskets. Demineralisation was completed by immersion of the labelled baskets in a glass beaker containing 0.1M EDTA in 2.5% glutaraldehyde in 0.06 M cacodylate buffer (pH 6) at 4˚C, with constant agitation and daily changes of the solution.

Decalcification was confirmed radiographically and by probing the tissues with a fine needle, after which the mandibles were embedded in Xantopren heavy bodied impression material contained in wax moulds. Under a stereomicroscope, the right and left halves of the mandibles were sectioned mid-sagittally and the mesial root PDL isolated into tissue blocks with a single

Continuous bathing of the tissue with 0.06M cacodylate buffer was required to avoid dehydration. Tissue segments were then placed in metal capped 2 ml soda vials half filled with 0.06M cacodylate buffer. Under a stereomicroscopic, tissue blocks were removed from their vials and oriented into silicone rubber moulds, embedded in LX-112 resin (Ladd Research Industries, Inc., Burlington, USA) and cured in an incubator for two days at 37˚C and 60˚C.

Tissue blocks from the mid-sagittal plane of the right and left mesial root PDL of the mandibular first molars were selected. These blocks were mounted on a Reichert-Jung Om-U4 ultramicrotome and trimmed to a trapezoidal mesa (Figure 4.1). A glass knife prepared using an LKB Type 780 1B knifemaker was aligned in the knife holder and used to cut one micron sections. The PDL was sampled at 160 µm intervals providing 7 to 9 levels from the alveolar crest to the root apex. At each level, 1 µm sections were assessed with routine toluidine blue staining to check orientation and aid mesa trimming. Grids were stained with 0.5% uranyl acetate for 8 minutes at 37˚C and modified Reynolds' lead citrate for 4 minutes, followed by drying (Appendix 3). Thorough washing of the grids in double distilled water occurred between each staining step.

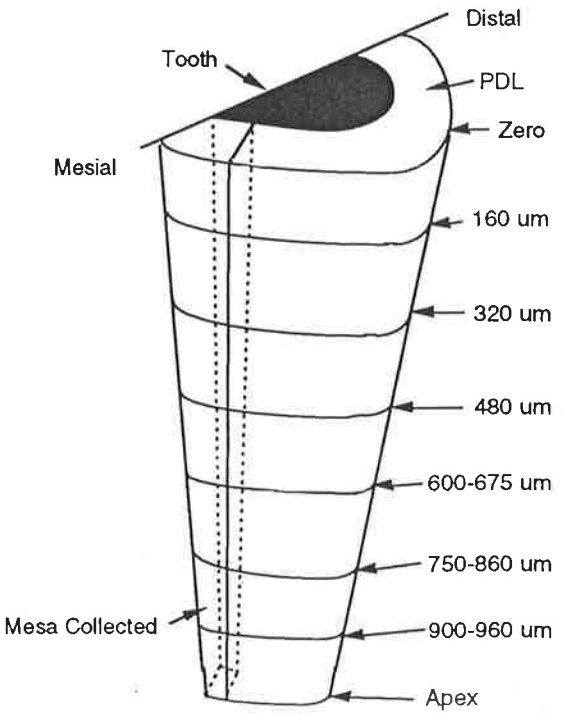

Figure 4.1 Diagram representing the outline of the trapezoidal mesa of tissue collected along the mesial root length from alveolar crest to the apex.

4.2 Transmission Electron Microscopy

Initially, sections were checked and oriented in a JEOL 100-S TEM at 80 kV and then carbon coated in a Dentron vacuum evaporator using ultra-'F' purity carbon rods. The JEOL 100-S TEM was also used for a pilot survey to determine an adequate sample of blood vessels for inclusion in the study (Section 4.2.3). Final specimen assessment was completed with a JEOL 2000FX at 120 kV at The University of Adelaide Centre for Electron Microscopy and Microstructure Analysis (CEMMSA) and a Phillips CM-10 at 80 kV at Flinders Medical Centre, in conjunction with a manual tilt goniometer (section 4.2.6). The use of the JEOL 2000FX was lost due to flooding of CEMMSA, and as a result, the Phillips CM-10 was used as a replacement.

4.2.1 Blood Vessel Classification

Blood vessel classification was based on:

1) Luminal diameter: the mean luminal diameters of the blood vessels were measured with digital calipers.
2) Structure of the blood vessel walls.

The criteria suggested by Rhodin (1967, 1968), Clark (1986), and Freezer (1984) were used, namely:

1) Arteriovenous anastomoses: luminal diameter of 12 to 15 μm; relatively thick-walled vessels; endothelium surrounded by a sphincter-like media; myelinated and unmyelinated nerves present in the adventitia.
2) Terminal arterioles: luminal diameter of 10 to 30 μm (Clark, 1986) with one or two layers of smooth muscle cells surrounding the endothelium.
3) Arterial capillaries: luminal diameter of five to 10 μm with endothelial cell nuclei bulging luminally; numerous microvilli projecting into the lumen from the encircling one to two endothelial cells; occasional single fenestrae.
4) Venous continuous capillaries: pericytic or apericytic such that the pericytes enclosure of the endothelium may be partial, complete, or absent (Freezer, 1984). Sims (1983) proposed the term 'apericytic' for venules without a complete layer of pericytes or veil cells; luminal diameter of 4 to 7 μm (Rhodin, 1968; Freezer, 1984); morphologically similar to fenestrated capillaries; up to 6 endothelial cells comprising the vessel wall.
5) Venous fenestrated capillaries: pericytic or apericytic; luminal diameter 4 to 7 μm (Rhodin, 1968; Freezer, 1984); fenestrae present; abluminally bulging nuclei.

6) Postcapillary-sized venules: pericytic or apericytic; luminal diameter 8 to 30 μm (Rhodin, 1968; Freezer, 1984); relatively thin-walled (Sims, 1983); sometimes fenestrated; up to 9 endothelial cells comprising the vessel wall.
7) Collecting venules: luminal diameters up to 50 μm surrounded by a continuous layer of pericytes.

4.2.2 Sample Size

Tissue blocks were sectioned at 160 μm intervals beginning at the crest of the alveolar bone representing the zero level, through to the root apex representing the end level. An average of 8 levels per mouse PDL resulted. Five blood vessels for each level were randomly selected as representative of each level (Chintakanon, 1990). Final sample size was derived following discussions with the Statistical Consulting Group, The University of Adelaide. One measurable junction was required for each of five blood vessels resulting in a constant number of five junctions per level.

As previously discussed (section 4.1), PDL tissue blocks were taken from right and left sites from each of four animals for young and old groups, representing 16 PDL tissue blocks (young = 8 blocks, old = 8 blocks). From each PDL tissue block, five junctions per level (coronal to apical) for 7 to 9 levels were randomly selected, resulted in a minimum sample size of 640 junctions for each of young (n=320) and old (n=320) mice.

4.2.3 Pilot Study

An initial survey of the sample found that more than 5 PCV were present at each level in the specimens studied (Appendix 2). Venous capillaries and collecting venules numbered less than 5 per level, and were excluded from the study due to lack of a statistically adequate sample size. Therefore, only PCV were included in the study. However, PCV contain 88% of the mouse PDL vascular volume (Freezer and Sims, 1987), that is, the predominant vascular segment of the PDL microvascular bed.

A range of PCV were found between quadrats, which varied from one to five in number. Further, the location of PCV across the lateral thirds of the PDL varied (tooth 1/3, middle 1/3 and bone 1/3), such that PCV were not commonly observed in the tooth 1/3 but occurred more frequently in the bone 1/3. Therefore, one endothelial junction from each PCV was not recorded for each PDL level across each third of the PDL. However, the location of each

PCV, with an endothelial junction that was assessed, was recorded in the tooth 1/3, middle 1/3, or bone 1/3 (Section 4.2.4).

4.2.4 Blood Vessel Location

A polaroid photograph (Freezer, 1984) of the final mesa (x100) was used to assist in identifying the PDL located at the most mesial area of the tooth. Each grid was examined, beginning at the top left hand corner of the grid and proceeding systematically across the grid from left to right and in the reverse for the adjacent row below, until PCV within the grid square were identified (Figure 4.2).

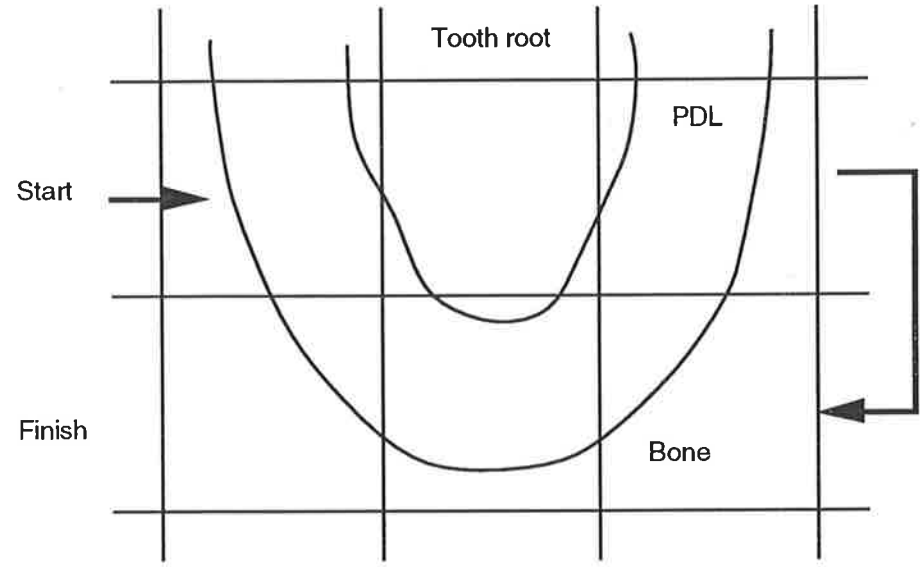

Figure 4.2 Preferred quadrat sampling procedure.

Electron micrographs of PCV were exposed at a magnification of x500 to cover all the area in that grid square. An image wobbler, switched off immediately prior to exposure, was used to assist in focussing at the lower magnification. If there were less than five blood vessels in the first grid square, then the adjacent grid square was examined. The PCV were recorded as being located in the tooth 1/3, middle 1/3, and bone 1/3 of the PDL (Figure 4.3). If any PCV was present in both regions, it was classified into the region of the PDL where the major part of it was located.

PCV were excluded if:

1) No junctions were identified in that vessel.
2) Less than 3/4 of the vessel was identified if it intersected with the grid bar which would make assessment of the luminal diameter difficult.

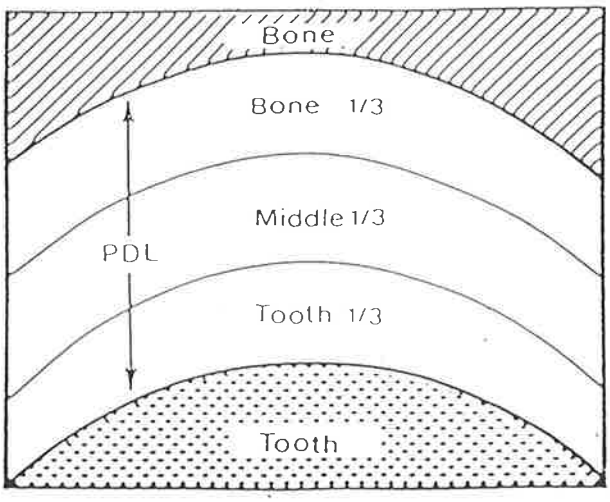

Figure 4.3 Representation of the periodontal ligament divided into three regions, tooth, middle, and bone circumferential thirds.

4.2.5 Endothelial Junction Inclusion

Each PCV was divided into 4 quadrants (Figure 4.4). The first 'complete' endothelial junction was selected by examining the upper left quadrant first. If no junction was found, examination continued clockwise from first quadrant until a 'complete' endothelial junction was found.

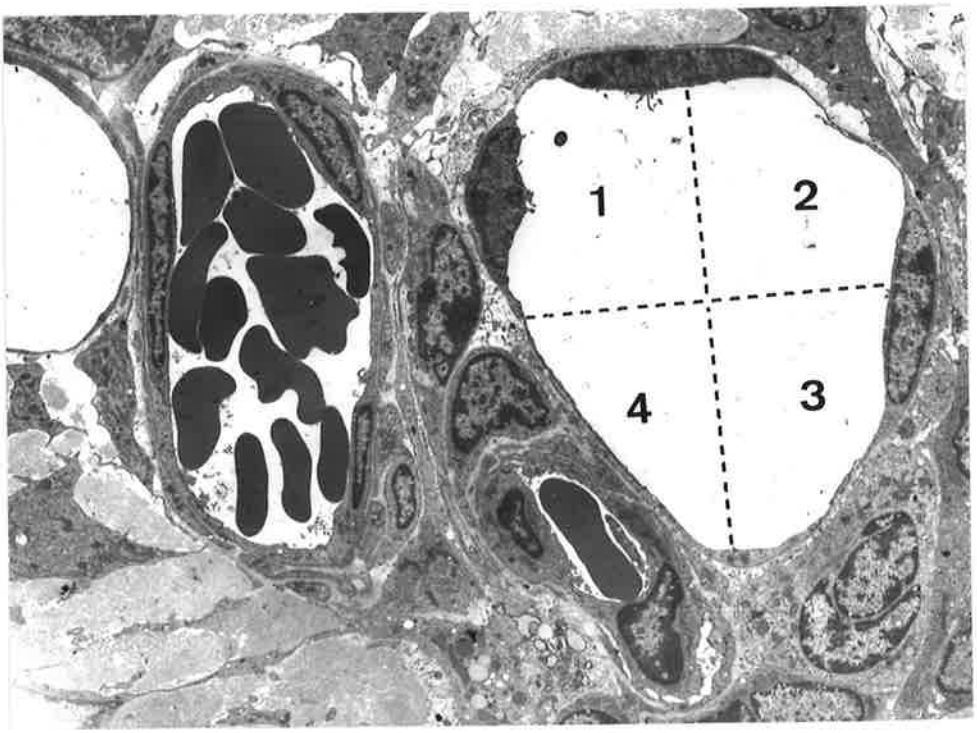

Figure 4.4 Representation of a poscapillary-sized venule divided into 4 quadrants. Observation began in quadrant 1 and progressed through each quadrant until the first 'complete' junction was selected. Final magnification (Mag.) = x2,900

Criteria used to distinguish a 'complete' junction were:

1) Clearly identified 'entrance' to the junction on the luminal side with well defined opposing plasmalemma membranes
2) Clearly identified 'exit' to the junction on the abluminal side with well defined opposing plasmalemma membranes

4.2.6 Goniometer

Utilising the manual tilt goniometer, complete junctions were viewed at a magnification of x80K, at zero tilt and at various tilts (>15°) in either a clockwise (+) or anti-clockwise (-) direction around the horizontal axis of the specimen holder. This method was used to assess the space between the closely apposed external laminae of the plasma membranes enabling classification of the junction as tight (no opening between external laminae) or close (opening between external laminae). Further electron micrographs at this magnification, that is, at zero and tilted angles were exposed. Ilford Electron Microscope Film was used for the micrographs, with an exposure time of three seconds and an automatic aperture opening. Micrographs for five junctions per level were obtained.

4.2.7 Magnification Calibration

A micrograph of a replicating graticule (E.F. Fullam Inc., Schendectady, N.Y., 2160 lines/mm) was exposed at both the low and high magnifications every TEM photographing session to enable standardisation of micrograph magnification.

4.3 Developing and Printing

Electron micrographs were developed for four minutes at 20°C using Kodak D19 developer rinsed in deionised water for one minute and fixed for a minimum of five minutes in Ilford Hypam Rapid Fixer at 20°C. Following fixation, the micrographs were rinsed for a further 15 minutes and air-dried for two hours. Using a Durst Laboratory 54 enlarger, the negatives were printed on multigrade Ilfospeed photographic paper, using a grade 5 filter to obtain adequate contrast. The prints were developed for one minute using Ilfospeed paper developer and fixed for five minutes with Ilford Hypam Rapid Fixer, followed by rinsing and drying. Prints were enlarged from the original negatives to produce the equivalent of x150K for the measurement of junction dimensions.

4.4 Morphometry of Junctional Dimensions

4.4.1 Endothelial junction classification

Endothelial junctions, classified by Casley-Smith (1983) into four types, include close junctions, tight junctions, open junctions and gap junctions. The following classifications were used in the present study (derived from Casley-Smith *et al.*, 1975; Casley-Smith, 1983; Simionescu and Simionescu, 1984):

1) Close Junction: a junction where the two outer lamellae of opposing cells were separated along the junction length and a 'close region' was identified.
   Close Region: a region where the two outer lamellae of opposing cells narrowed within the intercellular cleft (endothelial junction) to be separated by a small gap of 6 to 8 nm (Figure 4.5). The distance along the intercellular cleft at the location of the close region was defined as the close region junction size measured (section 4.4.3.5).
2) Tight Junction: a junction where the two outer lamellae of opposing cells were separated along the junction length and a 'tight' region was identified.
   Tight Region: a region where the two outer lamellae of the opposing cells were fused within the intercellular cleft. The distance along the intercellular cleft at the location of the tight region was defined as the tight region junction size measured (section 4.4.3.5).
3) Open Junction: the junction where an intercellular width increased greater than 100 nm along the junction depth.
4) Gap Junction: the junction where the two plasma membranes were closely opposed with an intercalated appearance between them.
5) Endothelial Junction without 'close' or 'tight' regions: a junction where the two outer lamellae of opposing cells were separated along the entire junction length with an intercellular width less than 100 nm (which defines an open junction). No 'close' or 'tight' regions were identified.
6) Endothelial Junction with multiple 'close' or 'tight' regions: a junction where more than one 'close' and/or 'tight' region were identified within the intercellular cleft.

The terminology for the dimensions of complete tight and close junctions used in the present study, were as follows (modified from Casley-Smith *et al.*, 1975; Casley-Smith, 1983; Simionescu and Simionescu, 1984):

1) Junction length: the distance between the luminal and abluminal surfaces following the course of the junction.

2) Junction width: the shortest distance across an endothelial junction between the external lamina of the plasma membranes of two adjacent endothelial cells.
3) Junction thickness: the shortest distance across the blood vessel wall at the site of a junction, from luminal to abluminal side.
4) Junction size (of junction region): the length along a close or tight region within the endothelial junction.

4.4.2 Random Assignment of the Study Sample

Each specimen was assigned a number from a random numbers table (Ott, 1988) and placed in sequence, blind to the observer, to eliminate observer bias during measurement procedures.

4.4.3 Method of Measurement

The junctional dimension assessments were completed on the enlarged printed electron micrographs, using an image analysis system, the Manual Optical Picture Analyser (MOP-3) (Carl Zeiss Inc., West Germany) and a Max-Cal electronic digital calliper (Fowler and NSK, Japan) with an accuracy of $\pm$ 0.03 mm and a resolution of 0.01 mm.

4.4.3.1 Junction Length

Each plasmalemma membrane of the PCV endothelial cell wall, curved continuously from the luminal and abluminal aspects of the intercellular cleft to form the luminal and abluminal sides of the blood vessel, respectively. At the outer and inner aspects of each plasmalemma membrane, the curvature of the membrane from the intercellular cleft to the lumen and the ablumen was convex and concave, respectively. The deepest point of the concavity on the inner aspect of a plasmalemma membrane determined the 'point of reflection'. The distance from one 'point of reflection' to the opposing membrane 'point of reflection' on the luminal side and abluminal side of the endothelial junction was defined as junction width 1 and junction width 4, respectively (section 4.4.3.2). Junction length was measured beginning from the midpoint between the two opposing membranes at the luminal end (junction width 1), along the junction, to the corresponding end point, at the abluminal end (junction width 4), as shown in Figure 4.5. Three measurements of each junction length were taken and then averaged.

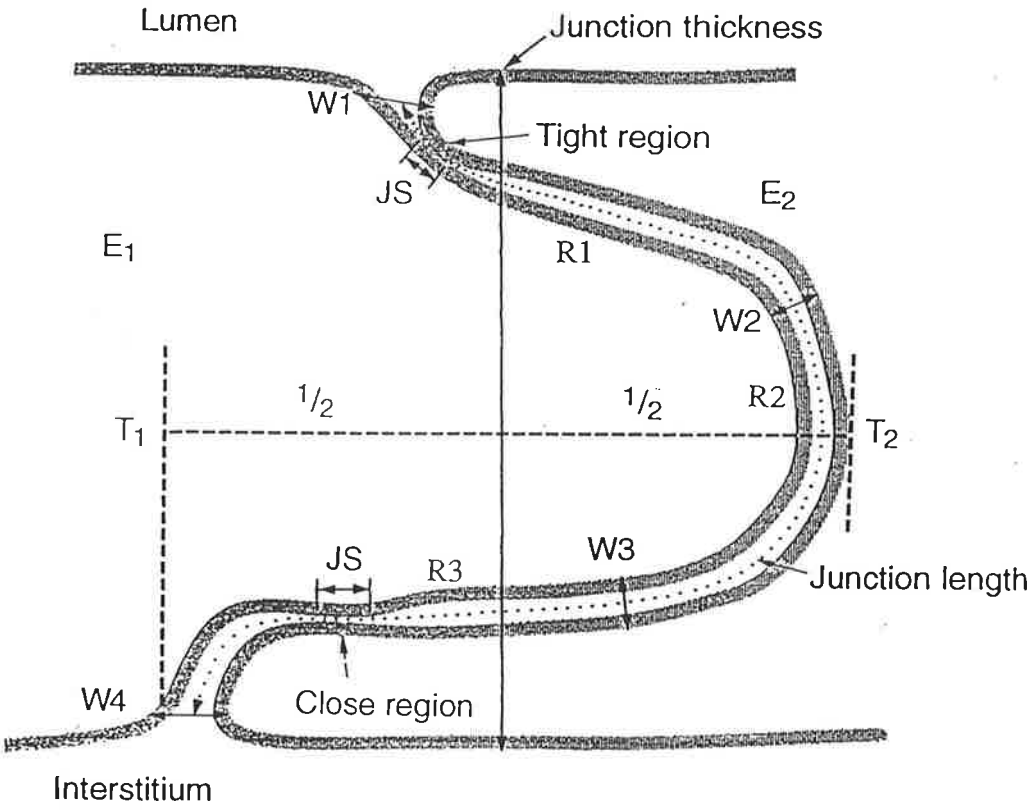

Figure 4.5 Representation of the method of measuring:
(1) junction length from lumen to ablumen, (2) PCV endothelial wall thickness (junction thickness), (3) junction width 1, 2, 3 and 4 (W1, W2, W3 and W4), (4) junction size (JS). E1 and E2 represent adjacent endothelial cells; R1, R2, R3 indicate the luminal 1/3, middle 1/3 and the abluminal 1/3 areas, respectively, to indicate the location of tight and/or close regions along the length of the junction. Junction thickness was measured at a location determined by the distance 1/2 way between the extension of the junction at T1 and T2.

4.4.3.2 Junction Thickness

Junction thickness represented the thickness of the PCV endothelial wall at the location of an endothelial junction. It was recorded, using a digital calliper, by measuring from the outer lamellae on the luminal side of the blood vessel to the abluminal side at a position determined as halfway between the outer extent of the endothelial junction (Figure 4.5).

4.4.3.3 Junction Length to PCV Wall Thickness Ratio - 'Meander"

A variable, termed 'meander', was defined as the ratio of the junction length to the PCV thickness at the junction. This ratio was calculated to determine

whether there was a relationship between the thickness of the PCV endothelium and the length of the endothelial cell junction. This is important because an increased length of the endothelial cell junction may not be related to a decreased permeability because there may be a compensatory decrease in the thickness of the PCV endothelial wall. As noted by Bundgaard (1988), an increase in the length of the diffusion pathway will result in decreased permeability. Therefore, it is expected that with an increased ratio, the permeability of the endothelial junction would be decreased (section 3.5). A log transformation of the ratio was used for statistical analysis (section 4.5).

4.4.3.4 Junction Width

The width measurements for each junction will be divided into four components, namely:

W1 - the width at the luminal side from one endothelial cell membrane 'point of reflection' (section 4.4.3.1), to the opposing endothelial cell membrane 'point of reflection'.

W2 - the width at one third distance along the length of the junction.

W3 - the width at two thirds distance along the length of the junction.

W4 - the width at the abluminal side from one endothelial cell membrane 'point of reflection' (section 4.4.3.1), to the opposing endothelial cell membrane 'point of reflection'.

Three measurements of each junction width were taken with a digital calliper and averaged. Accurate definition of the outer lamellae of the two opposing cells presented occasional difficulty due to the plane of the section. As a result, the width of the junctions were measured between the darkest lines on the inner lamellae of the two opposing cells which was more clearly defined than the outer lamellae (Figure 4.5). The width of two unit membranes (15 nm) was subtracted from the measured width (Casley-Smith, 1969), to give the absolute distance between the two opposing membranes (Figure 4.5).

4.4.3.5 Junction Type and Location

Close and tight junction regions that were observed at various depths along the intercellular cleft were recorded (Appendix 1). The location of the close or tight regions along the length an intercellular cleft were defined as (Figure 4.5):

Region 1 (R1) - one third of the distance along the intercellular cleft from the luminal entrance, that is, the luminal third. The beginning and end points of R1 correspond to W1 and W2, respectively.

Region 2 (R2) - one third of the distance along the length of the intercellular cleft from the end of region 1 to the beginning of region 3, that is, the middle third. The beginning and end points of R2 correspond to W2 and W3, respectively.

Region 3 (R3) - one third of the distance along the length of the intercellular cleft from the end of region 2 to the abluminal exit of the junction, that is, the abluminal third. The beginning and end points of R3 correspond to W3 and W4, respectively.

4.4.3.6 Junction Region Size

The length of close or tight regions within the endothelial junction was measured using a digital calliper. Three measurements of each region were recorded and averaged. The size (length) of tight regions was defined as the distance that the two outer lamellae of opposing endothelial cells were fused. The size (length) of close regions was defined as the distance that the two outer lamellae of opposing endothelial cells narrowed within the intercellular cleft (endothelial junction) to be separated by a small gap of 6 to 8 nm (Figure 4.5).

4.4.4 Random Assessment of Measurement and Junction Classification Error

Every tenth specimen was selected from the randomly assigned specimens resulting in 13 specimens which were used for measurement error. New electron micrographs were enlarged to x150K and developed from the negatives of the chosen specimens. Two junctions from each of these specimens were measured blind under the same conditions as previously.

The data was tested for normality and constant variance. Provided these assumptions were satisfied, a paired t-test was used for data analysis, otherwise a Wilcoxon signed-rank nonparametric test was used (Statview 512+, Brainpower Inc., California, USA). A significance level of $p < 0.05$ was used.

No significant differences were found between the first and second measurements. The coefficients of variation for the different parameters were 1.8% for junction length, 2.4% for junction thickness, 2.5% for junction

width 1, 2.8% for junction width 2, 4.4% for junction width 3 and 4.8% for junction width 4.

The kappa coefficient (Cohen, 1960; 1968) was used as a measure of association to describe and test the degree of agreement in classification of tight and close regions between first and second observations. This calculation yielded a measure of 1.00 indicating no significant differences were found between first and second classifications.

4.5 Statistical Analysis

Statistical analysis was completed using Genstat^{TM} 5 Release 3 (AFRC Institute of Arable Crops Research, Harpenden, UK). PDL levels were measured precisely. However, the number of levels changed from tooth to tooth due to different root lengths between animals, so there were differing numbers of values at each PDL level, for example, there was an additional level in the old mice for the apex class. Therefore, when differing root lengths for different animals were adjusted statistically to match, the observed data were then based on the class limit calculations. This feature was more relevant below the 480 μm level.

Class limits	Observed range
0-80	0
80-240	160
240-400	320
400-560	480
560-720	660-675
720-880	750-860
880-1000	900-960
> 1000	1000-1999 (Apex)

Initially, data were tabulated to give arithmetic means with standard error values, and classified by mouse group, PDL level and side (left and right). This procedure averaged the junctions within the PDL levels so all the above means could be used in the analysis. Arithmetic means do not account for the variation in the numbers of measurements, that is, the data set was unbalanced. The means for each PDL level, therefore, were estimated using

an analysis of covariance (Ott, 1988), with the effect of mice as a covariant.

Age effects were estimated between young and old mice groups. These age effects were, therefore, tested using a multiple regression technique by comparing the effect of age with the residual between mouse variance. By assuming that the occurrence of PCV across the PDL from tooth root to alveolar bone was independent for each mouse group, a test of significance could be made. In this case a generalised linear model with a poisson distribution (Ott, 1988) was used to test for the effect of age. A chi-square analysis was carried out to test whether there were differences in the proportion of close and tight junctions associated with increasing age.

With respect to junction length/junction thickness ratio, the simple ratio was not used because a small change in the junction thickness would skew the result. A log transformation of the ratio data, termed 'meander' (section 4.4.3.3), was calculated to obtain normality for analysis of variance.

CHAPTER 5 RESULTS

5.1 Blood Vessel Type

The blood vessels assessed were postcapillary-sized venules (PCV). Of these, the types of PCV identified were apericytic and pericytic vessels. Figure 5.1 and 5.2 are low and high magnification views of pericytic and apericytic PCV. Some fenestrated PCV also were identified (Figure 5.3).

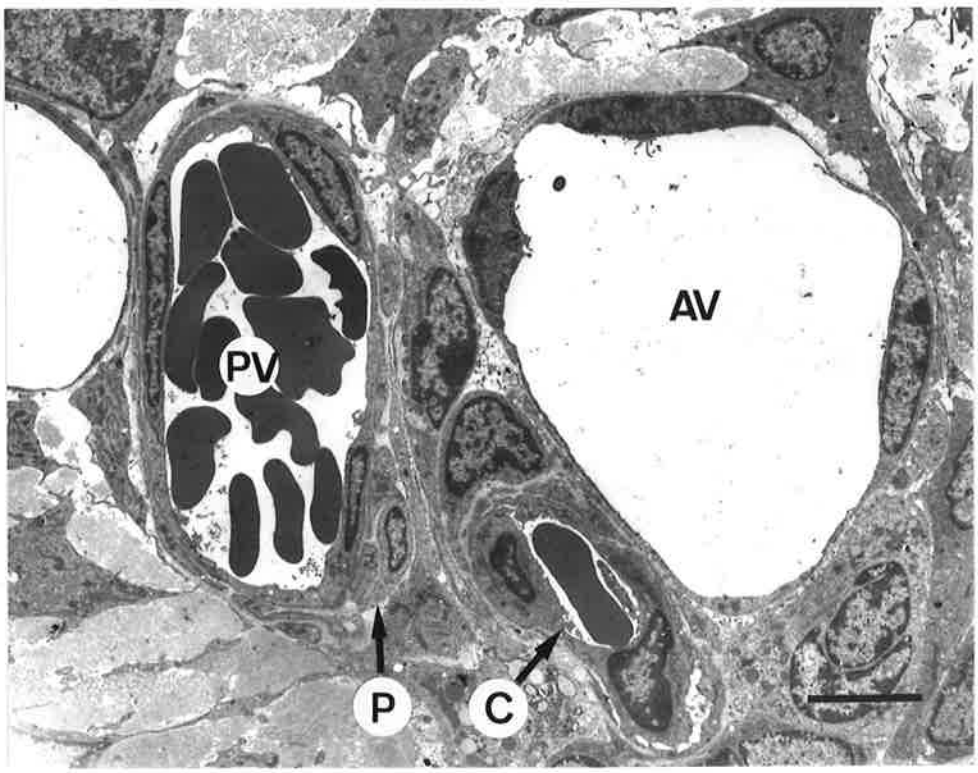

Figure 5.1 A arterial capillary (C) which lies in close proximity to an apericytic postcapillary-sized venule (AV) and a pericytic postcapillary-sized venule (PV) partially surrounded by a pericyte (P). Uranyl acetate and Reynolds' lead stain.
Mag. = x2,900 Bar = 5 μm.

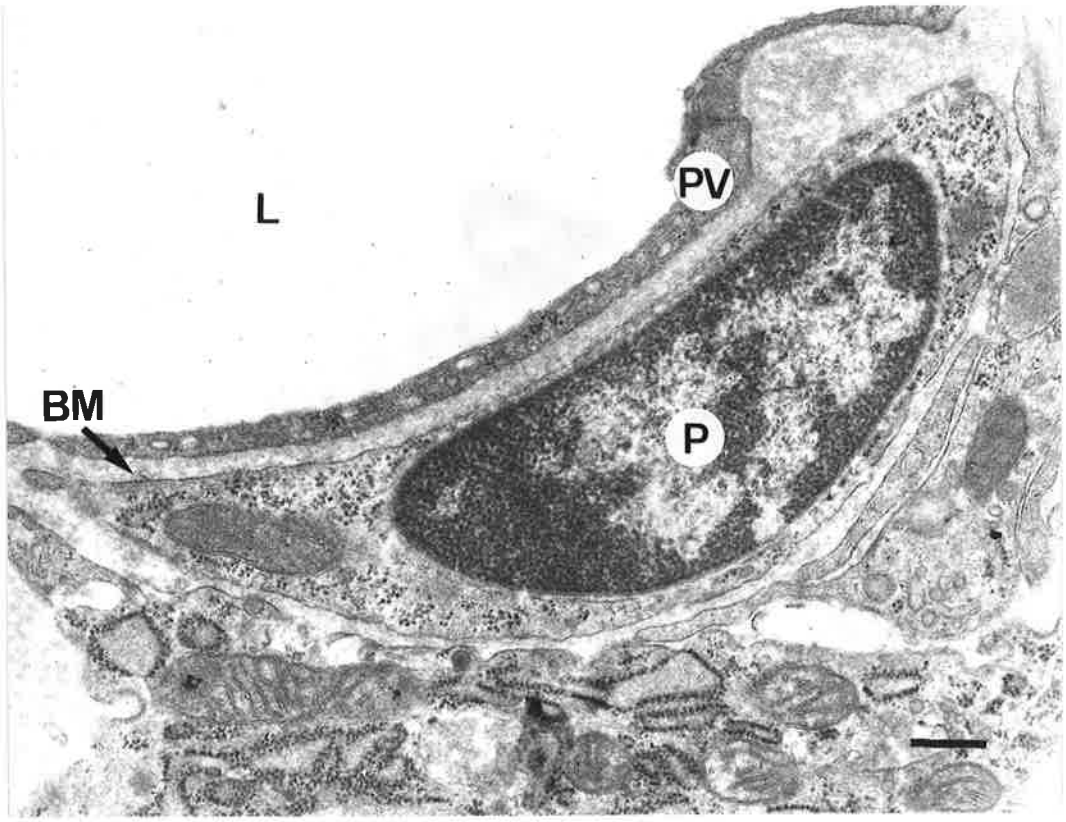

Figure 5.2 A pericytic postcapillary-sized venule endothelial wall (PV), a pericyte (P) and basement membrane (BM). L, luminal side. Uranyl acetate and Reynolds' lead stain.
Mag. = x4,000 Bar = 2.5 μm.

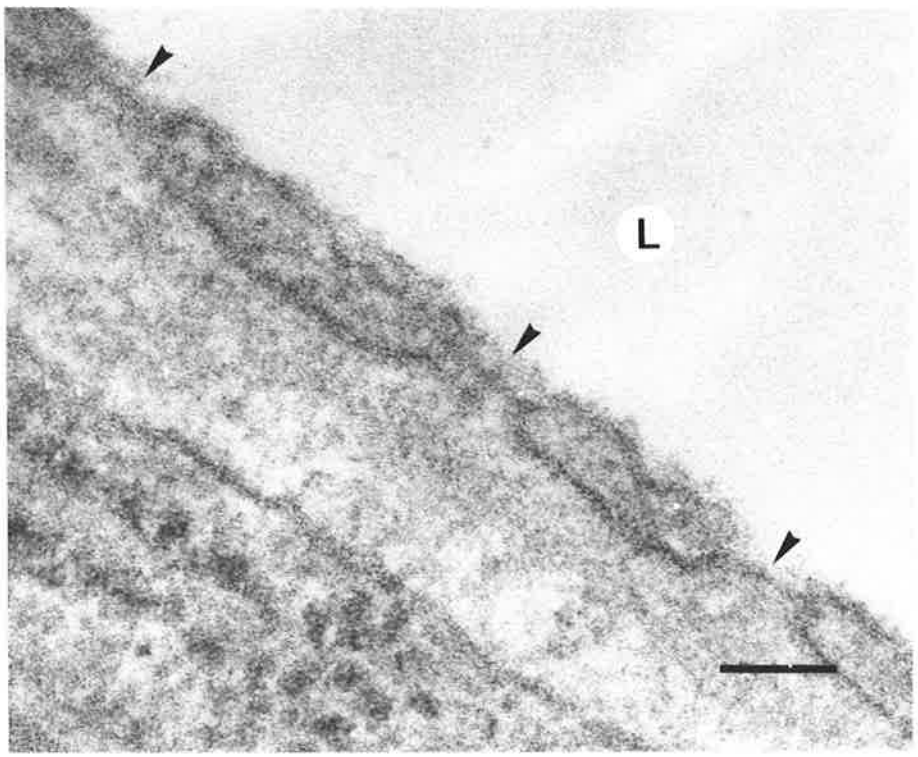

Figure 5.3 The endothelial wall of a fenestrated postcapillary-sized venule. The arrow heads indicate fenestrae each with a diaphragm; L, luminal side. Uranyl acetate and Reynolds' lead stain.
Mag. = x150K Bar = 100 nm

There was no effect of age on blood vessel type (Table 5.1). Apericytic PCV were more common in both groups at all PDL levels (coronal to apical). The number of apericytic PCV increased significantly with increasing depth of the PDL from the alveolar crest to the apex ($p < 0.05$) in each age group. A significantly increased ($p < 0.05$) number of pericytic PCV, relative to the total number of PCV, was found in each age group at the alveolar crest by comparison with the apex (Table 5.1).

Table 5.1 Total number of apericytic and pericytic postcapillary-sized venules in each PDL level for young (Y, n=4) and old (O, n=4) mice. Range represents the minimum and maximum number of apericytic and pericytic postcapillary-sized venules in each PDL level for each mouse in young and old mice groups.

	Apericytic				Pericytic			
Level (μm)	Y	Range	O	Range	Y	Range	O	Range
0	26	5-8	28	5-10	14	2-5	12	0-5
160	24	4-8	26	5-8	16	2-6	12	2-5
320	35	8-9	32	6-9	5	1-2	7	1-3
480	31	3-11	30	6-9	10	0-7	7	1-3
600-675	32	6-9	26	4-8	8	1-4	9	1-4
750-860	38	7-10	32	4-10	4	0-3	6	0-6
900-960	33	6-11	29	3-10	12	1-4	4	0-2
Apex	52	8-18	54	10-17	8	2	10	0-4
Total	271		257		77		67	

5.2 Blood Vessel Diameter

Age had no effect on PCV diameter. The mean luminal diameter of the PCV at each PDL level (coronal to apical) for each group is shown in Table 5.2. There was a suggestion that the older vessels were 2.5 μm less in mean diameter. However, this effect was not significant at the $p < 0.05$ level, when tested against the between mouse variance, using the analysis of covariance.

Table 5.2 Luminal diameter (μm) of all postcapillary-sized venules (apericytic and pericytic) for young and old mice at each periodontal ligament level.

Level (μm)	Young		Old	
0	13.6†	14.3‡	13.1	12.1
	(1.8)		(1.0)	
160	15.3	13.5	12.6	12.8
	(1.1)		(1.3)	
320	13.3	16.8	13.3	12.4
	(1.1)		(1.3)	
480	15.1	15.5	14.5	12.0
	(0.9)		(1.5)	
600-675	14.9	14.8	13.8	9.4
	(1.3)		(0.7)	
750-860	14.9	14.6	13.2	12.3
	(0.8)		(0.9)	
900-960	15.0	16.5	12.3	12.8
	(1.0)		(1.0)	
Apex	14.4	13.6	13.8	14.3
	(1.2)		(1.2)	

† - Arithmetic means with standard error values in parentheses.

‡ - Mean values calculated using analysis of covariance. They were adjusted because of different numbers of values at each periodontal ligament level (Section 4.5).

5.3 PCV Location

The sampling of PCV in each of the three circumferential regions of the PDL were examined in a random order. Therefore, a difference between ages could be investigated, but not quantified. The number of PCV sampled in each mouse and in each of the three circumferential regions (tooth 1/3, middle 1/3 and bone 1/3) across the PDL, is summarised in Table 5.3 and Figure 5.4. Using a generalised linear model with a poisson distribution (Section 4.5), a significant increase in the number of PCV in the tooth 1/3 in the old mice ($\chi^2 = 14.7$, $p < 0.01$) was found, as shown in Tables 5.3, 5.4 and 5.5. These PCV were predominantly apericytic ($p < 0.001$). There was animal variability, such that one mouse in the aged group did not have any PCV in the tooth third of the PDL. Except for one mouse, no PCV were found located in the tooth third in young mice.

Table 5.3 Number of total postcapillary-sized venule (apericytic and pericytic) in each of 8 mice classified by location across the periodontal ligament from the root to the alveolar bone.

Mouse age	Region			
	Tooth 1/3	Middle 1/3	Bone 1/3	Total
Young (Y)	0	16	65	81
Y	0	20	66	85
Y	0	19	73	89
Y	1	21	67	89
Total Y	1	76	271	352
Old (O)	3**	11	60	74
O	4**	13	66	83
O	8**	29	46	83
O	0	17	67	84
Total O	15	70	239	324

** - Significant increase in old mice postcapillary-sized venule number located in the tooth circumferential 1/3 of the periodontal ligament ($p < 0.01$).

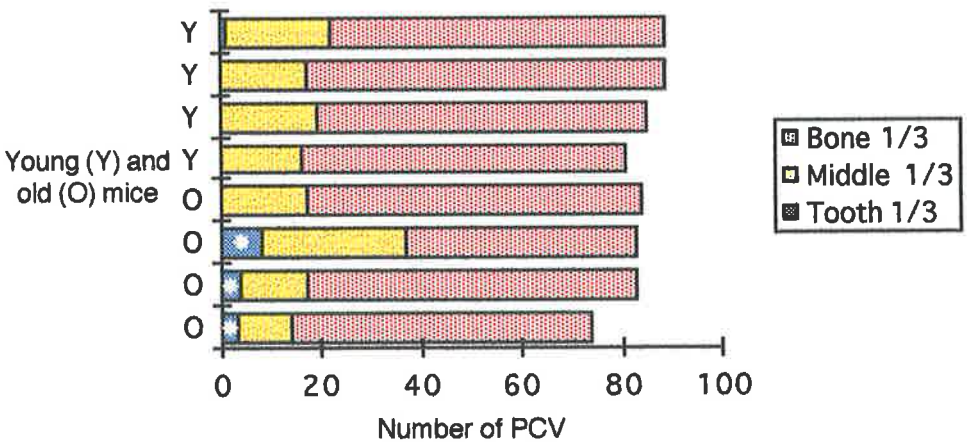

Figure 5.4 Plot of the number of all postcapillary-sized venule (PCV) according to the location within the periodontal ligament (PDL) from the root to the alveolar bone for each mouse. * - Significant increase in old mice PCV number located in the tooth circumferential 1/3 of the PDL ($p < 0.01$).

In young mice in the middle PDL circumferential 1/3 (Table 5.4), significantly fewer numbers of PCV ($p < 0.001$) were observed halfway down the PDL. The number of PCV in the PDL middle circumferential 1/3 in the old mice were more uniform and differed significantly from the young mice ($p < 0.001$) mid-way down the PDL. A significantly ($p < 0.05$) greater number of PCV were found in the apical bone third in old mice (Table 5.4). Although there was a greater number of PCV in the apical bone 1/3 in old mice (Table 5.4), this was not significant due to the inclusion of additional PDL levels at the apex (Section 4.5).

Table 5.4 Number of total postcapillary-sized venules for young and old mice classified by the location across the periodontal ligament from the tooth to the alveolar bone, and from coronal to apical levels.

Level	Region					
	Tooth 1/3		Middle 1/3		Bone 1/3	
	Young	Old	Young***	Old	Young	Old
0	1	2	19	12	20	26
160	0	1	6	6	34	31
320	0	1	4	12	36	26
480	0	3	3	8	38	26
600-675	0	3	0	12	40	20
750-860	0	4	6	8	33	26
900-960	0	1	10	6	34	26
Apex	0	0	25	6	36	58*
Total	1	15**	76	70	271	239

* - Significant increase in old mice postcapillary-sized venules number located in the bone 1/3 at the apex ($p < 0.05$).

** - Significant increase in old mice postcapillary-sized venules number located in the tooth cicumferential 1/3 of the periodontal ligmament ($p < 0.01$).

*** - Significant difference between young and old mice down the middle 1/3 of the periodontal ligament ($p < 0.001$).

The type of PCV also differed across the PDL as shown in Table 5.5. Although there were few vessels in the tooth 1/3, they were with a single exception, of the apericytic type. A significantly larger number of apericytic PCV ($p < 0.001$) in the tooth 1/3 of the old mice was found compared with the young mice. However, as shown in Table 5.1, the total number of apericytic PCV for young mice (271) was comparable to the number for old mice (257).

Table 5.5 Number and ratios of pericytic and apericytic postcapillary-sized venules (PCV) for young and old mice in each location horizontally across (tooth to alveolar bone) and vertically down (alveolar crest to the apex) the periodontal ligament.

PCV type	Region						
	Tooth 1/3		Middle 1/3		Bone 1/3		Total
	Young	Old	Young	Old	Young	Old	PCV
Pericytic	0	1	22	23	55	43	144
Apericytic	1	14***	54	47	216	196	528
Pericytic:Apericytic	0:1	1:14	1:2.5	1:2.0	1:3.9	1:4.6	
Pericytic:Total PCV	0:1	1:16	1:3.5	1:3.0	1:4.9	1:5.6	

*** - Significant difference between the number of apericytic postcapillary-sized venules in the tooth 1/3 in old mice ($p < 0.001$).

The total number of PCV for all levels of the PDL for young and old mice is shown in Figure 5.5. PCV were significantly ($p < 0.05$) more common in the bone third of the PDL, and declining in the middle third, with few found in the tooth third in young and old mice.

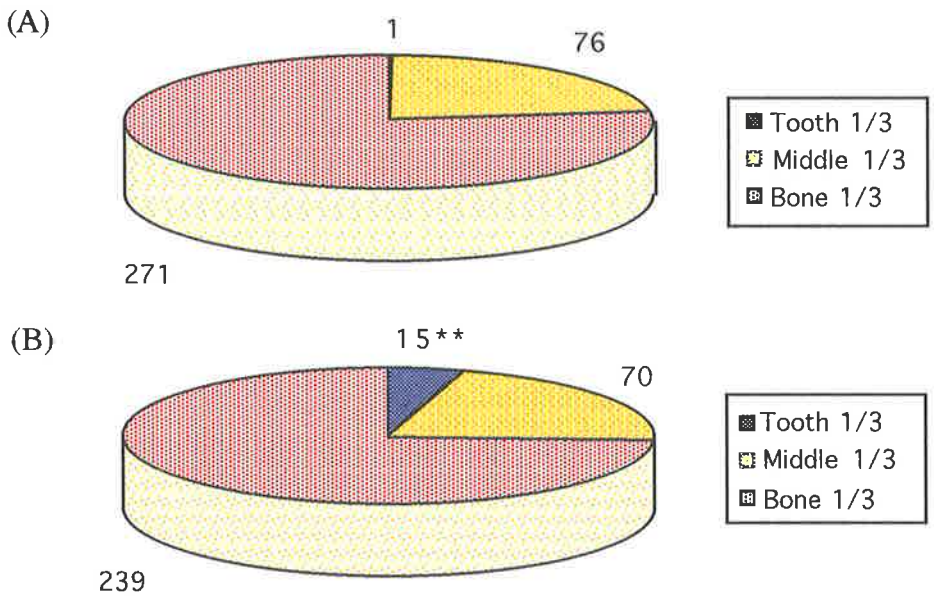

Figure 5.5 (A) and (B) Diagram of the total number of postcapillary-sized veunules for young (A) and old (B) mice located across the periodontal ligament (PDL) from the root to the alveolar bone, and for all levels of the PDL from the alveolar crest to the apex (** - Significant difference between young and old mice at the tooth 1/3 of the PDL, $p < 0.01$).

5.4 Junction Type

The sample of endothelial junctions that was assessed in the young and old mice, included junctions with close and/or tight regions or without close or tight regions. No gap or open junctions were identified in the sample. Figure 5.6 illustrates a junction in a PCV that has no close or tight regions, while figure 5.7 illustrates a more tortuous junction with a close region. Figure 5.8 is an example of a junction in which a tight region is visible.

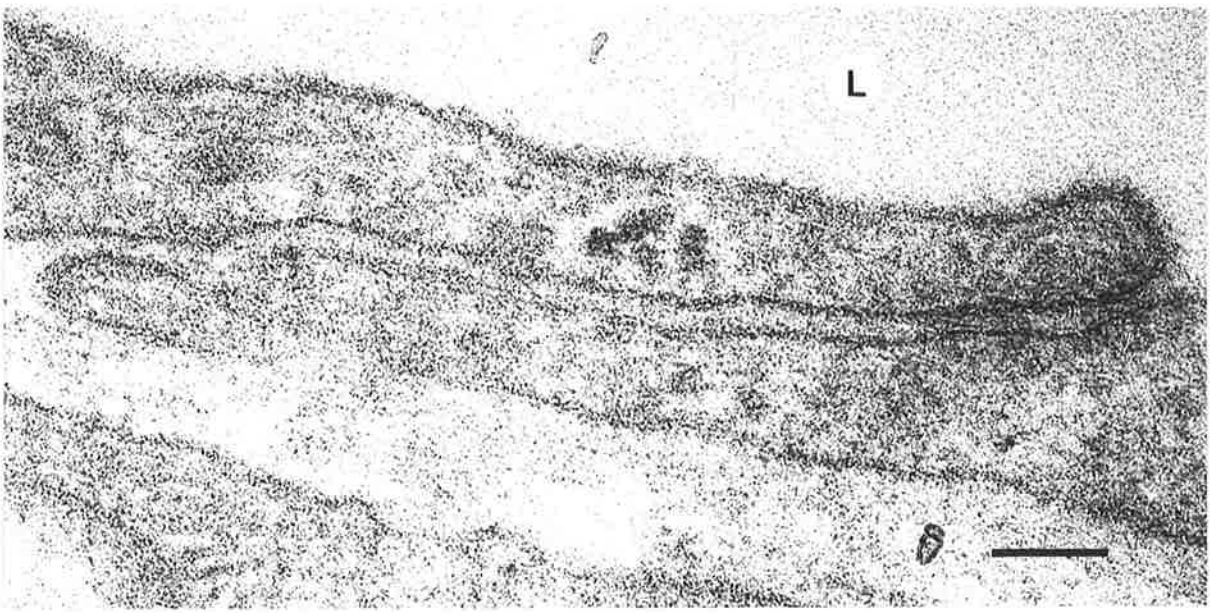

Figure 5.6 A 'simple junction' from a postcapillary-sized venule. No tight or close regions are present; L, luminal side. Uranyl acetate and Reynolds' lead stain. Mag. = x150K Bar = 100 nm

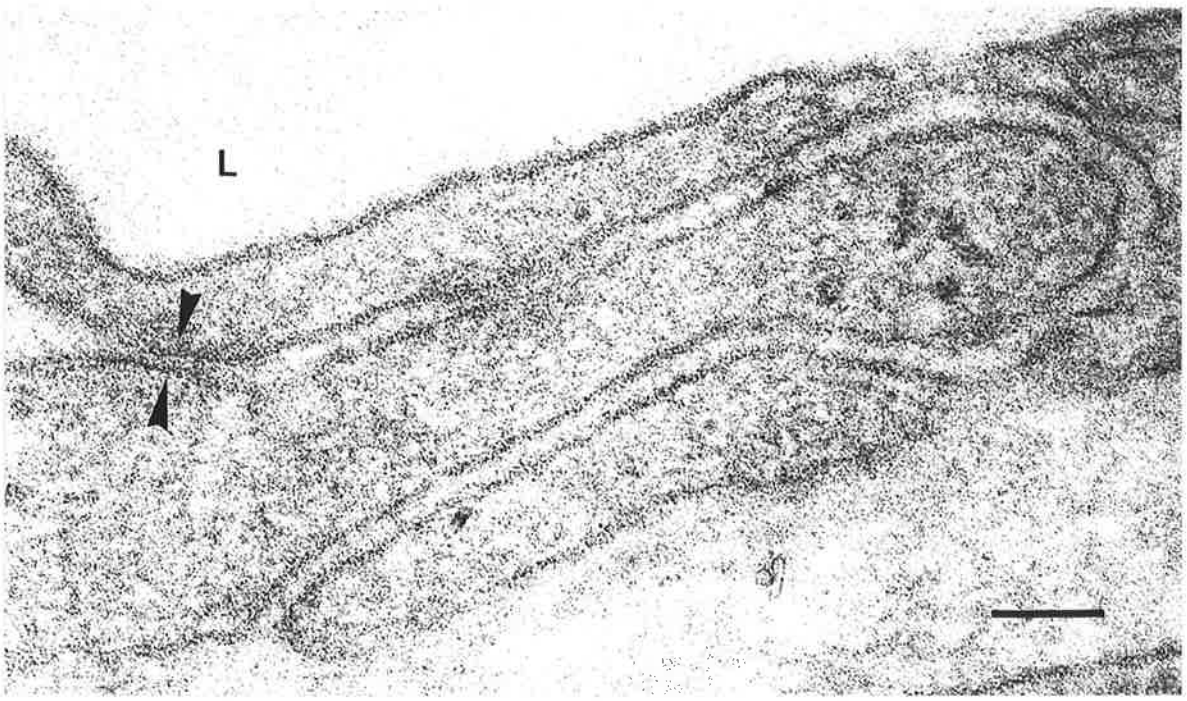

Figure 5.7 A tortuous junction from a postcapillary-sized venule. The arrow heads indicate a close region between the two opposing membranes; L, luminal side. Uranyl acetate and Reynolds' lead stain.
Mag. = x150K Bar = 100 nm

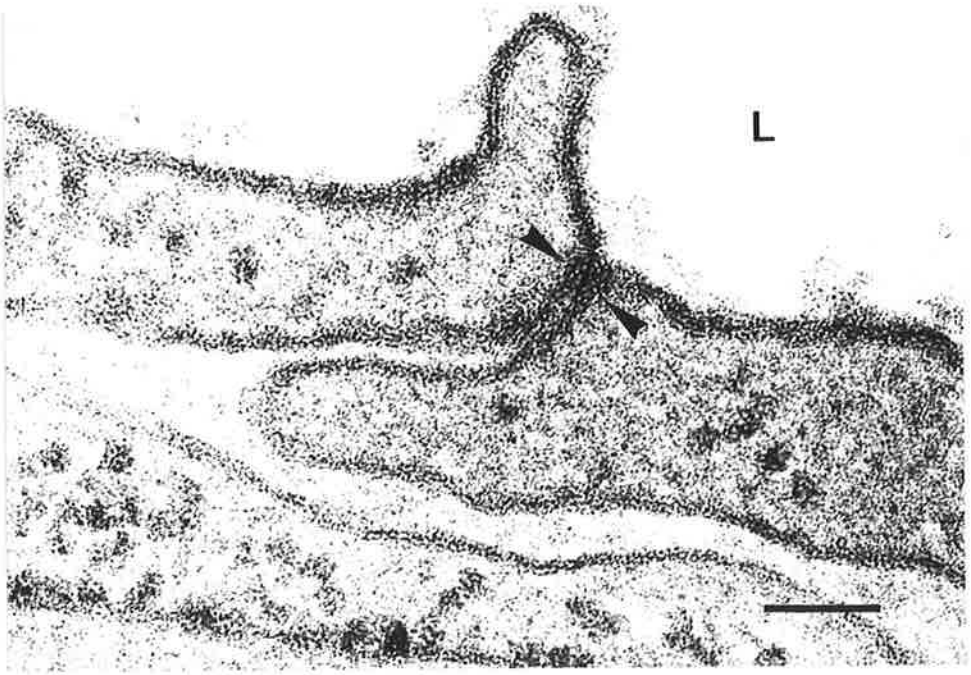

Figure 5.8 A 'simple junction' from a postcapillary-sized venule. The arrow heads indicate a tight region. One cell projects into the lumen as a microvillus; L, luminal side. Uranyl acetate and Reynolds' lead stain.
Mag. = x150K Bar = 100 nm

As previously noted (section 4.2.6), all tight junctions were assessed using a goniometer to enable distinction between tight and close regions. Figure 5.9 (A) demonstrates a junction that appears to be a tight junction, but on tilting the section 45° clockwise, the opposing endothelial cell membranes separate (Figure 5.9 B). This junction was therefore classified as a 'close junction'.

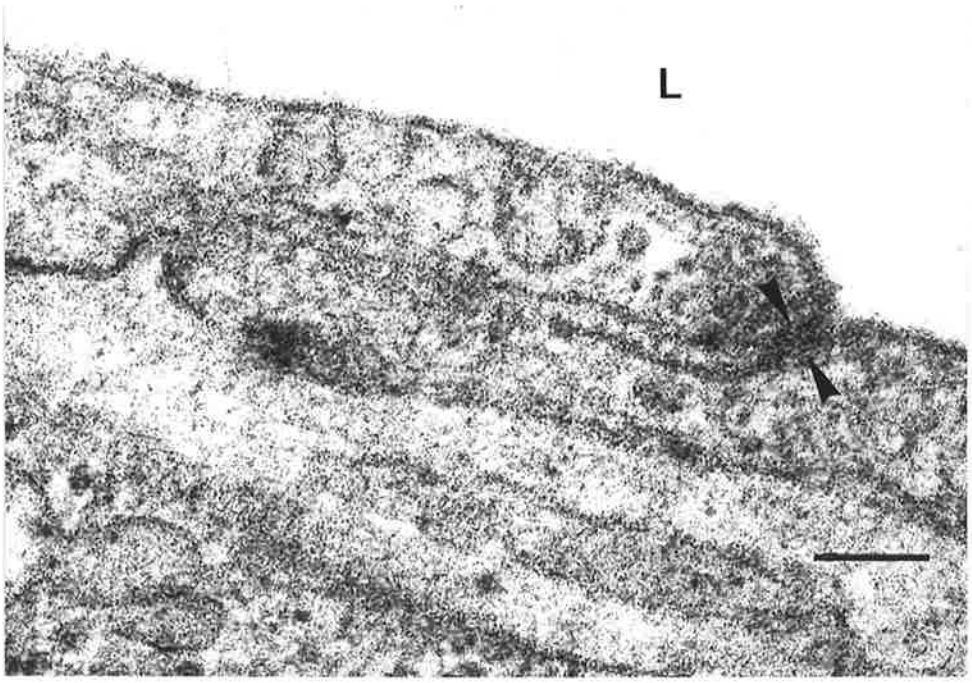

Figure 5.9 (A) The junction in figure (A) appears to have a tight region (arrow heads) at the luminal end where the two areas of membrane fuse; L, luminal side. Uranyl acetate and Reynolds' lead stain.
Mag. = x150K Bar = 100 nm

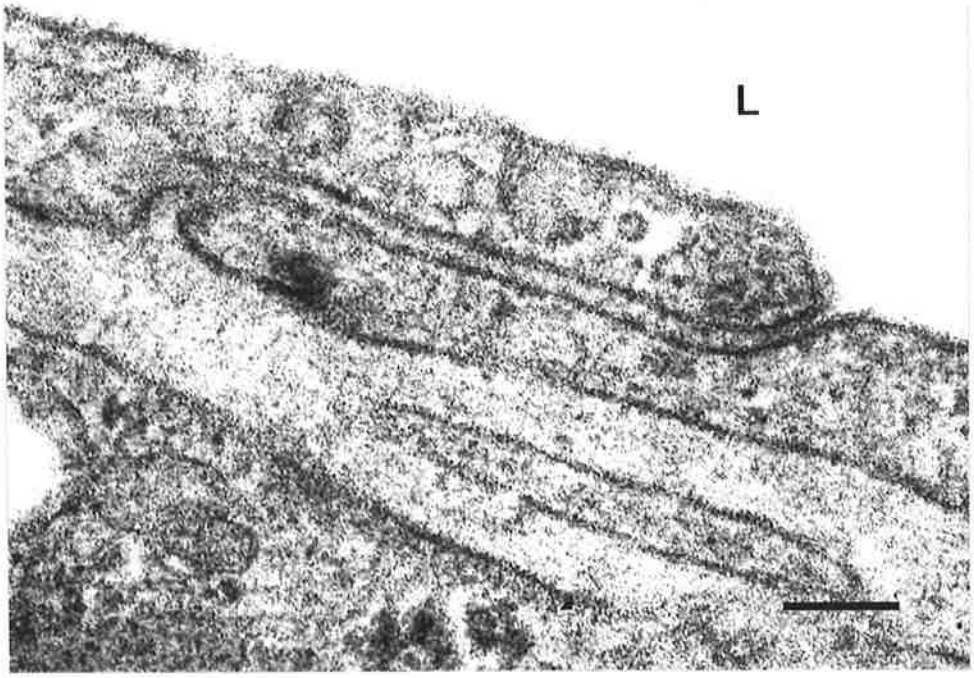

Figure 5.9 (B) Using a goniometer to tilt the same section, illustrated in figure 5.9 (A), 45° clockwise, the two fused areas appear to have a gap between them. This junction was therefore classified as a 'close junction'; L, luminal side. Uranyl acetate and Reynolds' lead stain.
Mag. = x150K Bar = 100 nm

Some junctions between endothelial cells had more than one close region. An example of this is illustrated in Figure 5.10(A) and Figure 5.10(B). Two close regions were identified in this junction, one close to the abluminal side and the other adjacent to the luminal side. Identification of these two regions as close was achieved through tilting of the section.

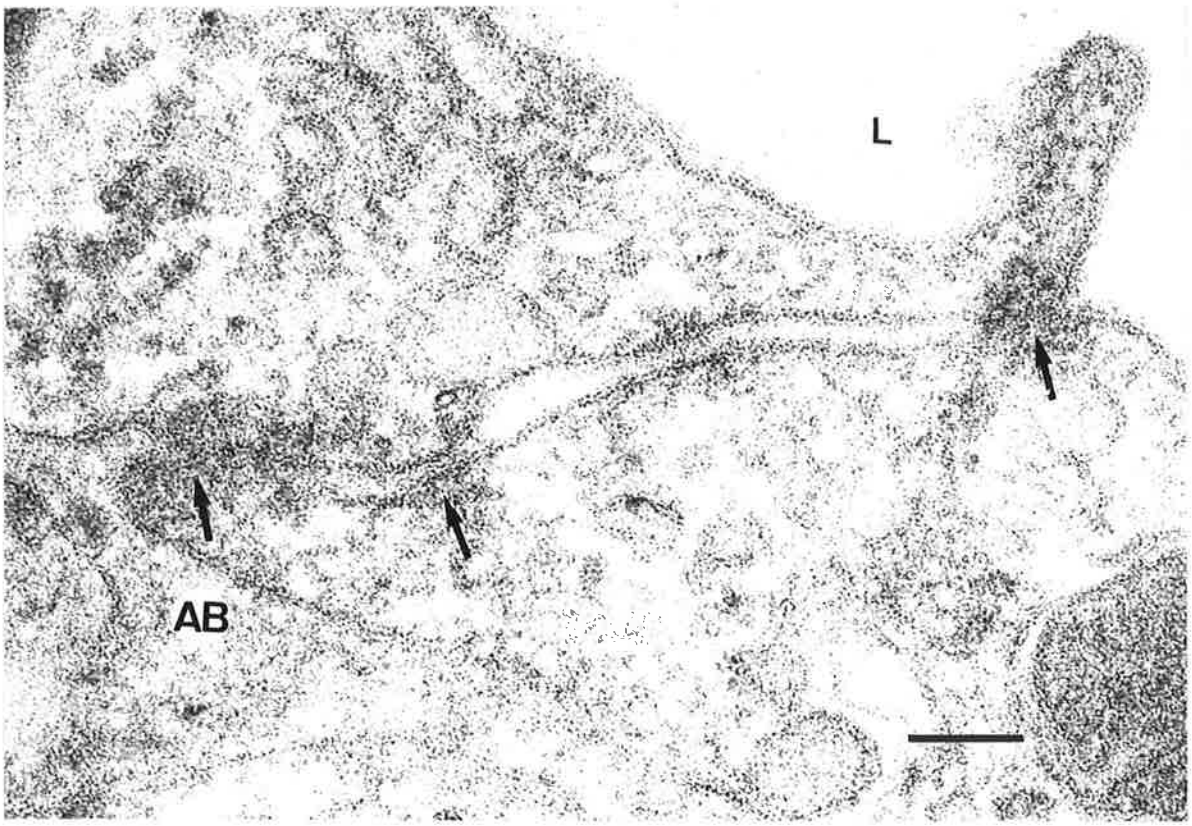

Figure 5.10 (A) A junction from a postcapillary-sized venule with three 'close regions' (black arrows) taken at a tilt of 0°. L, luminal side; AB, abluminal side. Uranyl acetate and Reynolds' lead stain.
Mag. = x150K Bar = 100 nm

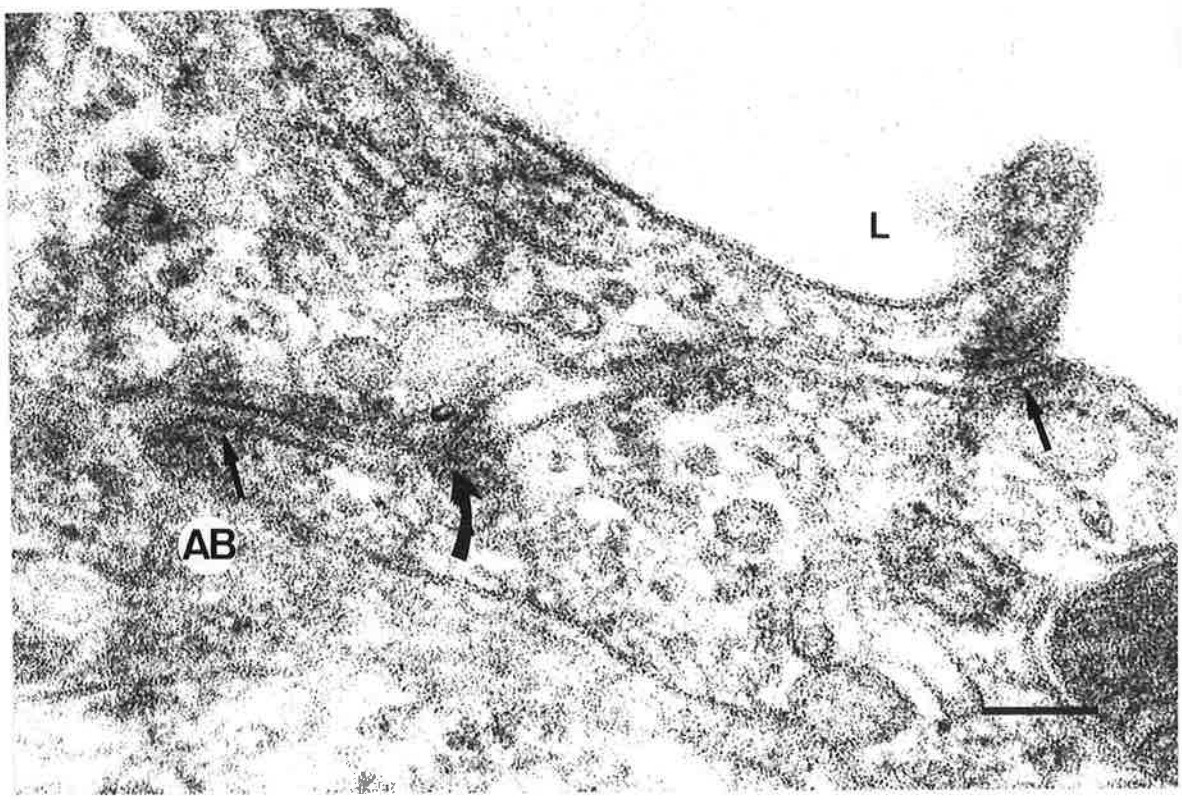

Figure 5.10 (B) A junction from a postcapillary-sized venule with three 'close regions'. The micrograph in figure 5.10 (A) was taken at 0°. After the section was tilted 45° the two opposing membranes of the close region toward the abluminal side (curved arrow) appeared to fuse. Whereas the two opposing membranes of the close region toward the luminal and abluminal side (black arrows) appeared to open. By tilting the section the dimensions of the junction were changed as seen in figure (B). L, luminal side; AB, abluminal side. Uranyl acetate and Reynolds' lead stain.
Mag. = x150K Bar = 100 nm

A chi-square analysis indicated that the junction types changed significantly with age ($\chi^2 = 19.3$, $p < 0.001$). The percentage of tight regions related to the total number of junctional regions (tight and close) was 14.1% ± 3.5% higher in old mice compared with young mice (Table 5.6). There was a significant difference in the close junctions between young and old mice. The proportion of close regions was 14.1% ± 3.5% higher in young mice by comparison with old mice (Table 5.6). The mean percentage of close regions for young and old mice was 88.8% and 74.7%, respectively (Table 5.6). The mean percentage of tight regions for young and old mice was 11.2% and 25.3%, respectively (Table 5.6).

Table 5.6 The mean percentage of tight and close regions in relation to the total number of tight and close junctional regions observed for young and old mice.

Junction Type	Tight	Close
Young	11.2	88.8
Old	25.3***	74.7***
Difference (SD)	14.1 (3.5)	14.1 (3.5)

*** - Significant difference between young and old mice, $p < 0.001$ using a chi-square analysis.

There were significantly ($p < 0.01$) greater numbers of tight regions in the old mice when compared with the young mice at every PDL level (Table 5.7). The ratio of tight to close regions in the old mice is greater than that of the young mice at every PDL level (Table 5.7). Not only did the old mice have more tight regions, but they also have a higher proportion of tight/close regions.

There was a significant but small effect of PDL level (coronal to apical) on the number of close and tight regions for young and old mice ($p < 0.05$) with significantly more tight regions at the alveolar crest and the apex in each group (Table 5.7 and Figure 5.11).

Table 5.7 Effect of periodontal ligament level (alveolar crest to apex) on the total number of close and tight regions for young and old mice.

Level (μm)	Junction	Young	*n*†	Range‡	Old**	*n*	Range	All Mice
0	c§	33	4	5-9	40	4	7-13	73
	t¶	8	4	1-3	21	4	2-8	29*
160	c	31	4	3-13	34	4	8-9	65
	t	1	1	0-1	17	4	2-7	18
320	c	40	4	8-15	40	4	7-15	80
	t	1	1	0-1	14	4	2-4	15
480	c	28	4	3-12	41	4	9-12	69
	t	5	3	0-2	14	4	1-7	19
600-675	c	30	4	2-11	35	4	2-13	65
	t	3	2	0-2	7	3	0-3	10
750-860	c	33	4	3-12	40	4	3-16	73
	t	1	1	0-1	9	3	0-5	10
900-960	c	41	4	6-13	33	4	4-14	74
	t	3	2	0-2	9	3	0-5	12
Apex	c	49	4	7-18	62	4	3-24	111
	t	14	4	3-4	19	4	2-7	33*
Count	c	285		60-91	325		60-116	610
	t	36		7-10	110		20-31	146
Total		321			435			756

* - Significant difference for young and old mice combined, between tight region number at the alveolar crest and the apex compared with other periodontal ligament levels ($p < 0.05$).

** - Significantly greater number of tight regions in old mice at all periodontal ligament levels ($p < 0.01$).

† - Number of mice contributing to the number of junctions at each level.

‡ - Range from the smallest to largest number of junctions found in all mice at each level.

§ - Close region.

¶ - Tight region.

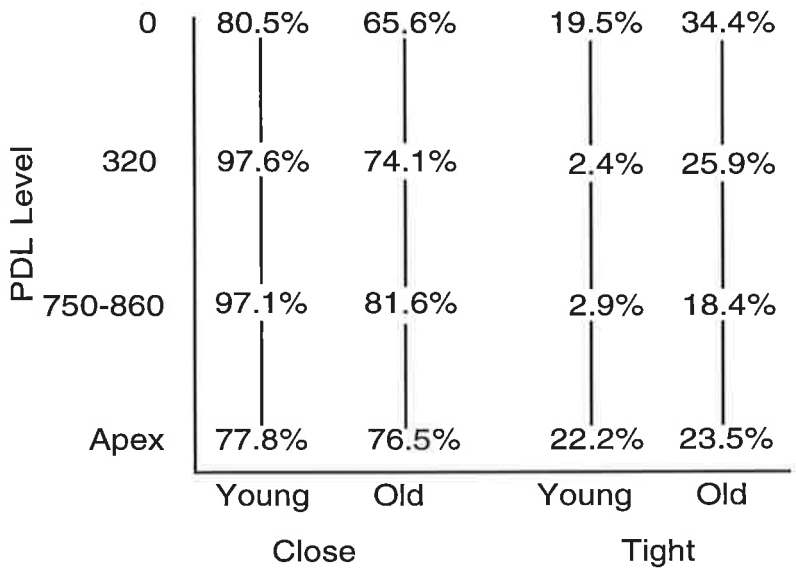

Figure 5.11 Summary of the percentage of close and tight junctions in relation to the total number of junctions observed for young and old mice against the periodontal ligament (PDL) level (μm) from the alveolar crest to the apex (summarised from Table 5.7).

Tight regions (86.1% in the young mice and 90.0% in the old mice) and close regions (66.7% in the young mice and 65.5% in the old mice) were largely confined to the luminal third of the PCV ($p < 0.05$), as shown in Table 5.8.

Table 5.8 Relationship between junction type and location of the junction region (tight or close) within the luminal third, middle third and, abluminal third of the junction.

Age	Junction Type	Region		
		L1/3	M1/3	Ab1/3
Young	Close	190*	54	41
	Tight	31*	1	4
Old	Close	213*	66	46
	Tight	99*	6	5

* - Significant difference between tight and close region number in each group in the luminal 1/3 compared with the middle and abluminal thirds, $p < 0.05$.

5.5 Junction Dimensions

5.5.1 Junction Length

Age had no significant effect on the length of the junctions. However, there was an effect of PDL level (Figure 5.12 and Appendix 4 in Table 8.4.2). For both groups at the level of 160 μm, the junction length was longer than at other PDL levels, however, overall this effect was not significant.

5.5.2 Junction Thickness

There was no significant effect of age. However, there was a significant effect ($p < 0.05$) of PDL level (coronal to apical) in both groups (Table 5.9). An examination of Figure 5.12 indicates a trend from slightly above average thickness at depth 0 μm, rising to a maximum at depth 160 μm and then steadily declining towards the apex in young and old mice.

5.5.3 Length:Thickness Ratio - 'Meander'

'Meander' was defined as the log of the ratio of the junction length to the thickness (Appendix 4, Table 8.4.2). There was a difference between depths within each group, however, this was not significant.

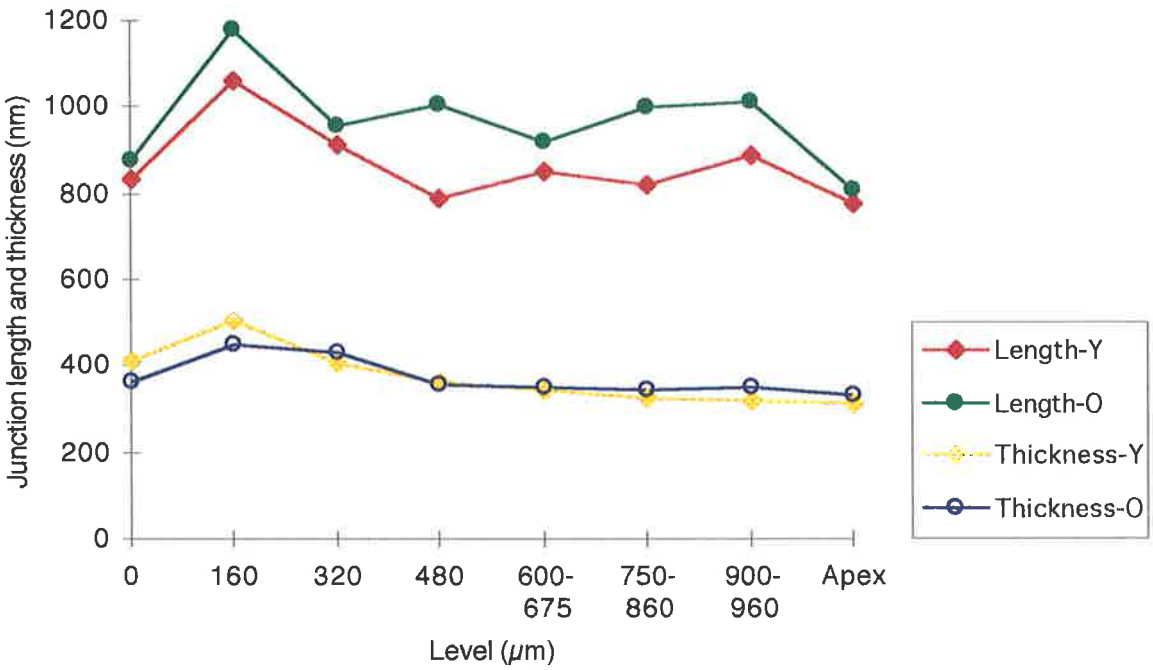

Figure 5.12 Plot of the mean junction length and thickness (nm) against periodontal ligament level (μm) from the alveolar crest to the apex, for young and old mice.

5.5.4 Junction Width

There was a significant effect of age and PDL level (coronal to apical) on junction width 2 (W2), that is, a third of the distance along the endothelial junction from the luminal to the abluminal side of the PCV. At the apex, W2 was 3.6 nm ± 0.88 nm wider in the old mice than in the young mice ($p < 0.05$) as shown in Table 5.9 and Appendix 4, Table 8.4.1. There was a significant ($p < 0.05$) difference of PDL level (coronal to apical) in junction width 1 (W1) for young and old mice. Junction width 1 increased in each group with increasing PDL level, from a low value (18.7nm in young mice; 21.7nm in old mice) at the alveolar crest, to a high value (26.2nm in young mice; 23.3nm in old mice) at the apex (Table 5.10). Junction width 2 (W2) also increased significantly ($p < 0.05$) with increasing PDL level (Appendix 4, Table 8.4.1) from a low value at the 960 µm PDL level (16.3nm in young mice; 19.5nm in old mice) rising sharply at the apex (20.5nm in young mice; 24.1nm in old mice).

Table 5.9 Summary of changes in junction width 1 (JW1), junction width 2 (JW2) and junction thickness (J Thickness) with periodontal ligament level for young and old mice. Values represent arithmetic means with standard errors in parenthesis. Complete data are presented in Appendix 4, Tables 8.4.1 and 8.4.2.

Level	J Thickness		JW1		JW2	
(µm)	Young*	Old*	Young	Old	Young	Old
0	413.4	365.1	18.7	21.7	17.1	20.5
	(30.1)	(38.0)	(0.5)	(1.1)	(1.0)	(1.0)
320	410.3	432.5	20.6	19.8	18.2	20.1
	(34.6)	(44.6)	(2.7)	(3.2)	(0.6)	(0.6)
750-860	328.9	345.3	24.6	20.0	18.6	18.8
	(26.8)	(33.2)	(3.9)	(1.9)	(1.5)	(0.8)
Apex	325.5	328.9	26.2†	23.3†	20.5‡§	24.1§
	(32.1)	(33.0)	(0.2)	(2.3)	(1.0)	(3.0)
Mean	372.2	372.4	22.8	21.7	18.1	20.3

* - Significant decrease in junction thickness from the alveolar crest to the apex for each age group ($p < 0.05$).

† - Significant increase in junction width 1 at apex by comparison with the alveolar crest for each age group ($p < 0.05$).

‡* - Significant increase junction width 2 at the apex in old mice by comparison with young mice ($p < 0.05$).

§ - Significant increase in junction width 2 at the apex by comparison with other periodontal ligament levels for each age group ($p < 0.05$).

5.5.5 Junction Size

There was no effect of age on junction size. There was no difference in the junction size regardless of the PDL level studied, or the type of junction studied. The junction size data specific for each PDL level for both tight and close junctions are shown in Table 5.10.

Table 5.10 Size (nm) of junctional regions (tight and close) at different periodontal ligament levels from the alveolar crest to the apex, for young and old mice.

PDL level	Young		Old	
0	29.4† (2.7)	29.4‡	26.9 (0.7)	26.7
160	32.9 (2.0)	31.6	28.8 (0.8)	28.4
320	27.2 (1.9)	27.7	28.1 (1.2)	28.2
480	26.1 (1.3)	25.8	28.5 (4.0)	28.5
600-675	29.0 (2.1)	29.6	29.7 (3.0)	29.7
750-860	29.4 (2.0)	30.5	28.4 (1.9)	27.1
900-960	27.5 (1.7)	27.1	27.7 (2.3)	28.1
Apex	26.0 (1.1)	27.1	29.2 (3.8)	29.8

† - Arithmetic means of tight and close regions with standard error values in parentheses. These values for tight and close regions were combined as there was no significant difference between the size of tight and close regions as shown in Table 5.11

‡ - Mean values calculated using analysis of covariance. They were adjusted because of different numbers of values at various periodontal ligament levels (Section 4.5).

No significant difference was found between junction size in each region of the junction , that is, luminal, middle and abluminal thirds, as shown in Table 5.11. Tight regions were typically 2.8 ± 2.4 nm shorter than close junctions in each region, but this difference was not significant.

Table 5.11 Junction size (nm) of tight and close regions located in young (Y) and old (O) mice located in the luminal third (L1/3), middle third (M1/3) or abluminal third (Ab1/3) along the length of the endothelial junction.

Age	Junction Type	Region Location					
		L1/3		M1/3		Ab1/3	
Y	Close	28.9†	28.9‡	29.4	29.4	27.2	26.5
		(0.7)		(0.8)		(2.2)	
	Tight	25.0	24.9	16.6	16.6	23.3	23.5
		(1.0)		§		(3.0)	
O	Close	28.8	28.5	29.5	29.3	31.0	28.5
		(1.2)		(0.7)		(2.9)	
	Tight	27.9	27.8	28.6	27.5	28.1	26.8
		(1.3)		(2.4)		(3.3)	

† - Arithmetic means with standard error values in parentheses.

‡ - Mean values calculated using analysis of covariance. They were adjusted because of different numbers of values at this periodontal ligament level (Section 4.5).

§ - n=1 at this location for young mice.

CHAPTER 6 DISCUSSION

6.1 General Discussion

6.1.1 Mouse as an Experimental Model

The mouse model for investigating the PDL microvasculature with ageing has been used by a number of previous studies (Masoro *et al.*, 1981; Sims *et al.*, 1992a; 1992b; 1993). Hazzard *et al.* (1992) suggested that there are no perfect animal models for ageing research because animal models are not completely isomorphic to the human condition. The authors stressed the need for multiple animal models in order to broaden scientific knowledge of an animal species in its own right, and also its application to the study of ageing in general. Extrapolating findings from animal models to human conditions is based on representation over a broad number of different species of various aspects of human functions.

The molar eruption pattern and dentition are similar for mice and rats which have a full complement of teeth by 35 days (Navia, 1977). By one year old, mice show signs of an ageing dentition, such that teeth are worn, some teeth have exfoliated or have periodontal disease and bone loss (Sims, personal communication, 1993).

6.1.2 Retention, Participation Aspects

Reduction in the sample numbers may occur via damage to the specimen during preparation, processing and TEM study. Possible ways damage may occur are: (1) contamination of the specimen, (2) removal of material from the specimen via ionisation of water vapour by the electron beam, (3) radiation damage with the electron beam, and (4) failure to precondition a specimen in the TEM. To minimise damage, the electron microscopes used were fitted with anticontamination devices and one field of the specimens was not viewed for lengthy periods of time, particularly at high magnification levels.

6.1.3 Fixing Agents and Endothelial Junctions

In the present study, tissues were fixed simultaneously with glutaraldehyde and osmium tetroxide which has been shown to reduce lipid extraction and cell shrinkage (Trump and Bulger, 1966). The advantages of using these simultaneous fixatives are as follows (Franke *et al.*, 1969):

1) Increased contrast of membranes and other lipid containing structures,
2) Preservation of nucleoprotein structures, for example, ribosomes and chromatin strands,
3) Preservation of cytoplasmic microtubules,
4) High staining of polysaccharide containing structures, and
5) Elimination of precipitation contaminants caused by fixation.

Perfusion fixation was used in the present study because:

1) Osmium tetroxide and glutaraldehyde preserve tissue to a depth of 0.25 mm and 0.5 mm, respectively (Glauert, 1978; Hayat, 1981). Therefore, immersion fixation is unsuitable to preserve the PDL.
2) It results in uniform fixation of tissue required for electron microscopy (Veerman, 1974).

Demineralisation using EDTA at 4°C in the present study, has been shown as the best procedure to reduce the amount of cellular dissociation (Fejerskov, 1971). Tissue dehydration commenced with 70% ethanol, which has been demonstrated to eliminate dimensional changes of cells (Weibel and Knight, 1964). The epoxy embedding materials used in this study reduce block shrinkage, and impart dimensional stability in the electron beam (Williams, 1977). According to Williams (1977), the heavy metal stains, modified Reynolds' solution and uranyl acetate used in the present study, reduce underestimation of tissue features due to poor section contrast.

6.1.4 Sample Size

Tissue samples previously prepared for TEM by Freezer (1984) and Sims *et al.* (1992 a, b) were evaluated. An initial pilot study of the specimens was completed, taking approximately four months, using the JEOL 100S to (1) evaluate the condition of the material and (2) assess the number of different blood vessel types for selection of an adequate study population. The findings of the pilot study, which are tabulated in Appendix 2, resulted in the selection of pericytic and apericytic PCV as the sample population that were found to possess adequate numbers at each level (section 6.3.2).

6.2 Accuracy in Measuring Method

6.2.1 The Interpretation of Two Dimensional Images from Three Dimensional Structures

The profile of an object in a ultramicrotome section is only a thin slice through that object. Cross-section profiles of endothelial junctions observed in ultra-thin section electron microscopy exhibit zones of apparent fusion and discrete gaps between membranes corresponding to tight and close regions. Magnification of muscle capillary endothelial cells at x450K did not reveal additional structural details of tight junctions (Pinto da Silva and Kachar, 1982). According to a recent review, the question of whether the composition of tight junctions represent lipidic structures or that proteins are involved in their formation and function remains open (Schneeberger and Lynch, 1992).

Measuring the width of a junction accurately requires the opposing membranes to be viewed at right angles (Figure 6.1). The apparent width of a junction will increase with the amount of obliqueness of the section and the membrane edges become less well defined (Weakley, 1981). Endothelial junctions are three-dimensional objects rather like a cranial suture. One part of the junction may be at right angles to the plane of section while another part is not.

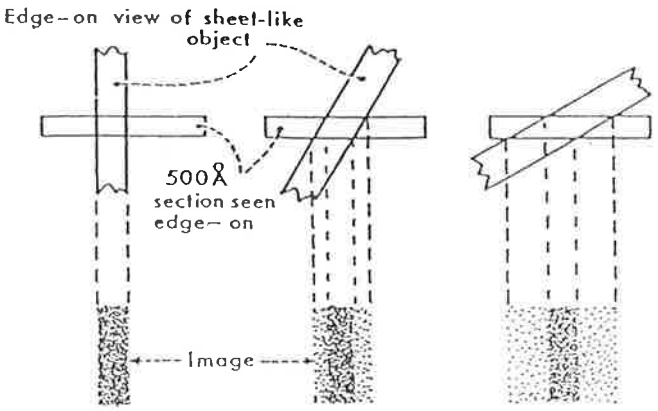

Figure 6.1 The dimension and definition of a sheet-like tissue section can vary when viewed at different angles through a section (Weakley, 1981).

6.2.2 Section Thickness

Contrast conditions and section geometry are important factors in the accuracy of measurements in electron microscopy (Palade *et al.*, 1979). Ultra-thin sections 70 nm thick were used in the present study. These are required to identify contact or separation between the plasmalemma membranes. If sections are too thick, fewer gaps and spaces between adjacent "unit membranes" can be distinguished. According to Bundgaard (1984), to identify a discrete gap in the line of contact, it must extend more than 50% through the thickness of the section. The criteria, used in the present study, to distinguish tight and close regions were areas of fusion of the opposing endothelial cells' outer lamellae, and separation of the outer lamellae by a gap of 6 to 8 nm, respectively (section 4.4.1).

6.2.3 Stained Sections

The depth that the stain penetrates the sections can affect contrast. According to Casley-Smith (1983), the majority of stains only penetrates the first 4 nm of a section. Therefore, sections are effectively 4 nm thick. Clough (1991) reported that staining techniques in different studies may account for differences found in the widths of endothelial junctions.

6.2.4 Goniometer

Endothelial junctions can be studied and tilted using a manual goniometer. This facility is essential for exploring the narrowest portions of junctions for accurate classification of each junction. Tight appearing regions of junctions may falsely appear to fuse because the standardised plane of sectioning of irregular PDL vessels used in this study may result in irregular cross-sectioned junctions during routine cutting. By manually tilting the specimen around a single axis with the goniometer, true fusion of the narrowest portions of opposed plasma membranes can be observed allowing definition of tight or close regions. However, as a specimen was tilted, the dimensions of the junction under observation changed. Therefore, measurements were taken from prints with zero tilt to standardise the measurement technique.

Simionescu *et al.* (1978) found a greater number of close junctions in postcapillary venules than in capillaries, whereas Casley-Smith (1983) reported equal numbers in capillaries and postcapillary venules using a goniometer. Casley-Smith (1983) attributed these differences to "the difficulties of observing close regions in the more convoluted junctions of

capillaries without using a goniometer stage." In the present study, use of a goniometer enabled accurate distinction between tight and close regions.

6.2.4.1 Effect of a Goniometer with a Rotation Facility on Tight and Close Region Classification

It has been reported that accurate distinction between tight and close regions is possible only when these junctional regions are viewed in a goniometer that allows observation of the junctional regions by tilting a specimen around an axis that is at 90° to the original tilt axis (Casley-Smith, personal communication, 1994).

A newly installed Phillips CM-100 TEM, possessing a goniometer with a rotation capability became available after completion of the collection and analysis of quantitative data on the endothelial junctions in the present study. This TEM enables the junctions to be viewed using a manual tilt goniometer to tilt the specimen around a single axis from 0°, through +60° or -60° and back to 0°. The specimen can then be rotated 90° and subsequently tilted through +60° or -60°. This effectively allows exploration of junctional regions through double axes at 90° to each other (x-y axes). A pilot survey of endothelial tight junctions was subsequently undertaken to confirm that these junctions had been accurately identified.

The results of this survey indicated that any alteration in the classification of junction type, and reinvestigation of the tight and close junctions classification, is not warranted. Figure 6.2 shows electron micrographs of one of the junctions viewed using both a single axis and a double axes goniometers. These findings suggest that single axis and double axes goniometers are equivalent with respect to measurement and classification of junctions.

Casley-Smith *et al.* (1975) raised the issue of the lengthy time involved in recording information on junction morphology using a double axes goniometer. It is noteworthy that he considered that this needed to be weighed against the accuracy of the information collected, and that 'the time involved speedily became quite disproportionate to the value of the information'.

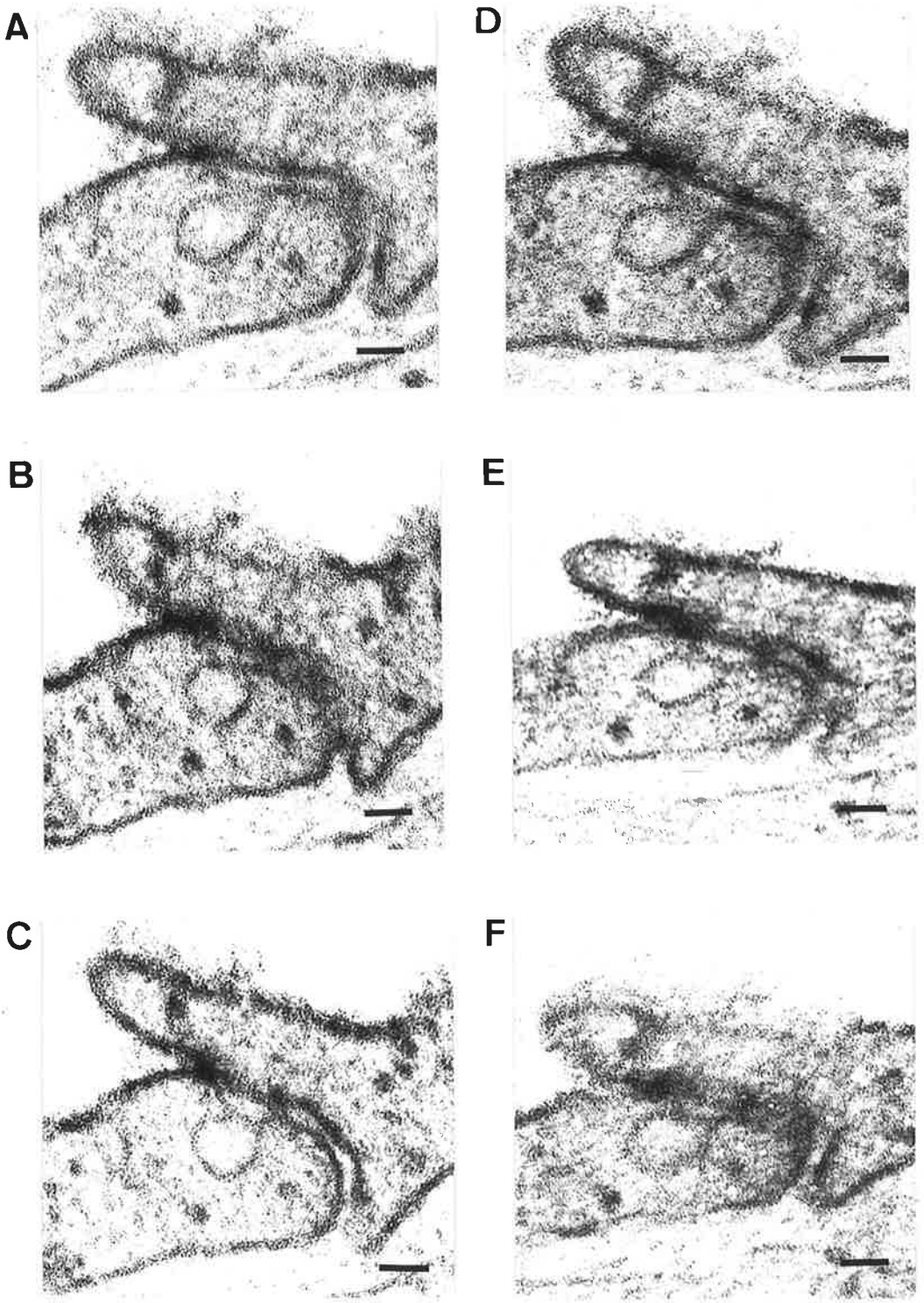

Figure 6.2 Electron micrographs of one endothelial junction with a tight region. A, B, and C represent views using a single axis goniometer; A: O°, B: +45° axis tilt, C: -45° axis tilt. D, E and F represent views of A, B and C rotated 90° in a double axes goniometer; D: O°, E: +45° axis tilt, F: -45° axis tilt. Note that the apposing plasma membranes at the tight region remain fused in all views. Mag = x150K Bar = 50 nm

6.2.5 Resolution and Accuracy of the Electron Microscope

The resolution of an electron microscope was formerly stated to be rarely better than 10Å (Casley-Smith, 1983). Therefore, tight regions may have undetected channels that pass through them. However, the resolution of the electron microscopes used in the present investigation were:

JEOL 100S	5Å
JEOL 2000FX	2.8Å
PHILLIPS CM-10	3.4Å

The polar heads of the amphipathic lipids of the bilayer and domains of membrane proteins immediately adjacent to it form the dense outer leaflet of the plasmalemma membrane. However, membrane glycoproteins up to 100Å, that extend above the plane of the outer leaflet, may not be discernible, for example, glycophorin of the erythrocyte plasmalemma (Marchesi *et al.*, 1976).

The small pore system of microvessels appear as patent channels across the endothelium separated by a gap of ~ 4 nm (Simionescu *et al.*, 1978) to ~ 6 nm (Casley-Smith, 1983). Hence, measurements made on electron micrographs give an indication of the size of given spaces. However, precise and definitive measurements of spaces between adjacent 'unit membranes' are difficult to make and extrapolation of results to *in vivo* must be viewed with caution (Palade *et al.*, 1979). Therefore, allowance has to be made for the finite resolution of the electron microscope, for the random angle at which the sections are taken and finally for the depth of penetration of stain into the sections.

6. 3 Blood Vessels

6.3.1 PCV Morphology

6.3.1.1 PCV Type

There was no effect of age on the PCV type, that is, apericytic or pericytic. However, there was a significant PDL effect. In young and old mice groups a significantly increased ($p < 0.05$) number of pericytic PCV, relative to the total number of PCV, was found at the alveolar crest by comparison with the apex. Apericytic PCV were more common overall. These findings of the current study were consistent with Freezer and Sims (1987) who found 70% of PCV were apericytic and 30% of PCV had associated pericytes. The PCV types differed between the lateral zones of the PDL. The few PCV in the tooth third

were with a single exception of the apericytic type. Freezer and Sims (1987) reported an absence of any pericytic PCV in the tooth third.

An increased number of pericytes surrounding endothelial cells is related to the increased degree of tightness of the interendothelial junction, that is, 'the better the microvascular barrier' (Shepro and Morel, 1993). Findings of the current study may result in variable tightness of the microvascular barrier across and down the PDL due to: (1) the larger number of apericytic PCV in the tooth third in the old mice, and that in young and old groups (2) the decreased proportion of pericytic to apericytic PCV in the tooth third by comparison with the middle and bone third , and (3) the decreased proportion of pericytic to apericytic PCV at the apical region by comparison with the alveolar crest.

It is suggested that the increased apericytic PCV in old mice may be a compensatory effect to increase vessel permeability. Therefore, more apericytic PCV in the aged mice may balance the increased number of tight regions found in the current study (section 6.4.1). In other words, in the aged mice PCV there are more junctional regions with fewer pericytic cells. However, it should be noted that an increase in the number of tight regions simply may be due to an increase in the number of endothelial cells per unit area of PCV. Investigation of the number of endothelial cells per unit area of PCV in young and aged mice is necessary to determine whether changes in numbers of endothelial junctions are correlated with endothelial cell numbers.

It may be postulated that alterations in the proportions of pericytic PCV to apericytic may indicate the PCV vessel wall becomes more permeable from the alveolar crest to the apex. As the mean number of tissue channels per μm^2 (MNTC/μm^2) increase with increasing interstitial fluid flow (Cooper *et al.*, 1990; Tang and Sims, 1992), if there is increased permeability of PCV in the apical regions, there would be an increase in the MNTC. However, Tang and Sims (1992) did not demonstrate any significant difference in the MNTC with increasing depth of normal rat PDL. This contrast may be due to species differences, or other factors important in controlling permeability, for example, distribution of junction type and/or other PDL microvessels that maintain a consistent amount of fluid flow, and not alterations in the MNTC with increasing depth of PDL. It may be postulated that the PCV vessel wall may have heterogenous permeability for the lateral zones of the PDL, that is, PCV permeability in the tooth third > middle third < bone third, and PCV

permeability in the tooth third is greater than the bone third of the PDL. The impact of this proposed alteration of the permeability of the PCV on the PDL permeability needs to take into account the distribution of PCV across the PDL. The numbers of PCV have been shown to increase from the tooth third to the bone third (section 5.3; Freezer and Sims, 1987). Therefore, it is suggested that the limited number of PCV in the tooth third are apericytic and are more permeable, while the bone third contains a greater proportion of pericytic PCV compared with the tooth third, suggesting less permeability. However, the majority of PCV in the bone third (which contains most PCV compared with the tooth third) are apericytic, and therefore, more permeable. Consistent with this hypothesis, is the reported steady increase in the MNTC/μm^2 from tooth third to the bone third of the rat PDL (Tang and Sims, 1992).

Further investigation is required to assess microvessel permeability in young and old mice in conjunction with assessment of cleft per unit area. This would be valuable by providing further morphological data on the blood vessels (including PCV) in the PDL, as it has been found that there is an increase in volume, length and surface density of pericytic and apericytic PCV in old mice by comparison with young mice (Sims, unpublished data, 1995). It is necessary to investigate these aspects to determine whether changes in volume, length and surface density of these vessels are associated with concomitant changes in junction number and the current findings of altered junction widths, proportion of apericytic and apericytic PCV and close and tight junctions with age.

6.3.1.2 PCV Diameter

There was no significant effect of age on PCV luminal diameter. The PCV diameters measured in the current study were smaller by comparison with those reported by Freezer and Sims (1987) which averaged 20.9 μm for PCV. However, it should be noted that in their calculation of average PCV diameter, collecting venules were included resulting in increased values. The diameters for PCV reported by Freezer and Sims (1987), and found in the present study, fall within the quoted ranges for PCV diameters (Rhodin, 1968; Simionescu and Simionescu, 1984; section 3.2.1).

6.3.2 Number and Location of PCV

The number of PCV differed between the lateral areas of the PDL with a significant increase in the number of PCV located in the tooth third in the old

mice. Another significant variation in PCV number that was demonstrated involved the middle circumferential third in the young mice. There was a steady reduction in PCV numbers from the alveolar bone to a minimum at the mid-point of the PDL, followed by a steady increase in numbers to the apex. The implications of this in relation to masticatory function need to be investigated. The absence of this trend in the old mice, where the numbers of PCV did not reduce in the middle circumferential third down the length of the PDL, was consistent with an increase in the vascularity of the PDL with age (Sims, unpublished data, 1995).

The current findings are consistent with the anisotropic distribution of the PDL microvascular bed of mice and humans. The number of PCV in young mice sampled in the current study was found to coincide with the volume distribution of PCV (that is, number of PCV per unit area) previously reported (0% in the tooth third, 25% in the middle third and 75% in the bone third; Freezer and Sims, 1987). The sampling techniques were different for the two studies. Namely, the current study sampled five PCV at each level while Freezer and Sims (1987) stereologically assessed all microvessels at each level. The similar findings of the two studies indicated that the TEM section oritentation and sample size used in the current study approached randomness by adequately representing the PCV population in the PDL.

6.4 Endothelial Junctions

Vascular endothelium is considered a simple squamous epithelium joined into a continuous vessel by junctional regions between adjacent cells. These junctions are continuous around each endothelial cell. However, they are seen in cross-section in the electron microscope. Junctions may vary considerably from a reasonably straight gap between adjacent cells to very convoluted configurations (section 5.4).

The types of junction found in this study were: (1) junctions with tight regions, (2) junctions with close regions, (3) junctions with tight and close regions, and (4) junctions with no tight or close regions where the opposing membranes along the length of the junction were separated by a space larger than a close region which was often uniform. No open or gap junctions were found. These current findings were supported by the endothelial junctions identified in rat PDL (Chintakanon, 1990). Studies of endothelium of other oral tissues, namely cat and human pulp blood vessels with thin sections and a

freeze-fracture technique, did not find any gap junctions in the endothelium (Ekblom and Hansson, 1984). However, numerous gap junctions are found in arterioles and larger arteries, for example, the pulmonary vascular bed (Schneeberger and Lynch, 1992), but gap junctions are reported not to be present in capillaries and pericytic venules (Simionescu *et al.*, 1975).

6.4.1 Tight Regions

Tight regions constituted 11.2% for young and 25.3% for aged mice. This percentage for the young mice are slightly lower than the findings of Chintakanon and Sims (1994) where tight regions comprised 14.2% of the total junctions in PCV of normal rat maxillary molar PDL. However, species variation may explain this difference.

The junction types changed significantly with age. The percentage of tight regions was 14.1% ± 3.5% higher in the old mice. The old mice also had significantly greater numbers of both tight regions consistently at all PDL levels. The tight/close region ratio in the old mice (1:3.0) was greater than young mice (1:7.9). There was a significantly greater percentage of tight regions in young and old mice at both the alveolar crest and the apex.

Endothelial junctions of PCV provide important avenues for fluid movement across tensioned endothelial walls of the PDL microvascular bed (Cooper *et al.*, 1990; Tang *et al.*, 1993). Tang and Sims (1992) showed that a significant increase in MNTC/μm^2 in tensioned rat PDL reduced from the alveolar crest to the apex where MNTC/μm^2 for normal and tensioned PDL were comparable. Total junction number/μm was positively correlated with tissue channel/μm^2 in normal and tensioned PDL (Tang *et al.*, 1993). The increase in proportion of tight regions in the present study at both the alveolar crest and the apex may be important in relation to the PDL under tension as these two areas receive greatest pressure during lateral masticatory and orthodontic tipping movements. These tight regions may represent a functional adaptation to prevent, or reduce, an increase in pressure at these locations as a result of function. Chintakanon and Sims (1994) demonstrated that tight regions did not change after applying a continuous 30 minute tension load of 1.0 N and suggested that tight regions are permanent structures. The results of the present study support the findings of Chintakanon and Sims (1994) which indicate that the change in number of tight regions at the alveolar crest and the apex is not as a result of short-term mechanical stimuli as both groups of mice demonstrated this alteration.

The number and morphology of tight regions vary among different microvascular beds and has been correlated to the permeability of epithelia (Claude and Goodenough, 1973; Schneeberger and McCormack, 1984) and endothelium (Shivers, 1979; Rippe and Haraldsson, 1994). The permeability of capillaries to transvascular fluid, micromolecular and macromolecular movement has been shown to decrease with age (Duran-Reynals, 1946; Wangensteen *et al.*, 1977; Matalon and Wangensteen, 1977; Hruza, 1977). The significant increase in the number of tight regions found in the current study may result in decreased permeability of the PDL microvasculature. Tracer studies are needed to confirm whether there is decreased permeability of aged PDL. It is possible that the increased number of tight junctions is in part an adaptive response to balance other changes that increase microvasculature permeability, for example, decreased vessel wall thickness (Sims, 1992a; section 3.6), decreased diffusion pathway (Sims, 1993; section, 3.6), or the increase in the number of tooth third apericytic PCV in old mice PDL in the current study (section, 6.3.1.1). Stated another way, the increased number of tight junctions may be important in the maintenance of homeostasis.

Tight regions were mainly found in the luminal third of the junction which was similar to findings in the rat (Chintakanon and Sims, 1994). This contrasts with findings in other oral tissues where tight regions in feline and human pulp venules were found localised in the luminal or abluminal third or both (Ekblom and Hansson, 1984). It appears that tight regions were located at various sites within rat heart venule endothelial junctions forming a complex 'network of lines of contact' between adjacent endothelial cells (Bundgaard, 1984). Masticatory loads potentially may force fluid and molecules out of PCV and into tissue spaces and channels. The predominant location of tight junctions in the luminal third may be hypothesised to play a role in the PDL fluid system considered important in tooth support for functional loads up to 1.0 N (Wills *et al.*, 1976).

There was no effect of age on the junction size, that is, the length of close or tight regions, nor was there an effect of PDL level. The current findings of discrete close or tight regions within endothelial junctions were consistent with a 'zone of fusion' as opposed to punctate fusion sites in rat PDL (Chintakanon and Sims, 1994) and in dental pulp (Tabata and Semba, 1987).

6.4.2 Close Regions

There was a significant effect of age on the number of close junctions. The percentage of close regions was 14.1% higher in the young mice compared with the increased number of tight junctions in old mice. The percentage of close junctions in PCV of mice PDL from the current study was similar to that of Chintakanon and Sims (1994). Namely, close junctions represented 84.4% of junctions in the normal rat PDL and 78.4% in the tensioned PDL. It is expected that the greater number of close regions in PCV of young mice may result in increased permeability of young mice PDL microvasculature.

There was a significantly reduced number of close regions at the apex and alveolar crest. There was no change in the junction size of close regions regardless of the location along the length of the junction. Numbers of close regions were greatest in the luminal third (66.1%), reducing gradually from middle third (19.7%) to abluminal third (14.2%) along the length of the junctions. There was no effect of PDL level on the numbers of close junctions.

6.4.3 Junction Length

The length of endothelial junctions is inversely proportional to the vessel permeability (Bundgaard, 1988; section 3.5). Generally there was a reduction in junction length, however, there was no significant difference between age groups or with increasing PDL level. The decreasing junction lengths paralleled the reduction in PCV vessel wall thickness (section 6.4.5), suggesting increased permeability from crest to apex. There was no evidence to demonstrate an increase in junction convolutions leading to increased junction length, while the junction thickness decreased after 160 μm with increased PDL level.

6.4.4 Junction Thickness

There was no significant effect of age on junction thickness. However, there was a significant effect of PDL level, such that in all mice there was an increase in thickness from the alveolar crest to the 160 μm PDL level. From the 160 μm PDL level there was a steady decrease in thickness to the apex, in the young and old mice. These current findings of junction thickness changes in conjunction with the decreased proportion of pericytic PCV, decreased number of tight regions (except for an increase at the apex), a decreased junctional length and increased junctional width are consistent with increased permeability of PCV with progressive depth of mouse PDL.

The increased permeability towards the apex may be important in allowing adequate outflow of fluid from the microvasculature into the tissues to dissipate forces associated with masticatory load (section 6.4.1). Tracer studies and tissue channel mapping from the alveolar crest to apex of PDL under various loads are necessary to confirm this concept.

6.4.5 Junction Length to PCV Wall Thickness Ratio - 'Meander'

As noted previously (section 5.5.3), the length of the endothelial junction is greater than the thickness of the PCV endothelium at the junction site. This feature occurs because the majority of junctions have either an oblique, straight, or a tortuous convoluted pathway, from the luminal to abluminal sides. The variable, termed 'meander', was defined as the ratio of the junction length to the PCV thickness at the junction (section 4.4.3.3). There was no significant effect of age or PDL level on this ratio (section 5.5.3).

6.4.6 Junction Width

The junction width is directly proportional to the vessel permeability (Bundgaard, 1988). There was a significant increase in young and old mice, in junction width at the luminal entrance from the alveolar crest to the apex. A significant increase in young and old mice in junction width at position two (a third of the distance along the length of the junction from the lumen) was demonstrated at the apex. At the apex, the junction width at position two was significantly wider in older mice than younger mice. Together, these junction width changes suggested increased permeability with depth of PDL in young mice and an increased permeability of older mice at apical regions only. The findings of Cooper *et al.*, (1990), which demonstrated increased tissue channels in the apical regions of tensioned PDL, support the proposal of increased permeability of microvessels at the apex associated with function (Picton, 1986).

6.5 Suggestions for Future Research

An increase in the number of tight junctions in the aged mice was found in the current study. This supports the reported decrease in permeability of the microvasculature with age (Hruza, 1977). However, it may be proposed that an increase in the number of tight regions with age may be compensated for by the increased junction width a third of the distance from the lumen (JW2) in aged mice and may represent a functional modification to balance a reduced vascular permeability in aged PDL. The findings of this investigation raise questions regarding the functional effects of the significant differences in the number of tight junctions that were found. It may be that tight regions

in the aged mice have the same functional capacity as tight regions in the young mice.

The implications of the changes in junction dimensions and the location and number of pericytic PCV require investigation to provide a more comprehensive picture of some of the factors involved in PDL function. In particular, PDL functions that are relevant to changes in vascular permeability include the role played in: masticatory function, orthodontic tooth movement, continued tooth eruption to maintain occlusal contact, root resorption, and development and progression of periodontal disease. Aspects of these functions could be investigated under varying age conditions to determine whether age changes have functional implications.

Investigation of endothelial junction morphology provides information on only one aspect of microvessel permeability. As noted previously (section 3.5), Simionescu and Simionescu (1984) defined transmembranous (directly across the endothelium) and extramembranous routes (transcellular vesicles, channels, fenestrae and diaphragms, and intercellular endothelial junctions) for the exchange of water, gases, ions and small hydrophilic molecules. Therefore, investigation of various aspects of PDL permeability under the various conditions listed above may include study of:

- the relationship of morphological features of close and tight junction distribution and (1) dimensions in other PDL microvessels using stereological principles (Casley-Smith *et al.*, 1975), (2) the distribution of fenestrae (Casley-Smith, 1983; Simionescu and Simionescu, 1984), and (3) the development of tissue channels (Cooper *et al.*, 1990; Tang *et al.*, 1993);
- variations in blood pressure in aged tissue microvessels or under masticatory load (Rippe and Haroldsson, 1994);
- application of more recent models of microvessel permeability to previously collected morphological data (Tsay *et al.*, 1989; Wienbaum *et al.*, 1992).

CHAPTER 7 CONCLUSIONS

1) The types of endothelial junction that were found in this study included:
   1. Junctions with close regions
   2. Junctions with tight regions
   3. Junctions with both close and tight regions
   4. Junctions with neither close nor tight regions

2) No gap or open junctions were identified.

3) Young mice tight and close region percentages were 11.2% and 88.8%, respectively. Old mice tight and close region percentages were 25.3% and 74.7%, respectively.

4) Significant ageing effects that were found include:
   1. The junction types changed with age ($p < 0.001$). The percentage of tight junctions was 14.1% ± 3.5% higher in aged mice.
   2. The aged mice had consistently more tight regions at every PDL level ($p < 0.01$).
   3. The junction width 2 (W2), at the apex of the PDL was on average 3.6 nm ± 0.88 nm wider ($p < 0.05$) in older mice than younger mice.
   4. The number of PCV in the tooth 1/3 of the PDL was higher in old mice ($p < 0.01$), and of the PCV found significantly more ($p < 0.001$) were apericytic PCV.
   5. The number of PCV decreased significantly ($p < 0.001$) in young mice in the PDL middle cicumferential third halfway down the PDL.

6) Significant effects of PDL level from the alveolar crest to the apex for young and old mice that were found include:
   1. Each age group had a significantly higher number of tight regions ($p < 0.05$) at the alveolar crest and the apex.
   2. The junction width (W1), that is, at the PCV luminal entrance, increased significantly ($p < 0.05$) at the apex by comparison with the alveolar crest in each age group.
   3. The junction width (W2), that is, one third of the distance along the length of the endothelial junction from the PCV lumen, significantly ($p < 0.05$) increased for young and old mice from a low value

(16.3 nm in young, and 19.5 nm in old mice) at the 960 μm PDL level to 20.2 nm and 24.1 nm at the apex in young and old mice, respectivley.

4. Junction thickness was on average 372 nm (SE 32 nm) and 372 nm (SE 33 nm) in young and old mice, respectively. There was a significant trend ($p < 0.05$) for junction thickness for both groups to increase from slightly above average at the alveolar crest, rising to a maximum (508 nm in young, and 454 nm in old mice) at the 160 μm level and then steadily declining to the apex (316 nm in young, and 334 nm in old mice)
5. The relative number of pericytic PCV, compared with total PCV, changed significantly with PDL level ($p < 0.05$), decreasing from the alveolar crest to the apex.
6. Apericytic PCV were more common in both groups.

7) Tight regions (86.1% in young and 90.0% in old mice) were largely confined to the luminal side of the endothelial junctions ($p < 0.05$). Close regions were more common ($p < 0.05$) in the luminal third for both groups.

8) Age had no significant effect on junction length, thickness, size or the location of junction regions along the intercellular cleft. The junction length at the 160 μm level was higher for all mice than other PDL levels, however, this was not significnant. Tight regions were an average of 2.8 nm ± 2.4 nm shorter than close regions, but this was not statistically significant.

9) Age had no significant effect on PCV type (pericytic or apericytic) or PCV diameter. PCV diameter in the aged mice was smaller (2.5 μm) than the young mice, but this finding was not significant.

10) This study provided morphological evidence to support the reported age related decrease in permeability of the microvasculature (Hruza, 1977), for example, an increase in the number of tight junctions in the aged mice.

11) It may be proposed that an increase in the junction width a third of the distance from the lumen in aged mice may represent a functional adaptation to maintain vascular permeability in aged PDL. The question

arises, are the significant differences in the number of tight junctions found of functional importance? Therefore, permeability needs to be assessed. Further, the question is raised whether tight regions in the aged mice have the same functional capacity as young mice?

12) Studies assessing permeability in aged PDL in conjunction with other factors that contribute to permeability of the microvasculature, for example, blood pressure, the presence of disease, interstitial tissue structure (Rippe and Haroldsson, 1994; Cooper *et al.*, 1990; Tang *et al.*, 1993) are needed to confirm these concepts.

13) The current study, using the mouse model to investigate endothelial junctional morphology of the PDL microvascular bed, has provided useful information regarding variations in parameters related to permeability under the influence of ageing.

Appendix 1: Data Recording Sheet

Animal No.		Level		J Loc	(nm)	(nm)						(nm)			(nm)			(nm)	(nm)
BV No.	BV Type	BV Dia (u)	BV Loc	J Type	J Length	Width 1	Width 2	Width 3	Width 4	JT	JR	J Size	JT	JR	J Size	JT	JR	J Size	J Thick
Animal No.		Level																	
Animal No.		Level																	
Animal No.		Level																	

Legend
BV Type:
P-pericytic
AP-apericytic

BV Dia=
Luminal Diameter

Junction Type
C=Close;T=tight
JT=junction type
C=Close
T=Tight

Location:
1-tooth 1/3 PDL
2-middle 1/3 PDL
3-bone 1/3 PDL

JR=junction region
1-lumen to 1/3
2-1/3 to 2/3
2/3 to ablumen

Appendix 2: Results of the Pilot Study

Numbers of various vessel types in the mouse periodontal ligament.

Age of mice	Level	Venous capillary*	Postcapillary-sized venule*	Collecting venule*
Young†	1-3‡ (0 μm to 320 μm)	-	-	-
Young	4-6‡ (480μm to 760μm)	2.5	31	3
Young	7-9‡ (920μm to apex)	4	18	1
Old†	1-3‡ (0 μm to 480 μm)	4.7	9.7	1.5
Old	4-6‡ (480μm to 760μm)	4.5	11	0.3
Old	7-9‡ (920μm to apex)	3.8	8	1.3

* Mean number of vessels for right and left sides

† One mouse from each age group was assessed

‡ Mean number of vessels for three levels

From these results of the pilot examination of numbers of vessels at various levels of the PDL, it is clear that there are insufficient numbers of venous capillaries and collecting venules. There are, however, adequate numbers of postcapillary venules, that is, a minimum of five vessels will be available to study per level. It was concluded that only postcapillary venule endothelial junctions will be studied.

Appendix 3: Tissue Preparation and Electron Microscopy

Anaesthetic

Solution:	30% Urethane.
Preparation:	3g Ethyl Carbamate (Urethane) in 10ml of 0.9% Sodium Chloride.
Dosage:	0.1ml/10g body weight.
Shelf life:	2 to 3 days at 4˚C.
Route:	Intraperitoneal at room temperature.

Anticoagulant

Solution:	1000 I.U. Heparin Sodium in 9ml Ringer's fluid.
Preparation:	90mg Sodium Nitrate. 1ml Heparin Sodium (1000 units/ml). 9ml Ringer's fluid.
Dosage:	0.02ml/10g of body wight.
Shelf life:	7 days at 4˚C.
Route:	Intravenous (tail vein) at room temperature.

Glutaraldehyde Solution

Solution:	TAAB Glutaraldehyde 25% for electron microscopy.
Preparation:	Use stock solution.
Shelf life:	6 months at 4˚C.

Cacodylate Buffer

Solution:	0.06M Sodium Cacodylate.
Preparation:	25.68g Sodium cacodylate in 2000ml double distilled (d.d.) water adjust to pH 7.4 using 1N HCL at 20˚C.
Shelf life:	7 days at 4˚C.

Osmium Tetroxide Solution

Solution:	4% Osmium Tetroxide.
Preparation:	Place 2g of Osmium tetroxide in 50ml d.d. water. Place the ampoule in hot water to melt the Osmium tetroxide crystals. Remove from water and rotate the ampoule to allow the melted Osmium Tetroxide to form an even film over the inside. When the Osmium Tetroxide has again solidified remove the label and clean the outside of the ampoule

thoroughly with Ethyl alcohol. Then drop the ampoule into a thick walled bottle containing 50ml d.d. water and shake to break the ampoule. Wrap in foil to exclude light and leave in a fume cupboard.

Shelf life: 7 to 10 days. this solution can only be used when clear. If it becomes coloured, or darker, then its fixative properties are greatly reduced. Refrigeration is not advised as it increases the rate of oxidation and because Osmium Tetroxide is so highly toxic.

Tissue Fixing And Staining

The tissue blocks were processed through a propylene oxide series for TEM using the following regime, while being continuously rotated in separate vials at room temperature and using soda glass pipettes to change solutions:

1) washed overnight in 0.06M cacodylate buffer immediately after trimming.
2) post-fixed with 4% osmium tetroxide for one hour.
3) 15 minute wash with 0.06M cacodylate buffer.
4) 15 minute wash with 70% alcohol.
5) block staining with 1% uranyl nitrate in 70% ethanol for one hour
6)15 minute wash with 70% alcohol.
7) dehydration through a series of ethanol to propylene oxide.
    2 x 15 minutes in 70% alcohol.
    2 x 15 minutes in 80% alcohol.
    2 x 15 minutes in 90% alcohol.
    2 x 15 minutes in 100% anhydrous alcohol.
    2 x 15 minutes in propylene oxide.
    2 x 30 minutes in propylene oxide.
8) Infiltration was completed after:
    12 hours in 1:1 (propylene oxide:LX-112).
    12 hours in 1:3 (propylene oxide:LX-112).
    12 hour step of LX-112 embedding resin alone.

Sections of 1 μm were stained for two minutes, using millipored solutions of 1:1 of 0.05% toluidine blue and 1% borax to determine the zero level for commencing ultrathin sectioning, that is, the crest of the alveolar bone. The mesa was then reduced further to only include bone, PDL and tooth from the most mesial aspect of the root (Figure 11).

Tissue Sectioning

Ultrathin serial sections were cut in the silver interference range (approximately 70 nm) with a diamond knife set at a clearance angle of 10° and a cutting speed of 1 mm/second (Diatome, Switzerland). Sections were floated on millipored, double-distilled water and flattened with chloroform vapour. Sections were collected on the dull surface of clean uncoated VECO 200 mesh copper grids and dried face upwards on filter paper in a covered petri dish. Specimens were stored in a LKB specimen grid holder.

Perfusate

Solution:	5.6% Glutaraldehyde and 0.9% Osmium Tetroxide in 0.06M Sodium Cacodylate buffer (final pH 7.4).
Preparation:	7.5ml 0.06M Cacodylate buffer, pH 7.4. 3.0ml 25% Glutaraldehyde. 3.0ml 4% Osmium Tetroxide. 0.54g Dextran 70. Dissolve Dextran 70 in the 0.06M cacodylate buffer solution and add Glutaraldehyde. Adjust to pH 7.4 using 1N HCL 2 to 3 hours before. Immediately before perfusing add the 4% Osmium Tetroxide solution.
Shelf life:	10 to 15 minutes at room temperature.
Route:	Intracardiac via left ventricle.

Decalcifying Solution

Solution:	0.1M EDTA in 2.5% Glutaraldehyde, adjust to pH 6 using 1N HCL.
Preparation:	74.45g EDTA. 1800ml 0.06M Cacodylate buffer by gentle heating. Cool to 4˚C, add Glutaraldehyde, pH 6.0 at 4˚C using 1N HCL.
Shelf life:	7 days at 4˚C.

Block Stain

Solution:	1% Uranyl Nitrate in 70% alcohol.
Preparation:	1g Uranyl Nitrate. 70ml Ethyl alcohol. 30ml d.d. water.
Shelf life:	7 days at room temperature.

Embedding Medium (Lx-112)

From Ladd Research Industries, Inc., Burlington, USA

Because of the nature of the tissue to be sectioned a hard embedding medium was selected.

The weight per epoxide (W.P.E,) of the epoxy resin batch used was 141.

Volumetric rather than gravimetric measurements were used although this did not adversely affect the quality of the embedding medium.

Preparation:	For total volume approximating 130ml.
Mixture A:	28ml DDSA, 22ml LX-112 (shaken vigorously for 10 minutes).
Mixture B:	44ml NMA, 37 ml LX-112 (shaken vigorously for 10 minutes).
Mixture C:	A + B + 1.8ml DMP-30 (shaken vigorously for 10 minutes).

Light Microscopic Stains

(i) 0.05% Toluidine Blue

Solution:	0.05% Toluidine Blue in d.d. water.
Preparation:	0.05g Toluidine Blue. 100ml d.d. water. Dissolve by stirring.
Shelf life:	5 months at room temperature.

(ii) 1% Borax

Solution:	1% Borax in d.d. water.
Preparation:	1g Sodium Thiosulphate (borax). 100ml d.d. water. Dissolve by stirring.
Shelf life:	6 months at room temperature.

Grid Stains

(i) 0.5% Uranyl Acetate

Solution:	0.5% Uranyl Acetate in 70% alcohol.
Preparation:	0.125g Uranyl Acetate. 7.5ml Ethyl alcohol. 17.5ml d.d. water.
Shelf life:	7 days at room temperature.

(ii) Modified Reynolds' Lead

Preparation: (a) 1.33g Lead Nitrate.
1.76g Sodium Citrate.
30ml d.d. water.
(b) 8ml 1N Sodium Hydroxide.
Vigorously shake (i) and allow to stand for 30 minutes, add (ii) then dilute to 50 ml with d.d. water mixing by inversion.

Shelf life: 30 days at 4°C. Discard if pH drops below 11.

Radiographic Equipment

1. Kodak periapical ultraspeed film 22 x 35mm.
2. Siemens Heliodent machine.
   a. accelerating voltage: 50 kV.
   b. tube current: 7 mA.
   c. exposure time: 0.1 sec.

Transmission Electron Microscope

1. JEOL 100S (Jeol Ltd., Tokyo, Japan).
   Accelerating voltage of 60 kV.
   Beam current of 50 micro-amps.
   Gun bias setting of 5.
   Objective lens aperture of setting of 2 ,that is, 50μm.
   Condenser aperture setting of 1, that is, 300μm.

2. JEOL 2000FX (Jeol Ltd., Tokyo, Japan).
   Accelerating voltage of 120 kV.
   Spot size 4.
   Objective aperture setting of 75 μm.
   Condenser aperture setting of 120 μm.

3. PHILLIPS CM-10
   Emission 4.
   Accelerating voltage of 80 kV.
   Spot size 2.
   Exposure time 2.
   Emulsion 4.0.
   Data int. 8.0.
   Smallest aperture.

Table 8.4.1 Summary of changes in junction widths 1, 2, 3 and 4 (JW1, JW2, JW3 and JW4) with PDL level for young and old mice.

Level	JW 1				JW 2				JW 3				JW 4			
(μm)	Young		Old		Young		Old		Young		Old		Young		Old	
0	18.7¶	18.7**	21.7	21.7	17.1	17.1	20.5	20.5	17.1	17.1	20.1	20.1	22.7	22.7	27.3	27.3
	(0.5)		(1.1)		(1.0)		(1.0)		(1.2)		(1.6)		(1.2)		(3.0)	
160	18.6	18.6	19.2	19.2	16.8	16.8	19.9	19.9	17.8	17.8	17.8	17.8	24.0	24.0	23.3	23.4
	(2.2)		(1.0)		(1.8)		(1.0)		(2.0)		(0.6)		(2.3)		(1.5)	
320	20.6	20.6	19.8	19.8	18.2	18.2	20.1	20.1	19.1	19.1	19.0	19.0	28.7	28.7	25.4	25.4
	(2.7)		(3.2)		(0.6)		(0.6)		(1.2)		(0.7)		(1.8)		(3.2)	
480	24.6	24.6	23.3	23.3	17.3	17.3	20.2	20.2	18.2	18.2	19.4	19.4	27.7	27.7	27.7	27.7
	(1.5)		(2.4)		(0.4)		(0.9)		(0.9)		(1.2)		(1.4)		(1.1)	
600-675	23.7	23.7	21.5	20.5	19.3	19.3	18.4	17.4	17.6	17.6	19.0	18.7	29.1	29.1	26.1	25.4
	(1.9)		(2.5)		(2.1)		(2.3)		(0.4)		(1.1)		(1.9)		(2.2)	
750-860	24.6	24.6	20.0	20.0	18.6	18.6	18.8	18.8	19.3	19.3	18.5	18.5	28.3	28.3	25.6	25.6
	(3.9)		(1.9)		(1.5)		(0.8)		(0.9)		(0.4)		(4.0)		(0.5)	
900-960	23.6	23.6	25.5	25.5	16.3	16.3	19.5	19.5	18.7	18.7	19.9	20.6	25.9	25.9	24.8	26.5
	(3.0)		(1.5)		(0.9)		(1.2)		(1.3)		(1.4)		(4.2)		(0.8)	
Apex	26.2*	26.2	23.3*	22.9	20.5‡	20.2	24.1†‡	24.1	19.9	19.7	19.0	19.0	30.0	30.5	25.7	24.8
	(0.2)		(2.3)		(1.0)		(3.0)		(0.8)		(0.8)		(1.2)		(2.5)	
Mean	22.8		21.7		18.1		20.3		18.5		19.1		27.3		25.7	

* - Significant increase in junction width 1 at apex by comparison with the alveolar crest for each age group ($p < 0.05$). † - Significant increase junction width 2 at the apex in old mice by comparison with young mice ($p < 0.05$). ‡ - Significant increase in junction width 2 at the apex by comparison with other PDL levels for each age group ($p < 0.05$). ¶ - Arithmetic means with standard error values in parenthesis.

** - These means were calculated using analysis of covariance. They were adjusted because of different numbers of values at this PDL level (Section 4.5).

Table 8.4.2 Summary of changes in junction length, junction thickness and 'meander' with PDL level for young and old mice.

Level(μm)	Length				J Thickness				Meander			
	Young		Old		Young§		Old§		Young		Old	
0	838.0¶	838.0**	880.5	880.5	413.4	413.4	365.1	365.1	0.70	0.70	0.87	0.87
	(119.3)		(59.3)		(30.1)		(38.0)		(0.11)		(0.11)	
160	1065.5	1065.5	1184.0	1184.0	508.1	508.1	454.1	454.1	0.80	0.80	0.98	0.98
	(120.6)		(152.7)		(99.8)		(75.6)		(0.14)		(0.12)	
320	915.8	915.8	957.7	957.7	410.3	410.3	432.5	432.5	0.80	0.80	0.77	0.77
	(89.3)		(88.4)		(34.6)		(44.6)		(0.03)		(0.08)	
480	792.3	792.3	1011.3	1011.3	363.7	363.7	356.0	356.0	0.78	0.78	1.01	1.01
	(92.8)		(133.6)		(27.5)		(23.9)		(0.11)		(0.12)	
600-675	854.1	854.1	928.4	921.7	344.5	344.5	345.3	353.9	0.93	0.93	1.01	0.98
	(56.5)		(46.6)		(26.3)		(37.7)		(0.08)		(0.13)	
750-860	824.1	824.1	1000.2	1000.2	328.9	328.9	345.3	345.3	0.90	0.90	0.98	0.98
	(93.0)		(193.0)		(26.8)		(33.2)		(0.14)		(0.06)	
900-960	890.6	890.6	951.2	1012.8	319.8	319.8	334.7	350.1	0.95	0.95	1.01	1.03
	(122.4)		(104.8)		(22.7)		(12.2)		(0.16)		(0.11)	
Apex	840.7	776.8	790.3	812.3	325.5	316.5	328.9	333.9	0.86	0.83	0.88	0.89
	(216.3)		(78.8)		(32.1)		(33.0)		(0.17)		(0.08)	
Mean	846.2		966.1		372.2		372.4		0.83		0.94	

§ - Significant decrease in junction thickness from the alveolar crest to the apex for each age group ($p < 0.05$).

¶ - Arithmetic means with standard error values in parenthesis.

** - These means were calculated using analysis of covariance. They were adjusted because of different numbers of values at this PDL level (Section 4.5).

BIBLIOGRAPHY

Abdellatif, H. and Burt, B. (1987) An epidemiological investigation into the relative importance of age and oral hygiene status as determinants of periodontitis. *J Dent Res* **66**: 13-18

Adamson, R. (1990) Permeability of frog mesenteric capillaries after partial pronase digestion of the endothelial glycocalyx. *J Physiol* **428**: 1-13

Adamson, R. and Michel, C. (1993) Pathways through the intercellular clefts of frog mesenteric capillaries. *J Physiol* **466**: 303-327

Anderson, J., Balda, M. and Fanning, A. (1993) The structure and regulation of tight junctions. *Curr Opin Cell Biol* **5**: 772-778

Baez, S. (1977) Microvascular terminology. In *Microcirculation.* (Kaley, G. and Altura, B. Ed.) Baltimore, University Park Press. pp 24

Balda, M. and Anderson, J. (1993) Two classes of tight junctions are revealed by ZO-1 isoforms. *Am J Physiol* **264**: C918-C924

Bennett, H., Luft, J. and Hampton, J. (1959) Morphological classification of vertebrate blood capillaries. *Am J Physiol* **196**: 381-390

Berkovitz, B. (1990a) The structure of the periodontal ligament: an update. *Eur J Orthod* **12**: 51-76

Berkovitz, B. (1990b) How Teeth Erupt. *Dent Update* **6**: 206-210

Bernick, S. (1962) Age changes in the blood supply to molar teeth of rats. *Anat Rec* **144**: 265-274

Bernick, S. (1967) Age changes in the blood supply to human teeth. *J Dent Res* **46**: 544-550

Bradley, J. (1972) Age changes in the vascular supply of the mandible. *Brit Dent J* **132**: 142-144

Bridges, T., King, G. and Mohammed, A. (1988) The effect of age on tooth movement and mineral density in the alveolar tissues of the rat. *Am J Orthod Dentofac Orthoped* **93**: 245-50

Bundgaard, M. (1984) The three-dimensional organization of tight junctions in a capillary endothelium revealed by serial-section electron microscopy. *J Ultrastruct Res* **88**: 1-17

Bundgaard, M. (1988) The paracellular pathway in capillary endothelia. In *Vascular Endothelium in Health and Disease.* (Chien, S. Ed.) New York, Plenum Press. pp 3-8

Bundgaard, M. and Frøkjær-Jensen, J. (1982) Functional aspects of the ultrastructure of terminal blood vessels: a quantitative study on consecutive segments of the frog mesenteric microvasculature. *Microvasc Res* **23**: 1-30

Burn-Murdoch, R. (1988) Does interstitial pressure have a role in tooth eruption? In *The Biological Mechanisms of Tooth Eruption and Root Resorption.* (Davidovitch, Z. Ed.) Birmingham, AL, EBSCO Media. pp 225-232

Burn-Murdoch, R. (1990) The role of the vasculature in tooth eruption. *Eur J Orthod* **12**: 101-108

Burt, B. (1994) Periodontitis and ageing: Reviewing recent evidence. *JADA* **125**: 273-279

Casley-Smith, J.R. (1969) The dimensions and numbers of small vesicles in cells, endothelial and mesothelial and the significance of these for endothelial permeability. *J Microsc* **90**: 251-269

Casley-Smith, J.R. (1983) The structure and functioning of the blood vessels, interstitial tissues, and lymphatics. In *Lymphangiology.* (Földi, M. and Casley-Smith, J.R. Ed.) Stuttgart, F K Schattauer Verlag. pp 27-164

Casley-Smith, J.R., Green, H., Harris, J. and Wadley, P. (1975) The quantitative morphology of skeletal muscle capillaires in relation to permeability. *Microvasc Res* **10**: 43-64

Chakravarthy, U., Gardiner, T., Anderson, P. and Archer, D. (1992) The effect of endothelin 1 on the retinal microvascular pericyte. *Microvas Res* **43**: 241-254

Chintakanon, K. (1990) An ultrastructural study of vascular endothelial junctions in normal and tensioned rat periodontal ligament. *MDS Thesis, The University of Adelaide, South Australia*

Chintakanon, K. and Sims, M.R. (1994) Ultrastructural morphology of vascular endothelial junctions in periodontal ligament. *Aust Dent J* **39**: 105-110

Clark, A. (1986) A quantitative analysis of the effect of intrusion on apical periodontal ligament fenestrae of the rat maxillary molar. *MDS Thesis, The University of Adelaide, South Australia*

Claude, P. and Goodenough, D. (1973) Fracture faces of zonulae occludenties from "tight" and "leaky" epithelia. *J Cell Biol* **58**: 390-400

Clough, G. (1991) Relationship between microvascular permeability and ultrastructure. *Prog Biophys Molec Biol* **55**: 47-69

Clough, G. and Michel, C. (1988) Quantitative comparisons of hydraulic permeability and endothelial intercellular cleft dimensions in single frog capillaries. *J Physiol* **405**: 563-576

Cohen, J. (1960) A coefficient of agreement for nominal scales. *Educ Psychol Meas* **20**: 37-46

Cohen, J. (1968) Weighted Kappa: Nominal scale agreement with provision for scaled disagreement or partial credit. *Psychol Bull* **70**: 213-220

Cook, J., Wailgum, T., Vasthare, U., Mayrovitz, H. and Tuma, R. (1992) Age-related alterations in the arterial microvasculature of skeletal muscle. *J Gerontol* **47**: B83-B88

Cooper, S., Sims, M.R., Sampson, W.J. and Dreyer, C.W. (1990) A morphometric, electron microscopic analysis of tissue channels shown by ionic tracer in normal and tensioned rat molar apical periodontal ligament. *Archs Oral Biol* **35**: 499-507

Corpron, R., Avery, J., Morawa, A. and Lee, S. (1976) Ultrasrtucture of capillaries in mouse periodontium. *J Dent Res* **55**: 551

Cotran, R., Kumar, V. and Robbins, S. (1989). Diseases of Aging. In *Robbins Pathologic Basis of Disease*. Philadelphia, W B Saunders Co. pp 543-552

Crone, C. and Levitt, D.G. (1984) Capillary permeability to small solutes. In *Handbook of Physiology, Section 2, The Cardiovascular System, Microcirculation Part 1.* (Renkin, E.M. and Michel, C.C. Ed.) Bethesda, Am Physiol Soc. pp 411-466

Crowe, P. (1988) A TEM stereological analysis of the marmoset periodontal ligament following incisor crown fracture, root canal therapy and orthodontic extrusion. *MDS Thesis, The University of Adelaide, South Australia*

Dice, J.F. (1993) Cellular and molecular mechanisms of ageing. *Physiol Rev* **73**: 149-159

Douvartzidis, I. (1984) A morphometric examination of the periodontal ligament vasculature of the marmoset molar. *MDS Thesis, The University of Adelaide, South Australia*

Duran-Reynals, F. (1946) Age and infection-a review. *J Gerontol* **1**: 358-373

Edwall, L. (1982) The vasculature of the periodontal ligament. In *The Periodontal Ligament in Health and Disease.* (Berkovitz, B., Moxham, B. and Newman, H. Ed.) Oxford, Pergamon Press. pp 151-171

Ekblom, A. and Hansson, P. (1984) A thin-section and freeze-fracture study of the pulp blood vesses in feline and human teeth. *Archs Oral Biol* **29**: 413-424

Embery, G. (1990) An update on the biochemistry of the periodontal ligament. *Eur J Orthod* **12**: 77-80

Farquhar, M.G. and Palade, G.E. (1963) Junctional complexes in various epithelia. *J Cell Biol* **17**: 375-412

Fejerskov, O. (1971) The effects of different demineralisation agents on oral mucosa membrane. *Scan J Dent Res* **79**: 172-182

Foong, K. (1994) Sterology of blood vessels in the periodontal ligament of Man. *MDS Thesis, The University of Adelaide, South Australia*

Franke, W., Krien, S. and Brown, R. (1969) Simultaneous glutaraldehyde-osmium tetroxide fixation with post osmication. *Histochemie* **19**: 162-164

Freezer, S. (1984) A study of periodontal ligament mesial to the mouse mandibular first molar. *MDS Thesis, The University of Adelaide, South Australia*

Freezer, S. and Sims, M.R. (1987) A transmission electron-microscope stereological study of the blood vessels, oxytalan fibres and nerves of mouse molar periodontal ligament. *Arch Oral Biol* **32**: 407-412

Frøkjær-Jensen, J. (1984) The plasmalemmal vesicular system in striated muscle capillaries and in pericytes. *Tissue & Cell* **16**: 31-42

Gabbiani, G. and Majno, G. (1977). Fine structure of endothelium. In *Microcirculation.* (Kaley, G. and Altura, B.M. Ed.) Baltimore, University Park Press. pp 133-143

Gilchrist, D. (1978) Ultrastructure of the periodontal blood vessels. *MDS Thesis, The University of Adelaide, South Australia*

Glauert, A. (1978). *Practical Methods in Electron Microscopy. Fixation, Dehydration and Embedding of Biological Specimens*. Amsterdam, North Holland Pub. Co.

Goldman, R. (1970) Speculations on vascular changes with age. *J Am Geriatrics Soc* **18**: 765-779

Gottlieb, A., Langille, B., Wong, M. and Kim, D. (1991) Biology of disease. Structure and function of the endothelial cytoskeleton. *Lab Invest* **65**: 123-137

Gould, T., Melcher, A. and Brunette, D. (1977) Location of progenitor cells in periodontal ligament of mouse molar stimulated by wounding. *Anat Rec* **188**: 133-142

Grant, D. and Bernick, S. (1970) Arteriosclerosis in periodontal vessels of ageing humans. *J Periodont* **41**: 170-173

Grant, D. and Bernick, S. (1972) The periodontium of ageing humans. *J Periodontol* **43**: 660-673

Gundersen, H., Bendtsen, T., Korbo, L., Marcussen, N., Møller, A., Nielsen, K., Nyengaard, J., Pakkenberg, B., Sørensen, F., Vesterby, A. and West, M. (1988) Some new, simple and efficient stereological methods and their use in pathological research and diagnosis. *APMIS* **96**: 379-394

Harman, D. (1981) The ageing process. *Proc Natl Acad Sci USA* **78**: 7124-7128

Haugen, L. (1992) Biological and physiological changes in the ageing individual. *Int Dent J* **42**: 339-348

Hayat, M. (1981) *Principles and Techniques of Electron Microscopy. Biological Applications.* Baltimore, University Park Press.

Hazzard, D.G., Bronson, R.T., McClean, G.E. and Strong, R. (1992) Selection of an appropriate animal model to study ageing processes with special emphasis on the use of rat strains. *J Gerontol* **47**: B63-64

Holm-Pedersen, P., Agerbæk, N. and Theilade, E. (1975) Experimental gingivitis in young and elderly individuals. *J Clin Perio* **2**: 14-24

Hruza, Z. (1977) Connective tissue. In *Microcirculation*. (Kaley, G. and Altura, B.M. Ed.) Baltimore, University Park Press. pp 167-183

Iida, J., Warita, H. and Kurihara, S. (1992) *In vivo* reserach on the effect of mechanical stress on vascular permeability (a comparison between heavy and light forces). In *The Biological Mechanisms of Tooth Movement and Craniofacial Adaptation*. (Davidovitch, Z. Ed.) Columbus, The Ohio State University College of Dentistry. pp 221-230

Karnovsky, M.J. (1967) The ultrastructural basis of capillary permeability studies with peroxidase as a tracer. *J Cell Biol* **35**: 213-236

Lakatta, E.G. (1993) Cardiovascular regulatory mechanisms in advanced age. *Physiol Rev* **73**(2): 413-467

Lampugnani, M., Caveda, L., Breviario, F., Maschio, A. and Dejana, E. (1993) Endothelial cell-to-cell junctions. Structural characteristics and functional role in the regulation of vascular permeability and leukocyte extravasation. *Baillière's Clinical Haematology* **6**: 539-558

Lee, D., Sims, M.R., Dreyer, C.W. and Sampson, W.J. (1991) A scanning electron microscope study of microcorrosion casts of the microvasculature of the marmoset palate, gingiva and periodontal ligament. *Archs Oral Biol* **36**: 211-220

Levick, J.R. and Smaje, L.H. (1987) An analysis of the permeability of fenestra. *Microvasc Res* **33**: 233-256

Lew, K., Sims, M.R. and Leppard, P.I. (1989) Tooth extrusion effects on microvessel volumes, endothelial areas, and fenstrae in molar apical periodontal ligament. *Am J Orthod Dentofac Orthop* **96**: 221-31

Loe, H., Anerud, A., Boysen, H. and Morrison, E. (1986) Natural history of periodontal disease in man. Rapid, moderate and no loss of attachment in Sri Lanken laborers 14 to 46 years of age. *J Clin Periodont* **13**: 431-45

Luke, D.A. (1992) The structure and function of the dentogingival junction and periodontal ligament. *Br Dent J* **172**: 187-190

Magnusson, B. (1973) Autoradiographic study of erupting teeth in rats after intercardial injection of ^{131}I-fibrinogen. *Scan J Dent Res* **81**: 130-134

Majno, G. (1965). Ultrastructure of the vascular membrane. In *Handbook of Physiology. Section 2 Circulation Vol III.* (Hamilton, W. and Dow, P. Ed.) Baltimore, Waverley Press. pp 2293-2375

Marchesi, V., Furthmayr, H. and Tomita, M. (1976) The red cell membrane. *Ann Rev Biochem* **45**: 667-698

Masoro, E.J. (1981). CRC Handbook of Physiology of Aging. In (Masoro, E.J., Adelman, R.C. and Roth, G.S. Ed.) Boca Raton, CRC Press, Inc. pp 157

Matalon, S.V. and Wangensteen, O.D. (1977) Pulmonary capillary filtration and reflection coefficients in the newborn rabbit. *Microvasc Res* **14**: 99-110

McCulloch, C. and Melcher, A. (1983) Cell density and cell generation in the periodontal ligament of mice. *Amer J Anat* **167**: 43-58

Michel, C.C. (1988) Capillary permeability and how it may change. *J Physiol* **404**: 1-29

Moxham, B. (1988). The role of the periodontal vasculature in tooth eruption. In *The Biological Mechanisms of Tooth Eruprtion and Root Resortption.* (Davidovitch, Z. Ed.) Birmingham, AL, EBSCO Media. pp 207-223

Moxham, B., Shore, R. and Berkovitz, B. (1985) Fenestrated capillaries in the connective tissues of the periodontal ligament. *Microvasc Res* **30**: 116-124

Navia, J.M. (1977). The oral environment in experimental animals: The teeth, structure and composition. In *Animal Models in Dental Research.* (Navia, J. Ed.) Alabama, The University of Alabama Press. pp 169-173

Norton, L. (1988) The effect of ageing cellular mechanisms on tooth movement. *Dent Clin Nth Am* **32**: 437-446

O'Morchoe, C. and O'Morchoe, P. (1987) Differences in lymphatic and blood capillary permeability. *Lymphology* **20**: 205-209

Ott, L. (1988). *An Introduction to Statistical Methods and Data Analysis.* Boston, PWS-Kent Publishing Company.

Palade, G.E., Simionescu, M. and Simionescu, N. (1979) Structural aspects of the permeability of the microvascular endothelium. *Acta Physiol Scand Suppl* **463**: 11-32

Pappenheimer, J.R. (1953) Passage of molecules through capillary walls. *Physiol Rev* **33**: 387-423

Parlange, L. and Sims, M.R. (1993) A TEM stereological analysis of blood vessels and nerves in marmoset periodontal ligament following endodontics and magnetic incisor extrusion. *Eur J Orthod* **15**: 33-44

Phillips, C., Parker, K. and Wang, W. (1994) A models for flow through discontinuities in the tight junction of the endothelial intercellular cleft. *Bull Math Biol* **56**: 723-741

Picton, D. (1986) Extrusive mobility of teeth in adult monkeys (*Macaca fascicularis*). *Arch Oral Biol* **31**: 369-372

Picton, D. and Wills, D. (1978) Viscoelastic properties of the periodontal ligament and mucous membrane. *J Pros Dent* **40**: 263-272

Pinto da Silva, P. and Kachar, B. (1982) On tight-junction structure. *Cell* **28**: 441-450

Reitan, K. (1954) Tissue reaction as related to the age factor. *Dent Rec* **74**: 271-279

Renkin, E. (1977) Multiple pathways of capillary permeability. *Circ Res* **41**: 735-743

Rhodin, J.A.G. (1967) The ultrastructure of mammalian arterioles and precapillary sphincters. *J Ultrastruct Res* **18**: 181-223

Rhodin, J.A.G. (1968) Ultrastructure of mammalian venous capillaries, venules, and small collecting veins. *J Ultrastruct Res* **25**: 452-500

Rhodin, J.A.G. (1984a). Anatomy of microcirculation. In *Blood Vessels and Lymphatics in Organ Systems.* (Abramson, D. and Dobrin, P. Ed.) Orlando, Academic Press, Inc. pp 97-106

Rhodin, J.A.G. (1984b). Architecture of the vessel wall. In *Handbook of Physiology Section 2 The Cardiovascular System. Vol IV.* (Renkin, E. and Michel, C. Ed.) Bethesda, Am Physiol Soc. pp 1-31

Rippe, B. and Haraldsson, B. (1994) Transport of macromolecules across microvascular walls: The two-pore theory. *Physiol Rev* **74**: 163-219

Roberts, W. (1994) Bone Physiology, Metabolism and Biomechanics in Orthodontic Practice. In *Orthodontics. Current Principles and Techniques.* (Graber, T and Vanarsdall, R. Ed.) St. Louis, Mosby. pp 139-234

Rubin, L. (1992) Endothelial cells: adhesion and tight junctions. *Curr Opin Cell Biol* **4**: 830-833

Schneeberger, E. and Karnovsky, M. (1976) Substructure of intercellular junctions in freeze-fractured alveolar-capillary membranes of mouse lung. *Circ Res* **38**: 404-411

Schneeberger, E. and Lynch, R. (1984) Tight junctions: Their structure, composition, and function. *Circ Res* **55**: 723-733

Schneeberger, E. and Lynch, R. (1992) Structure, function, and regulation of cellular tight junctions. *Am J Physiol* **262**: L647-L661

Schneeberger, E. and McCormack, K. (1984) Intercelullar junctions in upper airway submucosal glands of the rat: a tracer and freeze fracture study. *Anat Rec* **210**: 421-433

Schroeder, H. (1991). *Oral Structural Biology. Embryology, Structure, and Function of Normal Hard and Soft Tissues of the Oral Cavity and Temporomandibular Joints.* New York, Thieme.

Severson, J.A., Moffett, B.C., Kokich, V. and Selipsky, H. (1978) A histologic study of age changes in the adult human periodontal joint (ligament). *J Periodont* **49**: 189-200

Sheiham, A. (1990) Dentistry for an ageing population: responsibilities and future trends. *Dental Update* **17**: 70-74

Shepro, D. and Morel, N. (1993) Pericyte physiology. *FASEB J* **7**: 1031-1038

Sheridan, J.D. (1980) Dye transfer in small vessels from the rat omentum: homologous and heterologous junctions. (Abst) *J Cell Biol* **87**: 61a

Shivers, R. (1979) The blood brain-barrier of a reptile, Anolis Carolinensis. A freeze fracture study. *Brain Res* **169**: 221-230

Simionescu, M. and Simionescu, N. (1984) Ultrastructure of the microvascular wall: functional correlations. In *Handbook of Physiology, Section 2, The Cardiovascular System, Microcirculation, Part 1.* (Renkin, E.M. and Michel, C.C. Ed.) Baltimore, American Physiological Society. pp 41-101

Simionescu, M. and Simionescu, N. (1991) Endothelial transport macromolecules: transcytosis and endocytosis. *Cell Biol Reviews* **25**: 5-80

Simionescu, M., Simionescu, N. and Palade, G. (1974) Characteristic endothelial junctions in sequential segments of the microvasculature. (Abst.). *J Cell Biol* **63**: 316a

Simionescu, M., Simionescu, N. and Palade, G. (1975) Segmental differentiations of cell junctions in the vascular endothelium. The microvasculature. *J Cell Biol* **67**: 863-885

Simionescu, N., Simionescu, M. and Palade, G. (1978) Structural basis of permeability in sequential segments of the microvasculature of the diaphragm. I. Bipolar microvascular fields. *Microvasc res* **15**: 1-16

Sims, D. (1986) The pericyte - a review. *Tissue & Cell* **18**: 153-174

Sims, M.R. (1980) Angular changes in collagen cemental attachment during tooth movement. *J Perio Res* **15**: 638-645

Sims, M.R. (1983) The microvascular venous pool and its ultrastructural associations in mouse molar periodontal ligament - periodontal microvasculature and nerves. *Aust Orthod J* **8**: 21-27

Sims, M.R. (1987) A model of the anisotropic distribution of microvascular volume in the periodontal ligament of the mouse mandibular molar. *Aust Orthod J* **10**: 21-24

Sims, M.R., Dreyer, C.W., Leppard, P.I. and Sampson, W.J. (1992a) Stereological changes in the microvascular bed of mouse molar periodontal ligament with ageing. *J Dent Res* : 677: Abst 97

Sims, M.R., Sampson, W.J. and Dreyer, C.W. (1993). Ageing changes in the periodontal ligament microvasculature. 69th Congress of the European Orthodontic Society, Stockholm, European Orthodontic Society.

Sims, M.R., Sampson, W.J., Leppard, P.I. and Dreyer, C.W. (1992a) Ageing changes in the periodontal ligament microvascular bed-luminal volumes. *J Dent Res* : 677: Abst 96

Skalak, R. (1988). Theoretical modelling of fluid transport through endothelial junctions. In *Vascular Endothelium in Health and Disease.* (Chien, S. Ed.) New York, Plenum Press. pp 9-16

Stutzmann, J. and Petrovic, A. (1989). Responsiveness of alveolar bone to orthodontic treatment in adult patients. In *Orthodontics in an Ageing Society.* (Carlson, D. Ed.) Ann Arbor, Michigan, Center for Human Growth and Development, The University of Michigan. pp 181-199

Tabata, S. and Semba, T. (1987) Examination of blood capillaries in rat incisor pulp by TEM of thin sections and freeze fracture replicas. *J Electron Microsc* **36**: 283-93

Takano-Yamamoto, T., Kawakami, M. and Yamashiro, T. (1992) Effect of age on the rate of tooth movement in combination with local use of $1,25(OH)_2D_3$ and mechanical force in the rat. *J Dent Res* **71**: 1487-1492

Tang, M. and Sims, M.R. (1992) A TEM analysis of tissue channels in normal and orthodontically tensioned rat molar periodontal ligament. *Eur J Orthod* **14**: 433-444

Tang, M., Sims, M.R., Sampson, W.J. and Dreyer, C.W. (1993) Short communication. Evidence for endothelial junctions acting as a fluid flux pathway in tensioned periodontal ligament. *Archs Oral Biol* **38**: 273-276

Tortora, G. and Grabowski, S. (1993). In *Principles of Anatomy and Physiology.* New York, Harpers Collins College Publishers. pp 10-11

Trump, B. and Bulger, R. (1966) New ultrastructural characteristics of cells fixed in a glutaraldehyde-osmium tetroxide mixture. *Lab Invest* **15**: 368-379

Tsay, R., Weinbaum, S. and Pfeffer, R. (1989) A new model for capillary filtration based on recent electron microscopic studies of endothelial junctions. *Chem Eng Comm* **82**: 67-102

van der Velden, U. (1984) Effect of age on the periodontium. *J Clin Periodont* **11**: 281-294

Vander, A., Sherman, J. and Luciano, D. (1970) Chapter 10 Circulation. In *Human Physiology: The Mechanism of Body Function*. New York, McGraw-Hill Book Company. pp 274

Veerman, A., Hoefsmit, E. and Boeré, H. (1974) Perfusion fixation using a cushoning chamber coupled to a peristaltic pump. *Stain Technol* **49**: 111-112

Wagner, R. (1988) In *Endothelial Cell Biology*. (Simionescu, N. and Simionescu, M. Ed.) New York, Plenum. pp 23-47

Wangensteen, O.D., Lysaker, E. and Savaryn, P. (1977) Pulmonary capillary filtration and reflection coefficients in the adult rabbit. *Microvasc Res* **14**: 81-97

Ward, B., Bauman, K. and Firth, J. (1988) Interendothelial junctions of cardiac capillaries in rats: their structure and permeability properties. *Cell Tissue Res* **252**: 57-66

Weakley, B. (1981) *A Beginner's Handbook in Biological Transmission Electron MIcroscopy*. Edinburgh, Churchill Livingstone.

Weinbaum, G., Tzeghai, P., Ganatos, P., Pfeffer, R. and Chein, S. (1985) Effect of cell turnover and leaky junctions on arterial macromolecular transport. *Am J Physiol* **248**: H945-H960

Weinbaum, S., Tsay, R. and Curry, F.E. (1992) A three-dimensional junction-pore-matrix model for capillary permeability. *Microvasc Res* **44**: 85-111

Weir, A. (1990) The maromoset periodontal ligament: A TEM analysis following incisor crown fracture, endodontic therapy, orthodontic extrusion and long term retention. Morphometric and stereological data. *MDS Thesis, The University of Adelaide, South Australia*

Weisfeldt, M.L., Lakatta, E.G. and Gerstenblith, G. (1988). Aging and cardiac disease. In *Heart Disease.* (Braunwald, E. Ed.) Philadelphia, W B Saunders. pp 1650-1662

Wiebel, E. and Knight, B. (1964) A morphometric study of the thickness of the pulmonary air-blood barrier. *J Cell Biol* **21**: 367-384

Wiedeman, M.P. (1984). Architecture. In *Handbook of Physiology, Sect. 2, Cardiovascular System, Vol IV.* (Renkin, E. and Michel, C. Ed.) Bethesda, Am. Physiol. Soc. pp 11-40

Willliams, M. (1977). *Practical Methods in Electron MIcroscopy. Quantitative Methods in Biology.* Amsterdam, North Holland Pub. Co.

Wills, D., Picton, D. and Davies, W. (1976) A study of the fluid systems of the periodontium in Macaque monkeys. *Arch Oral Biol* **21**: 175-185

Wissig, S.L. (1979) Identification of the small pore in muscle capillaries. *Acta Physiol Scand Suppl* **463**: 33-44

Wong, R.S.T. and Sims, M.R. (1987) A scanning electron-microscopic, stereo-pair study of methacrylate corrosion casts of the mouse palatal and molar periodontal microvasculature. *Archs Oral Biol* **32**: 557-566

Wu, N. and Baldwin, L. (1992) Transient venular permeability increase and endothelial gap formation induced by histamine. *Am J Physiol* **262**: H1238-H1247